АВТОМАТИКА
и
ТЕЛЕМЕХАНИКА

Vol. 21, No. 10, October, 1960
Translation Published April, 1961

THE UNIVERSITY OF MICHIGAN
MAY 23 1961
ENGINEERING LIBRARY

SOVIET INSTRUMENTATION AND
CONTROL TRANSLATION SERIES

Automation and Remote Control

(The Soviet Journal *Avtomatika i Telemekhanika* in English Translation)

■ This translation of a Soviet journal on automatic control is published as a service to American science and industry. It is sponsored by the Instrument Society of America under a grant in aid from the National Science Foundation, continuing a program initiated by the Massachusetts Institute of Technology.

SOVIET INSTRUMENTATION AND CONTROL TRANSLATION SERIES

Instrument Society of America Executive Board

Dr. Ralph H. Tripp
President
J. Johnston, Jr.
Past President
Philip A. Sprague
President-elect-Secretary
Henry J. Noebels
Dept. Vice President
E. A. Adler
Dept. Vice President
Adelbert Carpenter
Dept. Vice President
Nathan Cohn
Dept. Vice President
Francis S. Hoag
Dept. Vice President-elect
John C. Koch
Treasurer
Nelson Gildersleeve
Dist. I Vice President
H. Kirk Fallin
Dist. II Vice President
John R. Mahoney
Dist. III Vice President
F. R. Gilmer
Dist. IV Vice President
Milton M. McMillen
Dist. V Vice President
Otto J. Lessa
Dist. VI Vice President
J. Howard Park, III
Dist. VII Vice President
Roy Horton
Dist. VIII Vice President
Robert C. Mann
Dist. IX Vice President
Kenneth S. Vriesen
Dist. X Vice President
John J. McDonald
Dist. XI Vice President

Headquarters Office

William H. Kushnick
Executive Director
Charles W. Covey
Editor, ISA Journal
Herbert S. Kindler
Director, Tech. & Educ. Services
Ralph M. Stotsenburg
Director, Promotional Services
Ira S. French
Director, Public Relations

ISA Publications Committee

Charles O. Badgett, *Chairman*

Jere E. Brophy	George A. Larsen	Joshua Stern
Dr. Enoch J. Durbin	Thomas G. MacAnespie	Frank S. Swaney
Prof. Richard W. Jones	John E. Read	Richard A. Terry

Translations Advisory Board of the Publications Committee

Jere E. Brophy, *Chairman*

T. J. Higgins	S. G. Eskin	G. Werbizky

■ This translation of the Soviet Journal *Avtomatika i Telemekhanika* is published and distributed at nominal subscription rates under a grant in aid to the Instrument Society of America from the National Science Foundation. This translated journal, and others in the Series (see back cover), will enable American scientists and engineers to be informed of work in the fields of instrumentation, measurement techniques, and automatic control reported in the Soviet Union.

The original Russian articles are translated by competent technical personnel. The translations are on a cover-to-cover basis and the Instrument Society of America and its translators propose to translate faithfully all of the scientific material in *Avtomatika i Telemekhanika*, permitting readers to appraise for themselves the scope, status, and importance of the Soviet work. All views expressed in the translated material are intended to be those of the original authors and not those of the translators nor the Instrument Society of America.

Publication of *Avtomatika i Telemekhanika* in English translation started under the present auspices in April, 1958, with Russian Vol. 18, No. 1 of January, 1957. The program has been continued with the translation and printing of the 1958, 1959, and 1960 issues.

Transliteration of the names of Russian authors follows the system known as the British Standard. This system has recently achieved wide adoption in the United Kingdom, and is currently being adopted by a large number of scientific journals in the United States.

Readers are invited to submit communications on the quality of the translations and the content of the articles to ISA headquarters. Pertinent correspondence will be published in the "Letters" section of the ISA Journal. Space will also be made available in the ISA Journal for such replies as may be received from Russian authors to comments or questions by American readers.

1960 Volume 21 Subscription Prices:

Per year (12 issues), starting with Vol. 21, No. 1

General: United States and Canada	$35.00
Elsewhere	38.00
Libraries of nonprofit academic institutions:	
United States and Canada	$17.50
Elsewhere	20.50
Single issues to everyone, each	$ 6.00

1957 Volume 18, 1958 Volume 19, and 1959 Volume 20 issues also available. Prices upon request.

See back cover for combined subscription to entire Series.

Subscriptions and requests for information on back issues should be addressed to the:

Instrument Society of America
313 Sixth Avenue, Pittsburgh 22, Penna.

Translated and printed by Consultants Bureau Enterprises, Inc.

Copyright © 1961 by the Instrument Society of America

Automation and Remote Control

A translation of Avtomatika i Telemekhanika, a publication of the Academy of Sciences of the USSR

EDITORIAL BOARD OF AVTOMATIKA I TELEMEKHANIKA

D. I. Ageikin
M. A. Aizerman
A. B. Chelyustkin *(Assoc. Editor)*
E. G. Dudnikov
N. Ya. Festa
V. A. Ilin
A. G. Iosuf'yan
V. V. Karibskii
A. V. Khramoi
B. Ya. Kogan
V. S. Kulebakin
S. A. Lebedev
A. Ya. Lerner
A. M. Letov *(Assoc. Editor)*
V. S. Malov
B. N. Petrov
Yu. P. Portnov-Sokolov
B. S. Sotskov
A. A. Tal' *(Corresp. Secretary)*
V. A. Trapeznikov *(Editor in Chief)*
Ya. Z. Tsypkin
G. M. Ulanov
A. A. Voronov
S. V. Yablonskii

Vol. 21, No. 10 Russian Original Dated October, 1960 **April, 1961**

CONTENTS

	PAGE	RUSS. PAGE
An Estimate of the Maximum Deviation for a Given Trajectory. E. A. Barbashin	945	1341
On the Stability of an Aileron Control System Disturbed by Turbulence. P. S. Landa and S. P. Strelkov	953	1352
A Vector Method for Calculating One Class of Control Systems. S. M. Levin and L. G. Manusevich	962	1365
Certain Problems in the Design of Machines Which Classify Objects According to an Identifying Feature Which is Not Specified A Priori. E. M. Braverman	971	1375
Controlling a Servodrive Using One Null Indicator Which Performs the Functions of Two Null Indicators. V. D. Vershinin	979	1387
Taking the Weak Surface Effect into Account in Switching the Magnetic State of a Ferromagnetic Plate. M. G. Vitkov	984	1393
Selection of the Most Suitable Circuit for a Photoelectric Fluxmeter. I. G. Gutovskii	989	1401
Synthesis of Circuits Whose Operation is Described by Boolean Time Functions. D. A. Pospelov	997	1410
Survey and Classification of Multiplying Devices. A. A. Moslov	1000	1414
Letter to the Editor. J. Matyáš	1016	1433
Work of the All-Moscow Seminar on Magnetic Automation Components. G. V. Subbotina	1018	1435
List of Literature on Magnetic Components for Automation, Remote Control, and Computer Technology for 1959. G. V. Subbotina and I. S. Trefilova	1019	1436

ERRATA

Vol. 21, No. 8, August, 1960

Equation (3) on page 858 should read as follows:

$$x = \Phi(p)[x_y + W_{f1}(p)x_{i_1} + \ldots + W_{fk}(p)x_{ik} + \ldots],$$

On the same page, all the x's in Fig. 1 should be lower case (x_c, x_d, x_{co}, and x) rather than capitals.

AN ESTIMATE OF THE MAXIMUM DEVIATION FROM A GIVEN TRAJECTORY

E. A. Barbashin

Sverdlovsk

Translated from Avtomatika i Telemekhanika, Vol. 21, No. 10,
pp. 1341-1351, October, 1960
Original article submitted April 15, 1960

The method proposed in [1] is used to estimate the maximum deviation of motion from a given trajectory.

A method of choosing control functions and vectors is introduced for decreasing this deviation. The case of an infinite time interval is considered. The relation between the problem investigated and that of the accumulation of disturbances is studied.

We consider the system of differential equations

$$\frac{dx_i}{dt} = \sum_{k=1}^{n} a_{ik}(t)\,x_k + \sum_{k=1}^{m} b_{ik}u_k(t) \qquad (1)$$

$$(i = 1, 2, \ldots\ n, \quad m \leqslant n),$$

where $a_{ik}(t)$ are continuous functions on the interval $t_0 \leq t \leq t_0 + T$, and the b_{ik} are constants such that the "control" vectors $b_k(b_{1k}, b_{2k}, \ldots, b_{nk})$ $(k = 1, 2, \ldots, m)$ are linearly independent.

As in [1], we pose the problem of finding control functions $u_k(t)$, such that for $t_0 \leq t \leq t_0 + T$ the relation

$$x_i(t) = f_i(t) \qquad (i = 1, 2, \ldots, n) \qquad (2)$$

is satisfied, where $x_i(t)$ is the solution of the system (1) and $f_i(t)$ is a given system of functions with $x_i(t_0) = f_i(t_0)$. When $m < n$, this problem is, as a rule, insoluble, and so we try to find functions $u_k(t)$ [2] such that the expression

$$\|z\| = \max_i \max_{t_0 \leq t \leq t_0+T} |x_i(t) - f_i(t)| \qquad (3)$$

will be a minimum.

Following the ideas of [1], we will not try to find control functions guaranteeing that the value of $\|z\|$ is exactly a minimum, but will obtain an estimate of the form

$$\|z\| \leq A\|y\|,$$

where A is a constant and $\|y\|$ is the deviation from zero in some sense of another quantity y. We replace the difficult problem of finding $\min \|z\|$ by the simpler problem of finding $\min \|y\|$. The loss in accuracy of the approximation due to this procedure is not great for small values of $\|y\|$, while the decrease in difficulty in the numerical calculations is considerable.

In Section 1 we show that the method of choosing the control functions and vectors proposed earlier ensures a decrease, not only in the mean square value of the deviation, but also a decrease in the maximum deviation. It must be taken into consideration that the value of a control function at any given instant is chosen independently of the length of the interval over which the approximation is being carried out, and also independently of the value of this function at any other instant of time.

In Section 2, the same method of choosing the control functions [see the system (10)] is used to obtain other methods of estimating the maximum deviation. Although these other methods have no special advantages over the estimate of Theorem 1, they are of interest in several cases. In particular, Theorem 3 (and also Theorems 1 and 2) solves the problem of the accumulation of disturbances in a dynamic system. From this point of view, the results obtained are completely analagous to those obtained by B. V. Bulgakov in [3, 4]. We also note that the character of any of the three estimates of $\|z\|$ depends on the function space in which we consider y. An explanation of this phenomenon is given in the Appendix.

We consider the case $T = \infty$ in Section 3. It is natural to consider this case in connection with questions in the theory of stability. It is unfortunately impossible in the present paper to investigate this problem in the light of the ideas in the detailed investigation by Massera and Schäffer [5].

1. The Basic Estimate of the Maximum of the Deviation and the Choice of Control Functions

In the system (1) we make the change of variables

$$z_i = x_i - f_i(t) \qquad (i = 1, 2, \ldots, n),$$

and obtain the new system

$$\dot{z}_i = \sum_{k=1}^{n} a_{ik}(t) z_k + y_i(t) \quad (i = 1, 2, \ldots, n), \tag{4}$$

where

$$y_i(t) = \sum_{k=1}^{r} b_{ik} u_k(t) + \sum_{k=1}^{n} a_{ik}(t) f_k(t) - \dot{f}_i(t) \quad (i = 1, 2, \ldots, n). \tag{5}$$

The solution of the system (4) that satisfies the conditions $z_i(t_0) = 0$ is

$$z_i(t) = \int_{t_0}^{t} \sum_{k=1}^{n} w_{ik}(t, \tau) y_k(\tau) d\tau \quad (i = 1, 2, \ldots, n), \tag{6}$$

where $W_{ik}(t, \tau)$ are the elements of the fundamental matrix $\mathbf{W}(t, \tau)$ defined by the equation $d\mathbf{W}/dt = \mathbf{A}(t)\mathbf{W}$ and the condition $\mathbf{W}(\tau, \tau) = \mathbf{I}$ [$\mathbf{I}$ is the unit matrix, and $\mathbf{A}(t)$ is the matrix with its elements, coefficients $a_{ik}(t)$].

In what follows we will use the notation

$$\|z\| = \max_i \max_{t_0 \leqslant t \leqslant t_0 + T} |z_i(t)|,$$

$$y^2(t) = \sum_{i=1}^{n} y_i^2(t),$$

$$w_i^2(t, \tau) = \sum_{k=1}^{n} w_{ik}^2(t, \tau) \qquad (i = 1, 2, \ldots, n).$$

Let $y_i(t)$ be functions which are for the moment arbitrary, but such that the integral $\int_{t_0}^{t_0+T} y^2(t)\, dt$ exists.

The following theorem opens up the possibility of estimating $\|z\|$ in terms of the mean square value of the quantity $y(t)$.

Theorem 1. There exists a minimum number M, for which

$$\|z\| \leqslant M \left(\int_{t_0}^{t_0+T} y^2(\tau)\, d\tau \right)^{1/2}. \tag{7}$$

The number M can be obtained from the formula

$$M = \max_i \max_{t_0 \leqslant t \leqslant t_0 + T} \left(\int_{t_0}^{t} w_i^2(t, \tau)\, d\tau \right)^{1/2}. \tag{8}$$

If the functions $a_{ik}(t)$ are constants, then

$$M = \max_i \left(\int_{t_0}^{t_0+T} w_i^2(t_0 + T, \tau)\, d\tau \right)^{1/2}. \tag{9}$$

Theorem 1 evidently also solves the problem of the accumulation of disturbances when the mean square of the external forces is bounded. In fact, if

$$\int_{t_0}^{t_0+T} y^2(\tau)\, d\tau = L,$$

then the formula (7) gives the maximum deviation, equal to ML. From the proof of Theorem 1 given in the Appendix, it is obvious what form the functions $y_i(t)$ must take to give the maximum deviation.

It follows from Theorem 1 that $\|z\|$ can be decreased by decreasing the quantity $\|y\| = \left(\int_{t_0}^{t_0+T} y^2(\tau)\, d\tau \right)^{1/2}$.

The method of choosing the control functions $u_i(t)$ to ensure that $\|z\|$ is a minimum was given in Section 2 of [1]. In this paper it was shown that the control functions are determined by a system of equations of the form

$$\sum_{i=1}^{m} (\mathbf{b}_k, \mathbf{b}_i) u_i(t) = (\mathbf{r}(t), \mathbf{b}_k) \quad (k = 1, 2, \ldots, m), \tag{10}$$

where $(\mathbf{b}_k, \mathbf{b}_i)$ is the scalar product of the vectors $\mathbf{b}_k$ and $\mathbf{b}_i$, and $\mathbf{r}(t) = \mathbf{r}_1(t), \mathbf{r}_2(t), \ldots, \mathbf{r}_n(t)$ are vector functions satisfying the equation

$$r_i(t) = f_i(t) - \sum_{k=1}^{n} a_{ik}(t) f_k(t) \qquad (i = 1, 2, \ldots, n). \tag{11}$$

If $u_i(t)$ is chosen according to (10), then we will have

$$y^2(t) = \sum_{i=1}^{n} y_i^2(t) = \frac{\Gamma(\mathbf{b}_1, \mathbf{b}_2, \ldots, \mathbf{b}_m, \mathbf{r}(t))}{\Gamma(\mathbf{b}_1, \mathbf{b}_2, \ldots, \mathbf{b}_m)}, \tag{12}$$

where the numerator and denominator in the fraction on the right-hand side are the Gramme determinants corresponding to the systems of vectors.

Thus, we have

$$H^2 = \|y\|^2 = \frac{1}{\Gamma(b_1, b_2, \ldots, b_m)} \int_{t_0}^{t_0+T} \Gamma(b_1, b_2, \ldots, b_m, r(t))\, dt. \tag{13}$$

It should be noted that if the functions $u_k(t)$ are chosen according to (10), then

$$\sum_{k=1}^{m} b_k u_k(t) = \frac{1}{\Gamma(b_1, b_2, \ldots, b_m)} \begin{vmatrix} (b_1, b_1) \ldots (b_1, b_m), & b_1 \\ (b_m, b_1) \ldots (b_m, b_m), & b_m \\ (r, b_1) \ldots (r, b_m), & 0 \end{vmatrix}.$$

In Section 3 of [1], a recommendation is given for the choice of the control vectors $b_1, b_2, \ldots, b_m$, to give a minimum value for $\|y\|$ if the functions $u_k(t)$ are chosen according to (10). The choice of the control functions and the control vectors given in [1] thus contributes, not only to decreasing the mean square deviation, but also to decreasing the maximum deviation.

2. Other Estimates of $\|z\|$

In this section we give other estimates of $\|z\|$ which are independent of the estimate given in Section 1. Let $y_i(t)$ be an arbitrary function such that the integral $\int_{t_0}^{t_0+T} y(\tau)\, d\tau$ exists.

Theorem 2. The inequality

$$\|z\| \leqslant N \int_{t_0}^{t_0+T} y(\tau)\, dt \tag{14}$$

holds, where $N = \max_i \max_{t_0 \leq t \leq t_0+T_0} \max_{t_0 \leq \tau \leq t} w_i(t, \tau)$.

If all the eigenvalues $\lambda_i(t)$ of the matrix $A(t) + A^*(t)$ ($A(t)$ is the matrix having the coefficients $a_{ik}(t)$ as elements, $A^*(t)$ is its adjoint) are nonpositive for any value of t in the interval $t_0 \leq t \leq t_0 + T$, then $N = 1$, and

$$\|z\| \leqslant \int_{t_0}^{t_0+T} y(\tau)\, d\tau.$$

Formula (14) gives a new estimate of $\|z\|$. In connection with the choice of control functions, it follows from Section 2 of [1] that Theorem 2 gives no new information in choosing these functions, except that which follows from the system (10) investigated in the present paper. In fact, when the control functions are chosen according to (10), the minimum value of not only the integral $\int_{t_0}^{t_0+T} y^2(\tau)\, d\tau$, but also that of the integral $\int_{t_0}^{t_0+T} y(\tau)\, d\tau$ is ensured.

Theorem 3. There exists a least number C, such that

$$\|z\| \leqslant C \max_{t_0 \leq t \leq t_0+T} y(t). \tag{15}$$

This number is given by the formula

$$C = \max_i \max_{t_0 \leq t \leq t_0+T} \int_{t_0}^{t} w_i(t, \tau)\, d\tau. \tag{16}$$

If the functions $a_{ik}(t)$ are constant, then

$$C = \max_i \int_{t_0}^{t_0+T} w_i(t_0 + T, \tau)\, d\tau. \tag{17}$$

In addition to the basic problem, Theorem 3 also solves the problem concerning the accumulation of disturbances in the system for bounded external vector forces. If the functions $y_i(t)$ satisfy the inequality $y^2(t) = \sum_{i=1}^{n} y_i^2(t) \leqslant R^2$, then it follows from Formula (15) that $\|z\| \leq RC$, while, from the proof of Theorem 3 given in the Appendix, it follows that the upper bound of RC is attained for

$$y_k(\tau) = R \frac{w_{ik}(t, \tau)}{w_i(t, \tau)},$$

where t and i are chosen so that the maximum (16) is attained. If the functions $a_{ik}(t)$ are constant, then we have

$$\|z\| \leqslant R \max_i \int_{t_0}^{t_0+T} w_i(t_0 + T, \tau)\, d\tau.$$

The result of the solution in the present paper and in [1] differ from that in [3] in that here the sum of the squares of the external influences $y_i(t)$ is bounded, and not each separate influence.

We now return to the main problem. Since $y_i(t) = \sum_{k=1} b_{ik} u_k(t) - r_i(t)$, where the functions $r_i(t)$ are given by Formula (11), then according to [1] $y(t) = \left(\sum_{i=1}^{n} y_i^2(t)\right)^{1/2}$ gives the distance from a point A lying on the curve $z_i = r_i(t)$ to a point B in the plane Q generated by the vectors $b_1, b_2, \ldots, b_m$. At any given instant t, the distance AB will be a minimum if the functions $u_i(t)$ are chosen according to (10). In this case $\rho(t) = y^2(t) = AB^2$ are calculated from Formula (12), while,

for the indicated choice of the control functions the quantity $\rho(t)$ will be a minimum. In order to use Theorem 3, we must calculate the greatest value of the function $\rho(t)$ for $t_0 \le t \le t_0+T$. This can obviously be done by elementary methods. In fact, since $\rho(t)=-[\mathbf{r}(t), \mathbf{y}(t)]$, where $\mathbf{r}(t)$ is the vector with projections $r_i(t)$ and $\mathbf{y}(t)$ is the vector with projections $y_i(t)$, we have $\rho(t)=-(\mathbf{r}, \mathbf{y})-(\mathbf{y}, \mathbf{r})$.

But, according to [6] (p. 205),

$$\mathbf{y}(t)=\frac{1}{\Gamma}\begin{vmatrix} (\mathbf{b}_1, \mathbf{b}_1), & \dots, & (\mathbf{b}_1, \mathbf{b}_m), & \mathbf{b}_1 \\ \dots & \dots & \dots & \dots \\ (\mathbf{b}_1, \mathbf{b}_m), & \dots, & (\mathbf{b}_m, \mathbf{b}_m), & \mathbf{b}_m \\ (\mathbf{b}_1, \mathbf{r}), & \dots, & (\mathbf{b}_m, \mathbf{r}), & \mathbf{r} \end{vmatrix}$$

$$\mathbf{y}(t)=\frac{1}{\Gamma}\begin{vmatrix} (\mathbf{b}_1, \mathbf{b}_1), & \dots, & (\mathbf{b}_1, \mathbf{b}_m), & \mathbf{b}_1 \\ \dots & \dots & \dots & \dots \\ (\mathbf{b}_1, \mathbf{b}_m), & \dots, & (\mathbf{b}_m, \mathbf{b}_m), & \mathbf{b}_m \\ (\mathbf{b}_1, \dot{\mathbf{r}}), & \dots, & (\mathbf{b}_m, \dot{\mathbf{r}}), & \dot{\mathbf{r}} \end{vmatrix} \qquad (18)$$

where $\Gamma=\Gamma(\mathbf{b}_1, \mathbf{b}_2, \dots, \mathbf{b}_m)$ is Gramme determinant for the vectors $\mathbf{b}_1, \mathbf{b}_2, \dots, \mathbf{b}_m$.

From (18) we see that

$$(\dot{\mathbf{y}}, \mathbf{r})=$$

$$=\frac{1}{\Gamma}\begin{vmatrix} (\mathbf{b}_1, \mathbf{b}_1), & \dots, & (\mathbf{b}_1, \mathbf{b}_m), & (\mathbf{b}_1, \mathbf{r}) \\ \dots & \dots & \dots & \dots \\ (\mathbf{b}_1, \mathbf{b}_m), & \dots, & (\mathbf{b}_m, \mathbf{b}_m), & (\mathbf{b}_m, \mathbf{r}) \\ (\mathbf{b}_1, \dot{\mathbf{r}}), & \dots, & (\mathbf{b}_m, \dot{\mathbf{r}}), & (\mathbf{r}, \dot{\mathbf{r}}) \end{vmatrix}=(\dot{\mathbf{r}}, \mathbf{y}).$$

A necessary condition for a maximum is therefore

$$(\dot{\mathbf{r}}, \mathbf{y})=0; \qquad (19)$$

and this condition is satisfied if $\dot{\mathbf{r}} \neq 0$, or if $\dot{\mathbf{r}}$ is orthogonal to $\mathbf{y}$. We will not consider the case $\mathbf{y}=0$, since in this case $y^2=\sum_{i=1}^{n} y_i^2=0$, and there is consequently no maximum.

To obtain a necessary condition, we introduce the parameter s, denoting the arc length of the curve $z_i = r_i(t)$. We have

$$\frac{1}{2}\frac{d\rho^2}{dt^2}=-(\ddot{\mathbf{r}}, \mathbf{y})-(\dot{\mathbf{r}}, \dot{\mathbf{y}})=$$

$$=-\left(\frac{d^2\mathbf{r}}{ds^2}\dot{s}^2+\frac{d\mathbf{r}}{ds}\ddot{s}, \mathbf{y}\right)-\Gamma(\mathbf{b}_1, \mathbf{b}_2, \dots, \mathbf{b}_m, \dot{\mathbf{r}}).$$

The equality $(\dot{\mathbf{r}}, \dot{\mathbf{y}})=\Gamma(\mathbf{b}_1, \mathbf{b}_2, \dots, \mathbf{b}_m, \dot{\mathbf{r}})$ is obtained directly from (18).

When we take into consideration that $\left(\frac{d\mathbf{r}}{ds}, \mathbf{y}\right)=0$, we can write the sufficient condition for a maximum in the form

$$\left(\frac{d^2\mathbf{r}}{ds^2}, \mathbf{y}\right)\dot{s}^2+\Gamma(\mathbf{b}_1, \mathbf{b}_2, \dots, \mathbf{b}_m, \dot{\mathbf{r}})>0. \qquad (20)$$

In order to find the greatest value of $\rho(t)$, we must calculate $\rho(t)$ at the points t_0 and t_0+T, and also at the maximum points, and choose the greatest value of $\rho(t)$ from these values.

3. The Approximate Trajectory in the Case $T=\infty$

We now consider the possibility of approximating to the given trajectory for an infinite time interval. We first of all set an upper limit to the absolute value of the elements of the fundamental matrix, and assume ([7], p. 366) that

$$|w_{ik}(t, \tau)|<Be^{-\alpha(t-\tau)} \qquad (i=1, 2, \dots, n, k=1, 2, \dots, n). \qquad (21)$$

This condition is equivalent to assuming that any solution of the system

$$\dot{x}_i=\sum_{k=1}^{n} a_{ik}(t)x_k \qquad (i=1, 2, \dots, n) \qquad (22)$$

satisfies the inequality

$$|x_i(t)| \le B\left(\sum_{k=1}^{n} x_k^2(t_0)\right)^{1/2} e^{-\alpha(t-t_0)}.$$

In fact, an arbitrary kth column $w_{1k}(t, \tau), w_{2k}(t, \tau), \dots, w_{nk}(t, \tau)$ of the matrix $\mathbf{W}(t, \tau)$ satisfies the system (22) if $w_{ik}(\tau, \tau)=0$ for $i \neq k$ and $w_{ii}(\tau, \tau)=1$.

The condition (21) is always satisfied if the matrix $\mathbf{A}(t)=\|a_{ik}\|$ is constant and its eigenvalues have negative real parts.

It follows from Theorems 1, 2, and 3, that when the conditions (21) are satisfied,

$$\|z\| \le B\left(\frac{n}{2\alpha}\int_{t_0}^{\infty} y^2(\tau)\,d\tau\right)^{1/2}, \qquad (23)$$

$$\|z\| \le B\sqrt{n}\int_{t_0}^{\infty} y(\tau)\,d\tau, \qquad (24)$$

$$\|z\| \le B\frac{\sqrt{n}}{\alpha}\sup_{t_0 \le t < \infty} y(t). \qquad (25)$$

It is obvious that in order that the solution of the system (4) be bounded, it is sufficient that one of the conditions

$$\int_{t_0}^{\infty} y^2(\tau)\,d\tau<\infty, \qquad (26)$$

$$\int_{t_0}^{\infty} y(\tau)\,d\tau < \infty, \tag{27}$$

$$\sup_{t_0<t<\infty} y(t) < \infty \tag{28}$$

be satisfied.

I. G. Malkin showed in [8] that it follows from the boundedness of all solutions of the system (2), for arbitrary $y_i(t)$ satisfying condition (28), that condition (21) is satisfied.

We now consider what conditions must be imposed on the functions $f_i(t)$ in order that the inequalities (26), (27), and (28) be satisfied when the control functions are chosen according to (10).

Since from (12) we have

$$y^2(t) = \frac{\Gamma(\mathbf{b}_1, \mathbf{b}_2, \ldots, \mathbf{b}_m, \mathbf{r}(t))}{\Gamma(\mathbf{b}_1, \mathbf{b}_2, \ldots, \mathbf{b}_m)},$$

these conditions must obviously have the form

$$\int_{t_0}^{\infty} \Gamma(\mathbf{b}_1, \mathbf{b}_2, \ldots, \mathbf{b}_m, \mathbf{r}(t))\,dt < \infty, \tag{26'}$$

$$\int_{t_0}^{\infty} \sqrt{\Gamma(\mathbf{b}_1, \mathbf{b}_2, \ldots, \mathbf{b}_m, \mathbf{r}(t))}\,dt < \infty, \tag{27'}$$

$$\sup_{t_0<t<\infty} \Gamma(\mathbf{b}_1, \mathbf{b}_2, \ldots, \mathbf{b}_m, \mathbf{r}(t)) < \infty. \tag{28'}$$

Here the vector function $\mathbf{r}(t)$ is given by formula (11). It is also easy to show that the choice of the system of control vectors according to [1] will be possible if the condition $\int_{t_0}^{\infty} r^2(t)\,dt < \infty$ is satisfied.

Conclusions

1. The choice of control functions according to (10) makes it possible to decrease not only the mean square deviation, but also the maximum deviation.

2. The values at any given instant of time of control functions chosen according to (10) do not depend on the length of the time interval over which the approximation is being made, or on the values of the control functions at any other instant of time.

3. The choice of control functions according to (10) yields the possibility of selecting an optimal system of control vectors by using the method described in Section 3 of [1].

4. The proposed method makes it possible to avoid difficulties in numerical calculation, and permits a simple geometric interpretation and the application of modelling for the solution of the problem.

5. The proposed method is most effective for small $\min\|y\|$, and when the conditions (21) are satisfied.

APPENDIX

Proof of Theorem 1. From the relation (6) we have

$$|z_i(t)| \leqslant \int_{t_0}^{t} w_i(t, \tau)\, y(\tau)\,d\tau, \tag{29}$$

and when we use the Bunyakovskii-Schwartz inequality, we obtain

$$|z_i(t)| \leqslant \left(\int_{t_0}^{t} w_i^2(t, \tau)\,d\tau\right)^{1/2}\left(\int_{t_0}^{t} y^2(\tau)\,d\tau\right)^{1/2} \leqslant$$

$$\leqslant \left(\int_{t_0}^{t} w_i^2(t, \tau)\,d\tau\right)^{1/2}\left(\int_{t_0}^{t_0+T} y^2(\tau)\,d\tau\right)^{1/2}. \tag{30}$$

This inequality becomes an equality when the function $y_k(\tau)$ has the form

$$y_k(\tau) = \frac{w_{ik}(t, \tau)}{w_i(t, \tau)} \quad \text{for} \quad 0 \leqslant \tau \leqslant t,$$

$$y_k(\tau) = 0 \quad \text{for} \quad t \leqslant \tau \leqslant t_0 + T.$$

From (30) we obtain

$$\max_{t_0<t<t_0+T} |z_i(t)| \leqslant \max_{t_0<t<t_0+T} \left(\int_{t_0}^{t} w_i^2(t, \tau)\,d\tau\right)^{1/2}\left(\int_{t_0}^{t_0+T} y^2(\tau)\,d\tau\right)^{1/2},$$

from which the formulas (7) and (8) follow.

Now let $a_{ik}(t)$ be constant; we will show that $F(t, t_0) = \int_{t_0}^{t} w_i^2(t, \tau)\,d\tau$ is a monotonically increasing function of t. Actually, in this case ([9], p. 173) we have $w_{ik}(t, \tau) = w_{ik}(t-\tau)$. If we let $t_0 < t_1 < t_2$, we can write

$$F(t_2, t_0) = \int_{t_0}^{t_2} w_i^2(t_2 - \tau)\,d\tau =$$

$$= \int_{t_0}^{t_0+t_2-t_1} w_i^2(t_2-\tau)\,d\tau + \int_{t_0+t_2-t_1}^{t_2} w_i^2(t_2-\tau)\,d\tau.$$

After the change of variable $\eta = \tau - t_2 + t_1$ in the second integral we have

$$F(t_2, t_0) = \int_{t_0}^{t_0+t_2-t_1} w_i^2(t_2-\tau)\,d\tau + \int_{t_0}^{t_1} w_i^2(t_1-\eta)\,d\eta =$$

$$= \int_{t_0}^{t_0+t_2-t_1} w_i^2(t_2-\tau)\,d\tau + F(t_1, t_0).$$

Since the first integral is positive, we obtain the desired result.

Formula (9) follows from the fact that $F(t, t_0)$, as a monotonically increasing function, attains its maximum for $t = t_0 + T$.

We note that in the case of variable $a_{ik}(t)$, the conclusion that $F(t, t_0)$ is increasing is no longer true. Similarly, consider the equation $\dot{z} = -\tan t\, z$. The general solution of this equation is $z = c \cos t$, $w(t, \tau) = \cos t / \cos \tau$, $F(t, 0) = \int_0^t w^2(t, \tau) d\tau = \frac{1}{2} \sin 2t$. The function $F(t, 0)$ is evidently not monotonic in the interval $-\frac{\pi}{2} + \epsilon < t < \frac{\pi}{2} - \epsilon$ if ϵ is sufficiently small.

Proof of Theorem 2. We conclude from the inequality (29) that

$$|z_i(t)| \leqslant \max_{0 \leqslant \tau \leqslant t} w_i(t, \tau) \int_{t_0}^{t} y(\tau)\, d\tau;$$

when we increase the upper limit of integration to $t_0 + T$, we obtain

$$|z_i(t)| \leqslant \max_{t_0 \leqslant \tau \leqslant t} w_i(t, \tau) \int_{t_0}^{t_0+T} y(\tau)\, d\tau,$$

and (14) follows.

We now consider the case when the eigenvalues of the matrix $\mathbf{A}(t) + \mathbf{A}^*(t)$ are nonpositive for all $t \geq t_0$. In this case, the quadratic form $\sum_{i,k=1}^{n} a_{ik}(t)\, x_i x_k$ will also be nonpositive. It is known ([9], p. 172) that the matrix $\mathbf{W}(t, \tau)$ is equal to $\mathbf{F}(t)\mathbf{F}^{-1}(\tau)$, where $\mathbf{F}(t)$ is the fundamental matrix of the system $\dot{x} = \mathbf{A}(t)x$. It is thus easy to obtain the relation

$$\frac{d\mathbf{W}}{d\tau} = -\mathbf{W}\mathbf{A}(\tau),$$

from which it follows that the rows $(w_{i1}, w_{i2}, \ldots, w_{in})$ of the matrix $\mathbf{W}(t, \tau)$ satisfy the system

$$\frac{dw_{ik}}{d\tau} = -\sum_{m=1}^{n} a_{mk}(\tau)\, w_{im} \qquad (k = 1, 2, \ldots, n).$$

Recalling that $w_i^2(t, \tau) = \sum_{k=1}^{n} w_{ik}^2(t, \tau)$, we have

$$\frac{d}{dt} w_i^2(t, \tau) = -2 \sum_{k=1}^{n} w_{ik} \sum_{m=1}^{n} a_{mk}(\tau)\, w_{im} =$$

$$= -2 \sum_{k,m=1}^{n} a_{mk}(\tau)\, w_{ik} w_{im} \geqslant 0,$$

according to the conditions of the theorem. Thus, $\max_{t_0 \leqslant \tau \leqslant t} w_i^2(t, \tau) = w_i^2(t, t) = 1$. It should be noted that the condition that the eigenvalues of the matrix $\mathbf{A}(t) + \mathbf{A}^*(t)$ be nonpositive can be replaced by the Sylvester criterion, or by a modification of this criterion ([6], p. 250).

Proof of Theorem 3. It follows from (29) that

$$|z_i(t)| \leqslant \int_{t_0}^{t} w_i(t, \tau)\, d\tau \max_{t_0 \leqslant \tau \leqslant t} y(\tau),$$

and so

$$\max_{t_0 \leqslant t \leqslant t_0+T} |z_i(t)| \leqslant \max_{t_0 \leqslant t \leqslant t_0+T} \int_{t_0}^{t} w_i(t, \tau)\, d\tau \max_{t_0 \leqslant \tau \leqslant t_0+T} y(\tau), \tag{31}$$

which yields

$$\|z\| \leqslant C \max_{t_0 \leqslant \tau \leqslant t_0+T} y(\tau),$$

where

$$C = \max_{i} \max_{t_0 \leqslant t \leqslant t_0+T} \int_{t_0}^{t} w_i(t, \tau)\, d\tau.$$

The fact that C is the least of the numbers satisfying the inequality follows, because the right-hand side of the inequality (31) is attained for

$$y_j(\tau) = \frac{w_{ij}(t, \tau)}{w_i(t, \tau)}.$$

Reasoning similar to that used in the proof of Theorem 1 can also be used to prove the validity of Formula (17).

Note. We will consider the relation (6) as the application of an operator $\mathbf{W}$, which transforms the vector function $y(t)$ into the vector function $z(t)$. In the present paper $z(t)$ is an element of the space $C_n(t_0, t_0 + T)$, in which the norm is defined by the formula $\|z\| = \max_i \max_{t_0 \leq t \leq t_0+T} |z_i(t)|$.

For each of the three theorems, the function $y(t)$ lies in a different space.

In the first theorem, $y(t)$ lies in the space $L_{2n}(t_0, t_0 + T)$ with the norm $\|y\| = \left(\int_{t_0}^{t_0+T} y^2(t)\, dt \right)^{1/2}$.

In the second theorem, $y(t)$ lies in the space $L_{1U}(t_0, t_0 + T)$ with norm $\|y\| = \int_{t_0}^{t_0+T} y(t)\, dt$, and in the third theorem $y(t)$ lies in the space $C_n'(t_0, t_0 + T)$ with norm

$$\|y\| = \max_{t_0 \leqslant t \leqslant t_0+T} y(t).$$

In the first and third theorems we calculate the norm of the operator **W**, i.e., the least value of the number A for which the inequality $\|z\| \le A\|y\|$ is valid.

We note that the problem concerning the accumulation of disturbances in an arbitrary trajectory is essentially the problem of determining the norm of the operator **W**.

Example. We consider the system of differential equations

$$\dot{x}_1 = -x_1 + b_1 u(t)$$
$$\dot{x}_2 = -3x_2 + b_2 u(t) \qquad (b_1^2 + b_2^2 = 1). \tag{32}$$

The fundamental matrix $\mathbf{W}(t, \tau)$ of the system $\dot{x}_1 = -x_1$, $\dot{x}_2 = -3x_2$ has the form

$$W(t, \tau) = \begin{vmatrix} e^{-(t-\tau)}, & 0 \\ 0, & e^{-3(t-\tau)} \end{vmatrix}$$

Let the curve $x_1 = e^{-2t}$, $x_2 = e^{-2t}$ be given. By choosing u(t), we will try to find an approximation to this curve in the interval $0 \le t \le T$. It follows from (11) that $r_1(t) = -e^{-2t}$, $r_2(t) = e^{-2t}$. The system (10) yields $u(t) = e^{-2t}(b_2 - b_1)$. By using the formulas in (12) we obtain

$$y^2(t) = e^{-4t}[2 - (b_2 - b_1)^2],$$

and from (13),

$$H^2 = \int_0^T y^2(\tau)\, d\tau = \frac{2 - (b_2 - b_1)^2}{4}(1 - e^{-4T}).$$

In order to use Theorem 1, we must calculate the number M from (9). We have

$$M_1^2 = \int_0^T e^{-2(T-\tau)} d\tau = \frac{1}{2}(1 - e^{-2T}),$$

$$M_2^2 = \int_0^T e^{-6(T-\tau)}\, d\tau = \frac{1}{6}(1 - e^{-6T}),$$

and so

$$M = \max\left(\sqrt{\frac{1}{2}(1 - e^{-2T})},\ \sqrt{\frac{1}{6}(1 - e^{-6T})}\right).$$

We thus have $\|z\| \le MH$, and for $T = \infty$ we have

$$\|z\| \le \frac{\sqrt{2(b_2 - b_1)^2}}{2\sqrt{2}}.$$

If we now carry out the analysis according to Section 3 of [1], or if we investigate directly the result we have obtained, we can verify that for $b_1 = \sqrt{2}/2$, and $b_2 = -\sqrt{2}/2$, we can obtain an accurate representation of the given trajectory.

We now consider the method of estimation of Section 2 of the present paper. According to Theorem 2 we have N = 1.

On the other hand,

$$H_1 = \int_0^T y(\tau)\, d\tau =$$

$$= \int_0^T e^{-2t}\sqrt{2 - (b_2 - b_1)^2}\, dt = \frac{\sqrt{2 - (b_2 - b_1)^2}}{2}(1 - e^{-2T}).$$

From Theorem 2 we obtain

$$\|z\| \le NH_1 = \frac{\sqrt{2 - (b_2 - b_1)^2}}{2}(1 - e^{-2T})$$

and from $T = \infty$

$$\|z\| \le \frac{\sqrt{2 - (b_2 - b_1)^2}}{2}.$$

In order to apply the result of the third theorem, we calculate

$$C = \max\left\{\int_0^T e^{-(T-\tau)} d\tau,\ \int_0^T e^{-3(T-\tau)}\, d\tau\right\} =$$

$$= \max\left\{1 - e^{-T},\ \frac{1}{3}(1 - e^{-3T})\right\}.$$

Moreover,

$$\max_{0 \le t \le T} y(t) = \sqrt{2 - (b_2 - b_1)^2}.$$

Thus, according to (15), we obtain

$$\|z\| \le C\sqrt{2 - (b_2 - b_1)^2}$$

and for $T = \infty$

$$\|z\| \le \sqrt{2 - (b_2 - b_1)^2}.$$

As we can see, for $T = \infty$ the best estimate of $\|z\|$ is obtained from Theorem 1, and the worst from Theorem 3.

LITERATURE CITED

1. E. A. Barbashin, "An estimate of the mean square deviation from a trajectory," Avtomatika i Telemekhanika 21, No. 7 (1960).*
2. R. Bellman, "Notes on Control Process. 1. On the minimum of maximum deviation," Quarterly Appl. Math. 14 (1957).

* See English translation.

3. B. V. Bulgakov, "The accumulation of disturbances in linear oscillating systems with constant parameters," Doklady Akad. Nauk SSSR 51, No. 5 (1946).
4. B. V. Bulgakov and N. T. Kuzovkov, "The accumulation of disturbances in linear systems with variable parameters," Priklad. Matem. i Mekh. 14, No. 1 (1950).
5. J. L. Massera and J. J. Schäffer, "Linear differential equations and functional analysis," Ann. of Math. 67, No. 3 (1958).
6. F. R. Gantmakher, The Theory of Matrices [in Russian] (Gostekhizdat, 1950).
7. I. G. Malkin, The Theory of the Stability of Motion [in Russian] (Gostekhizdat, 1957).
8. I. G. Malkin, "A first approximation to stability," Coll.: Scientific Proceeding of the Kazan' Inst. of Aviation [in Russian] (1936) No. 3.
9. V. V. Nemytskii and V. V. Stepanov, The Qualitative Theory of Differential Equations [in Russian] (Gostekhizdat, 1949).

ON THE STABILITY OF AN AILERON CONTROL SYSTEM DISTURBED BY TURBULENCE

P. S. Landa and S. P. Strelkov

Moscow

Translated from Avtomatika i Telemekhanika, Vol. 21, No. 10,
pp. 1352-1364, October, 1960
Original article submitted February 22, 1960

The stable modes of an airplane wing are found with an analog computer for the case where there are no nonlinear elements in the aileron control system. It is shown that the presence in the control circuit of a gap in certain parameters leads to the excitation of hard oscillations in the system. The probability of exciting growing wing oscillations over a given period of time in which the air flow is turbulent is calculated.

An airplane wing in flight is a complex nonuniform oscillatory system with distributed parameters. An accurate solution of the wing stability problem is practically impossible, even with the help of modern computers. At present, only approximate methods are known for solving this problem to one or another degree of accuracy.

Replacement of the nonuniform distributed oscillatory system with a simplified lumped-parameter system, described by a finite number of ordinary differential equations, is the basis of all the approximate methods.

One of the most widely used replacement methods is the method of [1], which is derived from the work of Raleigh and Pitts, and has been developed further by Bubnov and Galerkin.

In the application of the Bubnov-Galerkin method to the simplest, but one of the most practically important cases, the airplane wing, in a steady flow of air, can be considered as an oscillatory system with two degrees of freedom, in which certain parameters depend on the flow velocity. This paper is devoted to a study of the oscillations and the stability of such a system when nonlinear elements and statistical influences caused by the turbulent state of the atmosphere have a substantial effect.

In the majority of works in which the flutter of a wing with an aileron is examined (see, for example, [2-4]), the system is assumed to be linear, and the aileron control stick to be either fixed or free. In actual systems, there are always nonlinear elements as a result of gaps, dry friction, etc. Therefore, it is quite interesting to analyze those cases in which the presence of these nonlinear elements cannot be overlooked because they can have a substantial effect,not only on the character of the movement, but also on the stability of the different states of movement. An example of such an effect was computed in [5].

Nonlinear flutter problems, like all problems of this type, can be solved analytically in an approximate manner by means of the harmonic linearization method (Krylov-Bogolyubov method),if it is known that nearly harmonic modes of oscillation predominate in the system. The Krylov-Bogolyubov method, as it applies to nonlinear flutter problems, is examined, for example, in [7]. The use of a mathematical analog for studying airplane wing flutter is presented in [4, 5, 6], and oscillatory systems with nonlinear hardness are examined in the latter two.

The influence of turbulence on an airplane was also examined in a number of papers (for example, in [8]). In these papers, the airplane was represented as a linear oscillatory system, and the problem was solved by the ordinary theory of stationary random processes in linear systems.

The presence of nonlinear elements in a system can lead to the appearance of periodic modes (both stable and unstable), with which linear theory cannot deal. The existence of unstable periodic modes corresponding to unstable limited cycles means that the excitation of hard oscillations in the system is possible. The latter case is especially interesting, both theoretically and practically.

In this case, the airplane can indeed fly safely only in quiet air, since dangerous oscillations of the wings cannot arise in the absence of disturbance (the system is stable in the presence of small oscillations). If random jolts, caused by atmospheric turbulence, act on the wing, dangerous growing oscillations can appear after some time. Therefore, the statistical evaluation of the probability of such oscillations arising over a given period of time is an important problem, whose solution will be presented later.

An approximate analytic solution of this problem for an airplane wing with an aileron is possible under

the condition that the oscillations in the system are nearly harmonic, that is, the complex system being examined can be replaced with some equivalent oscillatory system with one degree of freedom, whose spectral characteristic approximates that of the whole system in the region of the most important frequencies. Then the Fokker–Planck equation can be used to solve the problem in a way analogous to that done in [9, 10]. However, there is quite an amount of computation even with the simplifications mentioned, and the study of the system is exceedingly complicated over the whole range of the parameters $\underline{v}$ and $\underline{n}$, where $\underline{v}$ is the flight velocity, and $\underline{n}$ is the relative frequency of the rotary aileron oscillations. Therefore, the limits of the modes interesting to us were first determined by an analog method, and then the amplitudes of the limited cycles and the excitation probabilities were calculated for the values of the parameters obtained.

1. Basic Equations of the Bending Oscillations of a Wing with an Aileron

The Bubnov–Galerkin method gives the following equations for bending-aileron oscillations of a cantilever wing (Fig. 1):

$$M\ddot{h} + S_\beta\ddot{\beta} + M\omega_h^2 h = F_1(h, \dot{h}, \beta, \dot{\beta}, v) + F_2(v, t),$$

$$S_\beta\ddot{h} + I_\beta\ddot{\beta} + I_\beta\omega_\beta^2\beta = M_1(h, \dot{h}, \beta, \dot{\beta}, v) + M_2(v, t), \quad (1)$$

where M, I_β, S_β, ω_h, and ω_β are the average parameters of the wing and aileron, respectively, characterizing the wing mass, moment of inertia and static moment of the aileron, the natural frequency of wing bending oscillations, and the natural frequency of aileron rotary oscillations, determined by the elasticity of the control levers and cables; F_1 and M_1 are the average aerodynamic force and moment acting on the wing and aileron which are moving in air with a velocity $\underline{v}$; F_2 and M_2 are the random aerodynamic force and moment caused by the turbulent disturbances of the vertical component of flight velocity.

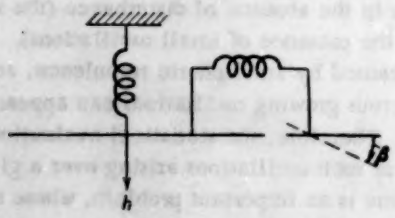

Fig. 1. Equivalent diagram of the bending oscillations of a wing with an aileron.

According to the theory based on the hypothesis of stationariness (see [11]), these aerodynamic forces and moments are expressed in the following manner:

$$F_1 = \pi\rho b^3 L\left\{-\frac{2v}{b}\frac{\dot{h}}{b} - \frac{L_a}{L}\alpha\frac{v}{b}\dot{\beta} - \frac{L_a}{L}\gamma\frac{v^2}{b^2}\beta\right\},$$

$$F_2 = 2\pi\rho Lbvu,$$

$$M_1 = \pi\rho b^4 L_a\left\{-\delta\frac{v}{b}\frac{\dot{h}}{b} - \zeta\frac{v}{b}\dot{\beta} - \varepsilon\frac{v^2}{b^2}\beta\right\},$$

$$M_2 = \pi\rho b^2 L_a\delta vu,$$

where ρ is the air density at the given altitude; L, the wing span; L_a, the aileron span; $\underline{b}$, the semichord of the wing; $\underline{v}$, the horizontal flight velocity; $\underline{u}$, the random vertical velocity appearing as a result of the turbulent state of the atmosphere; α, γ, δ, ζ, ϵ–coefficients which depend on the wing geometry.

The numerical values of the parameters basically correspond to the example given in [3]:

$$M = 38.3 \text{ kg}; \quad I_\beta = 0.0529 \text{ kgm}^2; \quad S_\beta = 0.175 \text{ kgm};$$

$$\omega_h = 30 \text{ rad/sec}; \quad L = 4.24 \text{ m}; \quad L_a = 1{,}9 \text{ m};$$

$$b = 0.762 \text{ m}; \quad \pi\rho = 3.105 \text{ kg/m}^3; \quad \alpha = 0.3458;$$

$$\gamma = 1.088; \quad \delta = 0{,}007; \quad \zeta = 0.0117; \quad \varepsilon = 0.0104.$$

For convenience in analysis we will introduce the dimensionless coordinates, velocity and time:

$$x = \frac{h}{b}, \quad y = \beta, \quad \bar{v} = \frac{v}{\omega_h b}, \quad \tau = \omega_h t.$$

Then Eq. (1) can be written in the form

$$\frac{d^2x}{d\tau^2} + x + a_{11}\bar{v}\frac{dx}{d\tau} + a_{12}\bar{v}^2 y + a_{13}\bar{v}\frac{dy}{d\tau} + a_{14}\frac{d^2y}{d\tau^2} = f_1(\tau), \quad \frac{d^2y}{d\tau^2} + n^2 y + a_{21}\bar{v}^2 y + a_{22}\bar{v}\frac{dy}{d\tau} + a_{23}\bar{v}\frac{dx}{d\tau} + a_{24}\frac{d^2x}{d\tau^2} = f_2(\tau), \quad (2)$$

where

$$n = \frac{\omega_\beta}{\omega_h}, \quad f_1(\tau) = \frac{1}{\omega_h^2 bM}F_2\left(\frac{\tau}{\omega_h}\right),$$

$$f_2(\tau) = \frac{1}{\omega_h^2 I_\beta}M_2\left(\frac{\tau}{\omega_h}\right).$$

The random functions $f_1(\tau)$ and $f_2(\tau)$ can be considered stationary and normal random processes which can be characterized sufficiently by giving their spectral densities, which, in their turn, are completely determined by the spectral density of the vertical component of turbulent air velocity u.*

*We will neglect the effect of fluctuations in the horizontal velocity, since they are significantly less than the flight velocity.

A graph of the spatial spectrum of the turbulence, given in [8], can be used to compute the spectral density of the random quantity u. As emphasized in this work, the values of spectral density shown on the graph are very approximate, since they depend strongly on the meteorological conditions, the local terrain, and the flight altitude. For example, the intensity of the turbulence increases sharply during a storm, and may differ from the value given on the graph by orders of magnitude.

2. Basic Equations of the Bending Oscillations of a Wing with the Aileron Controlled by a Hydraulic Amplifier

The presence of special aileron control mechanisms has a substantial effect on the oscillations of the entire system. Let us examine the schematic diagram of a hydraulic amplifier aileron control as shown in Fig. 2. The dotted lines designate a parasitic feedback path between the movement of the wing and system of aileron control levers and cables, and the hydraulic amplifier. Moreover, we will assume that a gap 2 can exist in the piston valve control system of the hydraulic amplifier 1. The deflection of the piston valve is composed of the displacement given by the pilot [the "controlling input" q(t)], and some additional displacement κh, due to the parasitic feedback loop and caused by the effect of wing oscillations on the aileron control drive. For simplicity, we will consider κh to be proportional to the vertical displacement of the wing h. The quantity κ will be called the feedback coefficient.

In the analysis, we will assume that the controlling input to the piston valve is constant, or that it changes very slowly in comparison to the oscillation period of the wing. Moreover, we will assume that the feedback coefficient κ can have only two values: +1 and −1.

If we limit ourselves to the linear portion of the servomotor characteristic, the oscillations in the system containing the hydraulic amplifier, for the case when the pilot exerts no controlling action, are described by the equations

$$\begin{aligned}
&\frac{d^2x}{d\tau^2} + x + a_{11}\bar{v}\frac{dx}{d\tau} + a_{13}\bar{v}^2 y + \\
&+ a_{13}\bar{v}\frac{dy}{d\tau} + a_{14}\frac{d^2y}{d\tau^2} = f_1(\tau), \\
&\frac{d^2y}{d\tau^2} + n^2(y - a_4 z) + a_{21}\bar{v}^2 y + a_{22}\bar{v}\frac{dy}{d\tau} + \\
&+ a_{23}\bar{v}\frac{dx}{d\tau} + a_{24}\frac{d^2x}{d\tau^2} = f_2(\tau), \quad \frac{dz}{d\tau} = a_3[\varphi(\varkappa x) - z].
\end{aligned} \tag{3}$$

Here, $z = r/b$ is the dimensionless coordinate of the servomotor shaft displacement 3, and the function $\varphi(\kappa x)$ determines the dependence between the displacements of the elements on the other side of the gap. Let us suppose that the gap size a can fluctuate within the limits $a = 0-0.01$. The coefficients a_3 and a_4 are, respectively, equal to 2 and 3. The remaining coefficients are determined by the parameters of the wing and aileron given above.

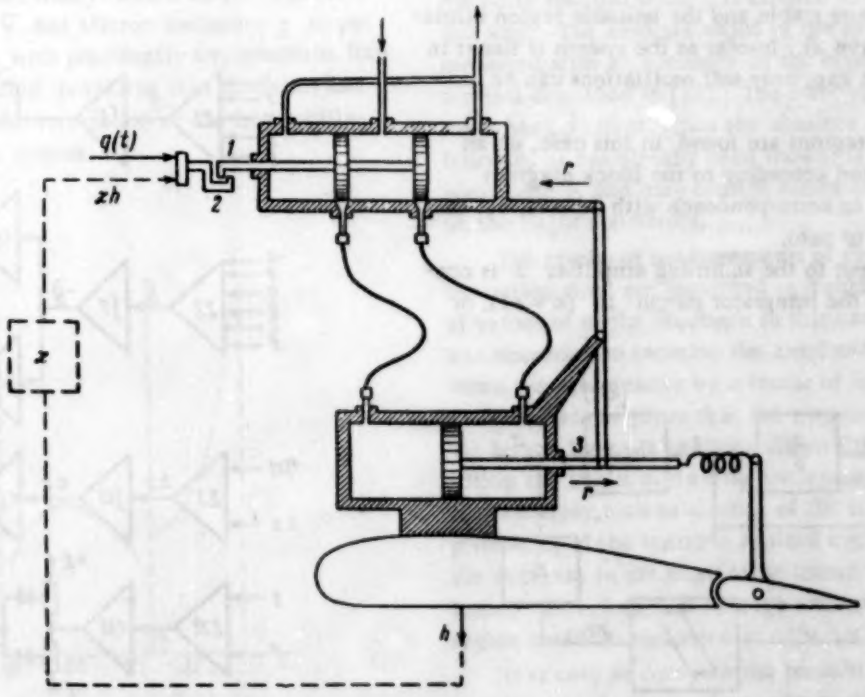

Fig. 2.

A block diagram of the system described by Eqs.(3) is shown in Fig. 3. The block with the transfer function $Y(p)$ includes the wing and the aileron, that is, it represents an oscillatory system with two degrees of freedom; $\xi(t)$ designates the turbulent input to the system.

3. Determining the Stable Regions of the System in the Absence of Random Disturbances

As has already been shown, at first, an electronic analog of the system is studied on a type MN-7 analog computer.

In order to check the correctness of the analog, and to clarify the effect of the servomotor on system stability, a curve was taken of the dependence of the critical speed of the plane, at which flutter arises, on the relative aileron frequency $\underline{n}$ with the aileron control stick fixed. In this case, the system is described by Eqs. (2), without the terms on the right.

The stable region is located outside the curve shown in Fig. 4 by the dashed line. The results agree with the data in [2-4].

If the control stick is not fixed, the unstable region changes substantially, due to the presence of parasitic feedback in the system. We note that the concept of an unstable region independent of the oscillation amplitude has meaning only for a linear system. Therefore, let us first examine how the unstable region changes in the case when there is no gap in the aileron control system. It appears that the unstable region expands (Fig. 4, curve 1) if the feedback is positive, which corresponds to $\kappa = +1$, but if the feedback is negative ($\kappa = -1$), the system becomes more stable, and the unstable region diminishes (Fig. 4, curve 2). Insofar as the system is linear in the absence of a gap, only soft oscillations can be excited in it.

The stable regions are found, in this case, on an analog constructed according to the block diagram shown in Fig. 5, in correspondence with Eqs. (3), but the gap is set equal to zero.

The first input to the summing amplifier 2 is connected either to the integrator output 15 ($\kappa = +1$), or to the inverter output 11 ($\kappa = -1$), depending on the sign of the feedback.

The presence of a gap makes it possible for hard oscillations to be excited in the system being analyzed, and for stable limited cycles to appear.

The performance of the system was studied as a function of the aileron relative frequency $\underline{n}$ for a fixed flight velocity, $\bar{v} = 0.8$. The following phenomena were observed: Soft oscillations were excited in the system when $n_1 \le n \le n_2$, which corresponds to an unstable region if the aileron control stick is fixed. If positive feedback existed, the oscillations grew toward infinity, but a

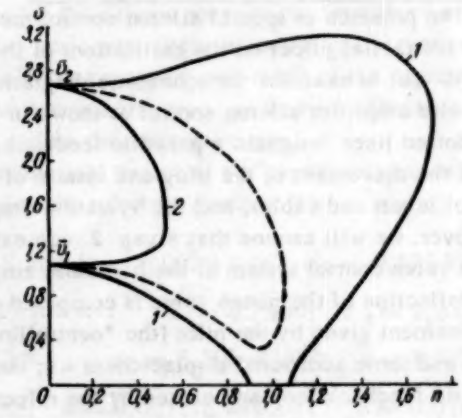

Fig. 4. Graph of the stable regions of the system.

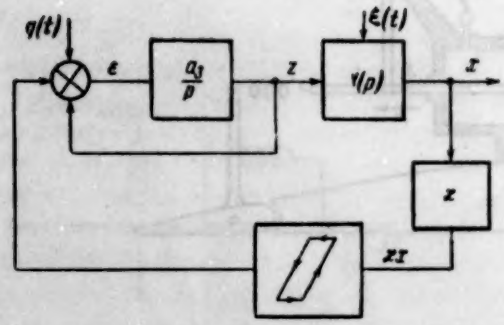

Fig. 3. Block diagram of the wing-aileron-hydraulic-amplifier system.

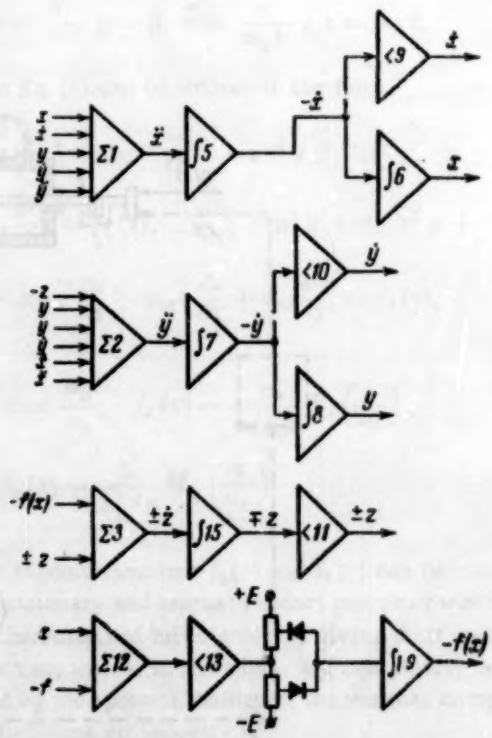

Fig. 5. Block diagram of an analog of the wing-aileron-hydraulic-amplifier system.

stable limited cycle, whose amplitude $A_{x\,ex}$ varied as a function of $\underline{n}$, appeared if the feedback was negative; this is shown in Fig. 6 by the solid line. The system is stable for all other values of $\underline{n}$, if the feedback is negative. If the feedback is positive, then for $n_1' \leq n \leq n_1$ and $n_2 \leq n \leq n_2'$, where n_1' and n_2' correspond to the limits of stability in the absence of a gap, hard oscillations are excited in the system. The dashed lines in Fig. 6 show the amplitude of the minimum initial disturbance, which must be imparted to the wing so that it can accomplish unattenuated oscillations, as a function of $\underline{n}$.

It is evident that this quantity characterizes the amplitude of the unstable limited cycle.

4. Measuring the Probability of System Excitation in the Presence of Turbulence

The same method as in [12] was used to measure the probability of system excitation as a function of time (for given parameters and amplitude of the fluctuating disturbances). For the same set of parameters, up to fifty time intervals were measured during which the system remained unexcited. The average excitation time τ_{av}' and probability $p(\tau)$ that the system will be excited at time $\tau' \geq \tau$ were computed from these measurements.

Strictly speaking, the noise of the special generator fed to the analog must have a spectrum similar to that of the turbulence. However, the spectral components of the noise in a narrow band near the free oscillation frequency of the system play the main role in system excitation. If the free oscillation frequency did not depend on the amplitude, then it would be possible for a fixed flight velocity $\overline{v}$ and aileron frequency $\underline{n}$ to put a random input $\xi(\tau)$, with practically any spectrum, into the system being studied, providing that spectrum had the same density as the turbulence at the free oscillation frequency of the system, ω_0'.

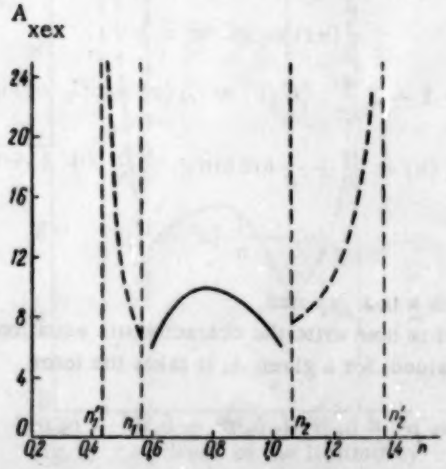

Fig. 6. Limited cycle amplitude as a function of the aileron relative frequency (experimental curves).

In reality, a weak dependence of the free oscillation frequency on the amplitude is observed in the nonlinear system being analyzed. This can be seen, for example, from Table 1, in which the oscillation frequencies measured at different wing displacements are shown for a number of values of $\underline{n}$.

Here the following designations are introduced: $\omega(0)$ is the system oscillation frequency corresponding to very small amplitudes; $\omega(A_1)$ is the oscillation frequency near an unstable limited cycle having an amplitude A_1; $\omega(\infty)$ is the frequency corresponding to very large amplitudes.

In view of the weak dependence of the oscillation frequency on the amplitude, and, consequently, the comparatively small change in the spectral density of the noise as the amplitude varies, noise having a uniform spectrum in the region of the system operating frequency, and whose spectral density agrees with that of the actual disturbance at some average frequency $S_{\ddot{u}\,av}'$, can be put into the system. The amplitude of this average spectral density as a function of $\underline{n}$ is also shown in Table 1. It is evident that the spectral density of the noise fed into the system must be varied in correspondence with the data of Table 1, as the relative aileron frequency $\underline{n}$ changes. In practice, this spectral density change is accomplished in the following manner. The signal from an ultralow-frequency noise generator (see [12]) is fed into the analog through one of the amplifiers whose amplification factor is varied as $\underline{n}$ changes in correspondence with the change in spectral density. An adequately accurate relation between the amplitudes of the noise spectral density is ensured as $\underline{n}$ changes, in this way. The absolute value of the spectral density is measured with an accuracy on the order of 25% by the method described in [12]. The error in this measurement has no effect, since the absolute value of the turbulence, as has already been shown, is given very approximately, and may change substantially, depending on the flight conditions.

The results of measurements of the average system excitation time are presented in Table 1 for a number of values of $\underline{n}$; the feedback in this case is positive. It was necessary to increase the amplitude of the turbulence spectral density by a factor of four in comparison with the data of [8] so that the measurement time would not be too long. It has been shown that as $\underline{n}$ increases within the limits $n_2 \leq n \leq n_2'$, the average excitation time grows sharply, both as a result of the increase in the amplitude A_1 of the unstable limited cycle, and because of the decrease in the equivalent intensity of the turbulence. Therefore, the average excitation time in this region could be measured at only one value, $n = 1.1$.

It is easy to compute the probability of system excitation as a function of time from the data obtained in measuring the average time. The results of the calculations for the case when $n = 0.55$ are shown as a graph in

TABLE 1

n	$10^5 A_1$	$\omega(0)$	$\omega(A_1)$	$\omega(\infty)$	$10^3 S'_{u\,av}$	τ'_{av}
0.5	2.10	0.888	0.871	0.873	5.72	180
0.55	1.44	0.892	0.892	0.891	5.56	132
1.1	1.74	1.125	1.100	1.105	3.82	334
1.2	2.20	1.188	1.123	1.155	3.53	—
1.3	3.60	1.295	1.162	1.221	3.06	—

Fig. 7. The exponential function $\exp(-\tau/\tau_{av})$ is shown by dashed lines on the same figure. It can be seen from the graph that the distribution observed does not have the exponential form predicted by theory for the excitation probability $p(\tau)$ in the case of sufficiently low noise. This difference can be explained by the fact that the noise acting on the system is high, so that the time that the mapping point spends in the phase space near the boundaries of excitation is comparable with its average dwell time in the region of the unexcited states.

One can conclude from this that the methods for theoretically computing the excitation probability, described in [9, 10] for the case of low noise, do not give accurate quantitative results. However, with the aid of these methods, one can obtain a theoretical estimate of the order of the average system excitation time, and this has practical value.

5. Theoretical Calculation of Airplane Wing Stability in the Presence of Turbulence

It has already been indicated that an analytic solution of the stability problem of a complex system affected by fluctuations is possible if certain restrictions are imposed on the system parameters, namely, oscillation in the system must be nearly harmonic. The results of studies on analogs have shown that this requirement is met sufficiently well over a wide range of change in the parameters.

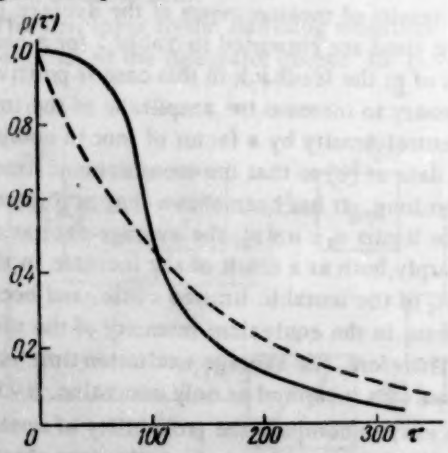

Fig. 7. Probability of system excitation for $n = 0.55$.

The idea of the method presented in this paper is as follows. The restriction mentioned above means that the solution of Eqs. (3) must be put in the form of almost harmonic oscillations with slowly changing amplitudes:

$$x = A\cos\omega\tau,\ y = B\cos(\omega\tau + \varphi_1),$$

$$z = C\cos(\omega\tau + \varphi_2).$$

Then Eqs. (3) can be linearized in the ordinary manner by using the harmonic linearization method (the Krylov–Bogolyubov method). We obtain an equivalent linear set of equations as a result, and their coefficients depend on the amplitude of the wing oscillations A. In operational form, this linearized set of equations is

$$\begin{aligned}
&(p^2 + a_{11}\bar{v}p + 1)\,x + \\
&+\ (a_{14}p^2 + a_{13}\bar{v}p + a_{12}\bar{v}^2)\,y = f_1(\tau), \\
&(a_{24}p^2 + a_{23}\bar{v}p)\,x + \\
&+\ (p^2 + a_{22}\bar{v}p + a_{21}\bar{v}^2 + n^2)\,y - a_4 n^2 z = f_2(\tau), \\
&-a_3\varkappa C(u)\,x + (p + a_3)\,z = 0,
\end{aligned} \tag{4}$$

where $C(u)$ is determined from the function $\varphi(\kappa x) = \varphi(\kappa A\cos\omega\tau)$ expressed as a complex Fourier series:

$$\varphi(\varkappa x) = \varkappa C(u)\,x + \ldots.$$

$$u = 1 - 2\frac{a}{A},\quad C(u) = C_1(u) + jC_2(u)\operatorname{sign}\omega,$$

$$C_1(u) = \frac{1}{2} + \frac{1}{\pi}\arcsin u + \frac{1}{\pi}u\sqrt{1-u^2},$$

$$C_2(u) = \frac{1}{\pi}(u^2 - 1);$$

the term a is a gap size.

Let us now write the characteristic equation for the set obtained, for a given A; it takes the form

$$L(p) = p^5 + b_1 p^4 + b_2 p^3 + b_3 p^2 + b_4 p + b_5 = 0. \tag{5}$$

Equation (5) is an algebraic equation with complex coefficients. Since the coefficients of the equation

specifically depend on the sign of ω, the roots of this equation must be complex conjugates of the form $p = -\delta(u) \pm j\omega(u)$. Therefore, one need only find the solution of Eq. (5) for positive values of ω, for example.

Let us investigate the behavior of the characteristic equation roots as a function of the relative aileron frequency $\underline{n}$ at a fixed flight velocity, $\bar{v} = 0.8$.

Let us assume that

$$p = -\delta(u) + j\omega_0 + j\omega_1(u) \qquad (6)$$

for finding an approximate solution of Eq. (5); we will define ω_0 so that when $p = j\omega_0$, the modulus of $L(p)$ will be maximum. Since the system has been assumed to be narrow-band, the following inequalities must be satisfied: $\delta(u) \ll \omega_0$, and $\omega_1(u) \ll \omega_0$.

Computation and experimental data show that ω_0 differs little from unity at all values of relative aileron frequency $\underline{n}$, and at any amplitudes which are of interest to us. Therefore, we can say that $\omega_0 = 1$.

By substituting expression (6) into Eq. (5), and restricting ourselves to terms of the first order of smallness relative to δ and ω_1, we get the linear set of equations which determine $\delta(u)$ and $\omega_1(u)$.

An analysis of the behavior of the attenuation coefficient $\delta(u)$ as a function of $\underline{n}$ gives results which qualitatively agree with experimental data.

For $n_1 \leq n \leq n_2$, the system is unstable, no matter how small the amplitudes, and the oscillations jump toward infinity if there is positive feedback. However, a stable limited cycle exists if there is negative feedback. The boundaries of the unstable region, n_1 and n_2, are determined from the equation

$$\delta(u)\big|_{u=-1} = 0.$$

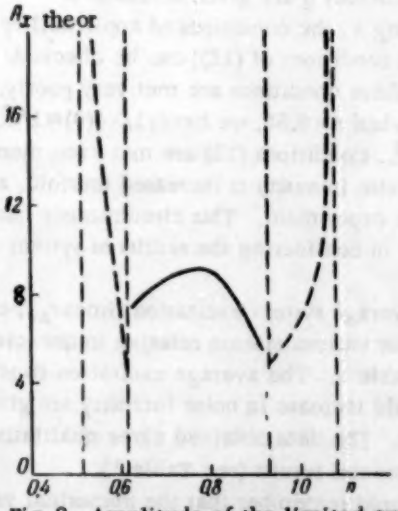

Fig. 8. Amplitude of the limited cycles as a function of relative aileron frequency (theoretical curves).

The solution of this equation gives $n_1 = 0.612$, $n_2 = 0.930$, which differs numerically somewhat from the data obtained from the analog ($n_1 = 0.565$, $n_2 = 1.06$). This difference can be explained by the inaccurate correspondence between the analog system parameters and the equation being investigated, and also by the approximateness of the theoretical calculations.

For the case of negative feedback, the amplitude of the stable limited cycle can be computed as a function of $\underline{n}$ over the range of values obtained for $\underline{n}$, by setting $\delta(u)$ equal to zero for a fixed $\underline{n}$.

The results of such a computation of the stable limited cycle amplitude are shown in the graph (Fig. 8, solid line).

The range of $\underline{n}$ over which the system will have hard excitation is determined from the equation

$$\delta(u)\big|_{u=1} = 0. \qquad (7)$$

By solving this equation, one can see that hard excitation of the system is possible only if the feedback is positive, for the values of system parameters which we have chosen. It should be mentioned here that the system may have hard oscillations for other parametric values even if the feedback is negative.

The solution of Eq. (7) is $n_1' = 0.514$, $n_2' = 1.08$, for $\kappa = 1$. Consequently, the hard oscillation mode occurs when $\underline{n}$ has values which satisfy the inequalities: $n_1' \leq n \leq n_1$ and $n_2 \leq n \leq n_2'$.

Setting $\delta(u)$ equal to zero for a fixed $\underline{n}$, we can find the dependence of the unstable limited cycle amplitude A_1 on $\underline{n}$, graphically. The results of these calculations are shown on the graph (Fig. 8, dashed lines) to a scale appropriate for the experiment, and are also given in Table 2. A knowledge of the unstable limited cycle amplitude is necessary for calculating the average excitation time of the system.

The oscillations in a complex system (3) are the sum of two "natural" oscillations whose frequency and attenuation decrement are a function of amplitude. Bending oscillations of the wing predominate in one of these oscillations, and rotary oscillations of the aileron in the other. It appears that the first "natural" oscillation attenuates very slowly, whereas the second attenuates much more rapidly. Therefore, the approximately linearized oscillatory system with two degrees of freedom (4) can be replaced by a certain equivalent oscillatory system with one degree of freedom, whose oscillations are nearly the same as the bending oscillations of the wing, that is, they have the same frequency and attenuation decrement.

We get an approximate equation describing the wing oscillations as a result of this replacement:

$$(p^2 + 2\delta p + \omega^2)\, x = \omega^2 \zeta(\tau), \qquad (8)$$

TABLE 2

n	$10^2 A_1$	$\omega(0)$	$\omega(A_1)$	$10^2\,\delta(0)$	$10^3 Su_{av}$	$10^3\lambda^{-1}$	τ_{av}	τ'_{av}
0.55	3.23	0.95	0.93	1.24	5.17	1.05	10^{14}	$5\cdot10^{4}$
0.6	1.39	0.96	0.94	0.29	5.06	0.97	1500	470
0.95	1.10	1.13	1.12	1.22	3.76	0.63	$6\cdot10^{5}$	400
1.0	1.41	1.15	1.13	4.83	3.67	0.71	$2\cdot10^{21}$	$9\cdot10^{5}$
1.05	1.96	1.15	1.16	8.76	3.55	0.81	$5\cdot10^{42}$	$4\cdot10^{11}$

where $\zeta(\tau)$ is the equivalent noise, whose intensity depends on the amplitude of the oscillations A, in the general case.

Now the Fokker–Planck equation can be used if the noise correlation time τ_{cor} is short in comparison to the system time constant, which is about $1/\delta$, and the noise intensity is small enough so that the following conditions are met:

$$\langle\zeta\zeta^*\rangle^{1/2} \ll A_1 \text{ for } \tau_{cor} \geqslant \frac{2\pi}{\omega}\,^{\dagger},$$
$$[\omega S(\omega)]^{1/2} \ll A_1 \text{ for } \tau_{cor} < \frac{2\pi}{\omega}, \qquad (9)$$

where $S(\omega)$ is half the spectral density of $\zeta(\tau)$ at the frequency ω.

Setting $x = Ae^{j(\omega\tau+\varphi)}$, $\dot{x} = Aj\omega e^{j(\omega\tau+\varphi)}$ and substituting them in Eq. (8), we get a shorter equation for A in the usual manner (see [10]):

$$\dot{A} = \frac{1}{2j\omega} e^{-j(\omega\tau+\varphi)}(p^2+\omega^2)x =$$
$$= -A\delta(A) + \frac{1}{\lambda A} + \zeta'(\tau), \qquad (10)$$

where $\zeta'(\tau)$ is the equivalent white noise having a correlation function $K(t) = 2\lambda^{-1}\delta(t)$, and $\lambda^{-1} = \frac{\omega^2}{4} S(\omega)$. Since the oscillation frequency depends on the amplitude, the intensity of the equivalent noise will also depend on amplitude.

The Fokker–Planck equation takes the following form in the given case:

$$\frac{\partial w}{\partial \tau} = -\frac{\partial}{\partial A}\left\{\left[-A\delta(A) + \frac{1}{\lambda A}\right]w\right\} + \frac{\partial^2}{\partial A^2}(\lambda^{-1}w). \qquad (11)$$

The stationary solution of this equation corresponding to null probability flow is expressed in the following way, as can be seen by direct substitution:

$$w(A) = C\,A\lambda \exp\left\{-\int_a^A \lambda A\delta(A)\,dA\right\};$$

the normalizing constant C_0 is approximately equal to $\delta|_{A=0} = \delta(0)$ if the following conditions are met:

$$1/\sqrt{\lambda\delta(0)} \ll A_1,\ 1/\sqrt{K_1} \ll A_1, \qquad (12)$$

where

$$K_1 = -\frac{d}{dA}[\lambda A\delta(A)]\Big|_{A=A_1}$$

It is now easy to obtain an expression for the average frequency of system transition through the excitation boundary, which is the inverse of the average excitation time, by a method analogous to the one given in [10]:

$$\gamma = \frac{1}{\lambda}\sqrt{\frac{K_1}{2\pi}}\,w(A_1) =$$
$$= \delta(0)\,A_1\sqrt{\frac{K_1}{2\pi}}\exp\left\{-\int_0^{A_1}\lambda A\delta(A)\,dA\right\}. \qquad (13)$$

Hence, a graph of $\lambda A\delta(A)$ as a function of A for different values of $\underline{n}$ must be plotted in order to compute the average excitation time of the system. Then the integral in the brackets of the exponential in (13) can be evaluated from this graph, and the value of K_1 found.

Calculations show that the equivalent noise intensity λ^{-1} depends weakly on A, the amplitude of the oscillations. Therefore, the average value of λ, which does not depend on amplitude, but is a function of $\underline{n}$, must be used when the average excitation time of the system is computed from (13). The average noise intensities for different $\underline{n}$ are given in Table 2.

Knowing λ, the conditions of applicability of the theory [the conditions of (12)] can be checked. It appears that these conditions are met very poorly. For example, when $n = 0.55$, we have: $1/\lambda\delta(0) \approx 1/\sqrt{K_1} \approx 3\cdot10^{-3}$, $A_1 \approx 3\cdot10^{-2}$. Conditions (12) are met even more poorly when the noise intensity is increased fourfold, as was done in the experiment. This circumstance has already been noted in considering the results of system studies on an analog.

The average system excitation times τ_{av}, calculated from (13) for various aileron relative frequencies $\underline{n}$, are given in Table 2. The average excitation times τ'_{av}, for a fourfold increase in noise intensity are given in the same table. The data obtained agree qualitatively with the experimental results (see Table 1).

We should remember that the numerical values of the average time obtained from theoretical calculations

†Here ζ^* designates the complex conjugate of ζ, and the sign < > designates a statistical average.

have meaning only as estimates of the quantities mentioned.

CONCLUSIONS

1. The presence of a parasitic positive feedback path in the control system causes the unstable region to expand. In this case, if there is a gap in the aileron control drive, the system can be excited only under definite initial conditions (in the absence of fluctuation disturbance), for certain parametric values.

2. The danger of growing oscillations of an airplane wing arises as a result of the excitation of hard oscillations in flight through turbulent air.

3. The probability of growing oscillations arising in a definite time interval depends on the intensity of the fluctuations caused by turbulent disturbance of the vertical flight velocity component, and this probability decreases sharply with a decrease in this intensity.

4. The basic role in system excitation is played by the spectral components of the turbulence near the natural bending oscillation frequency of the wing, ω_h, in other words, the amplitude of the spatial spectral density of the turbulence, $S_u^i(\Omega)$, at $\Omega = \omega_h/v$.

5. The theoretical methods presented in this paper in combination with a study of the system on an analog computer permit one to get statistical estimates for the excitation time of dangerous wing oscillations as a function of the flight velocity and natural frequency of the aileron.

The authors express gratitude to R. L. Stratonovich for much valuable advice and suggestions.

LITERATURE CITED

1. E. P. Grossman, Course on the Vibration of Airplane Parts [in Russian] (Oborongiz, 1940).
2. E. P. Grossman, "Flutter" (Trudy TsAGI No. 284, 1937).
3. R. H. Scanlan and R. Rosenbaum, Introduction to the Study of Aircraft Vibration and Flutter (The MacMillan Company, New York, 1951).
4. S. P. Strelkov, and A. A. Kharlamov, "A study of the flutter of a wing with an aileron," Naucha. Dokl. Vyssh. Shkol., Fiz.-Matem. Nauki 2, No. 2 (1959).
5. D. S. Woolston, H. L. Runyan, and T. A. Byrdsong, Some Effects of System Nonlinearities in the Problem of Aircraft Flutter (NACA, TN, 1955) p.3539.
6. D. S. Woolston, H. L. Runyan, and R. E. Andrews, "An investigation of the effects of certain types of structural nonlinearities on wing and control surface flutter," J. Aero. Sci. 24, No. 1 (1957).
7. S. F. Shen, "An approximate analysis of the nonlinear flutter problem," J. Aero. Sci. 26, No. 1 (1959).
8. Yu. M. Romanovskii, and S. P. Strelkov, "Concerning the effect of atmospheric turbulence on an airplane with elastic wings at different flight velocities," Izvest. Akad. Nauk SSSR, Otdel. Tekh. Nauk, Mekh. i Mashin., No. 4 (1959).
9. R. L. Stratonovich and P. S. Landa, "The effect of noise on a generator with hard oscillations," Izv. Vuz, Radiofizika 2, No. 1 (1959).
10. P. S. Landa, "Concerning the stability of servocontrol systems in the presence of random perturbations," Avtomat. i Telemekh. 21, No. 1 (1960).‡
11. A. I. Nekrasov, The Theory of a Wing in Nonsteady-State Flow [in Russian] (Izd. AN SSSR, 1947).
12. P. S. Landa, "An analog computer study of the effect of noise on a generator with hard oscillations," Izv. Vuz, Radiofizika 2, No. 3 (1959).

‡See English translation.

A VECTOR METHOD FOR CALCULATING ONE CLASS OF CONTROL SYSTEMS

S. M. Levin and L. G. Manusevich

Leningrad

Translated from Avtomatika i Telemekhanika, Vol. 21, No. 10,
pp. 1365-1374, October, 1960
Original article submitted April 18, 1960

A method for studying one class of control systems is examined. The method is based on constructing vector diagrams and finding the reflection of the parameter space on the amplitude-phase plane.

1. Statement of the Problem. Let the transfer function of an open-loop control system have the form

$$\Phi(p) = -\frac{M(p)}{D(p)} f(p), \tag{1}$$

where f(p) is the transfer function of a group of links containing no unknown parameters,

$$M(p) = \sum_{\nu=1}^{s} m_\nu A_\nu(p) + \sum_{\lambda=1}^{r} k_\lambda B_\lambda(p) + \sum_{\nu=1}^{s}\sum_{\lambda=1}^{r} m_\nu k_\lambda C_{\lambda\nu}(p),$$
$$D(p) = \sum_{\nu=1}^{s} m_\nu D_\nu(p). \tag{2}$$

Here m_ν and k_λ are the system parameters to be determined, and the coefficients of the polynomials $A_\nu(p)$, $B_\lambda(p)$, $C_{\lambda\nu}(p)$ and $D_\nu(p)$ depend on the parameters $l_\mu(\mu = 1, 2, \ldots, t)$ whose precise value is unknown. Let us call l_μ the "unreliable" parameters.

The transfer functions of a wide class of control systems can be reduced to the form of (1) and (2). In particular, the transfer functions of systems which are controlled by two or more physical quantities have such a form—for example, the transfer functions of airplane [1] and ship [2] control systems. In this case, the "reliable" parameters are those of the regulator, and the "unreliable" parameters are the aerodynamic and hydrodynamic coefficients.

The problem consists of determining the parameters, m_ν and k_λ, which ensure stability and the required system quality under the conditions that the "unreliable" parameters l_μ may vary between definite limits.

2. Initial Constructions. Let us first assume that the requirements on system quality are merely that the system must have a certain degree of stability [3], and let us consider the function $W(-\varepsilon + i\omega)$, representing each of the terms in (2) in vector form.

Having been given an initial system of parametric values $l_\mu(\mu = 1, 2, \ldots, t)$, let us construct the following vectors for each frequency ω:

$$\overline{A_\nu}(-\varepsilon + i\omega, l_\mu) = \sum_{\gamma=1}^{n_\nu} \overline{A_\nu^\gamma}, \tag{3}$$

where $|\overline{A_\nu^\gamma}| = a_\nu^\gamma(l_\mu) R^\gamma$; $\arg \overline{A_\nu^\gamma} = \gamma\left(\varphi + \frac{\pi}{2}\right)$; a_ν^γ are the coefficients of the polynomial $A_\nu(p)$; $R =$

$= \omega \sqrt{1+\left(\frac{\varepsilon}{\omega}\right)^2}$: $\varphi = \operatorname{arc\,tg} \frac{\varepsilon}{\omega}$; n_ν is the highest degree of the polynomial being examined.

When the parameters l_μ change, the vector $\overline{A}_\nu$ receives the increment

$$\overline{\Delta A}_\nu = \sum_{\gamma=1}^{n_\nu} \delta a_\nu^\gamma \overline{A}_\nu^\gamma, \tag{4}$$

where

$$\delta a_\nu^\gamma = \frac{a_\nu^\gamma [(l_1 + \Delta l_1), (l_2 + \Delta l_2), \ldots, (l_t + \Delta l_t)] - a_\nu^\gamma (l_1, l_2, \ldots, l_t)}{a_\nu^\gamma (l_1, l_2, \ldots, l_t)},$$

and Δl_μ is the increment of l_μ.

Considering only the linear members of δa_ν^γ expressed as a series in Δl_μ we represent δa_ν^γ in the form

$$\delta a_\nu^\gamma = \left(\frac{1}{a_\nu^\gamma}\right)_0 \sum_{\mu=1}^{t} \left(\frac{\partial a_\nu^\gamma}{\partial l_\mu}\right)_0 \Delta l_\mu. \tag{5}$$

The sign "0" indicates that the corresponding quantities are determined from the initial values of the parameters.

The vectors $\overline{B}(p)$, $\overline{C}_{\lambda\nu}(p)$, $\overline{D}_\nu(p)$ can be constructed analogously, and their increments found.

Next, having been given the initial parameters k_λ^0, m_ν^0, we construct geometric series for each frequency ω, which define the vectors $\overline{D(-\epsilon+i\omega)}$ and $\overline{-M(-\epsilon+i\omega)}$ $f(-\epsilon+i\omega)$ in correspondence with formulas (2). The latter vector is derived from the vector $\overline{-M(-\epsilon+i\omega)}$ by extending it $|f(-\epsilon+i\omega)|$ times and rotating it by an angle arg f $(-\epsilon+i\omega)$.

We will start these geometric series from point 0, and we will denote the ends by the letters D and M, respectively; we will indicate the parameters k_λ and m_ν, on which they depend, at each of the component vectors.

A change in the parameter k_λ by an amount $\delta k_\lambda = \frac{k_\lambda - k_\lambda^0}{k_\lambda^0}$ causes the vector $\overline{0M}$ to change by an amount

$$\overline{\Delta_{k_\lambda} M} = \delta k_\lambda \left[k_\lambda^0 \overline{B_\lambda}(p) + \sum_{\nu=1}^{s} k_\lambda^0 m_\nu^0 \overline{C_{\lambda\nu}}(p) \right]. \tag{6}$$

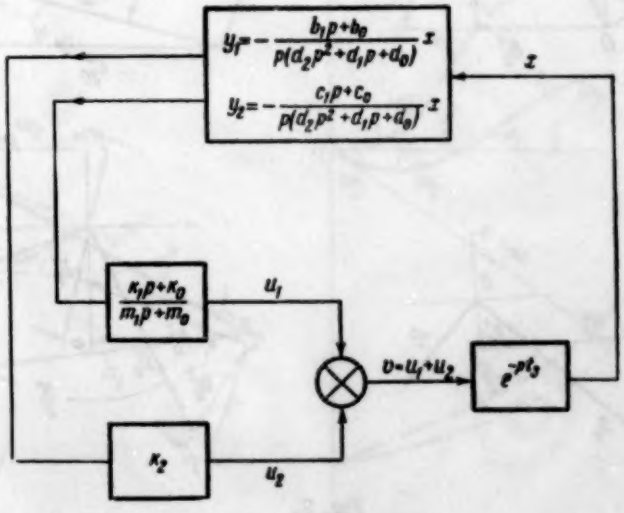

Fig. 1.

Analogously, a change in m_ν causes the vectors $\overline{0D}$ and $\overline{0M}$ to change by the amounts

$$\overline{\Delta_{m_\nu} D} = \delta m_\nu [m_\nu^0 \overline{D_\nu(p)}],$$

$$\overline{\Delta_{m_\nu} M} = \delta m_\nu \left[m_\nu^0 \overline{A_\nu(p)} + \sum_{\lambda=1}^{r} k_\lambda^0 m_\nu^0 \overline{C_{\lambda\nu}(p)} \right], \tag{7}$$

respectively.

When m_ν and k_λ change simultaneously, the increment of 0M is found from the formula

$$\overline{\Delta^{\Sigma}_{k_\lambda m_\nu} M} = \overline{\Delta_{k_\lambda} M} + \overline{\Delta_{m_\nu} M} + \overline{\Delta_{k_\lambda m_\nu} M}, \tag{8}$$

where

$$\overline{\Delta_{k_\lambda m_\nu} M} = \delta k_\lambda \delta m_\nu [k_\lambda^0 m_\nu^0 \overline{C_{\lambda\nu}(p)}].$$

The vectors plotted for initial values of the parameters are enclosed in square brackets in expressions (6), (7), and (8).

Hence, a change in a parameter corresponds to a proportional change in the lengths of the vectors representing it. If the system stability does not meet requirements on system quality, the construction must be done over for $\epsilon=0$.

It follows from (1) and the constructions described above that the ratio of the segments 0M to 0D equals the modulus of the amplitude-phase characteristic of an open-loop system (normal for $\epsilon=0$ or expanded $\epsilon>0$), and its argument is the angle χ between $\overline{0D}$ and $\overline{0M}$. The ratio of the lengths of M0 and MD and the angle between vectors $\overline{MD}$ and $\overline{M0}$ are equal to the modulus and argument, respectively, of the amplitude-phase characteristic of a closed-loop system with respect to the controlling input. The real part of the amplitude-phase characteristic is equal to the projection of $\overline{M0}$ along $\overline{MD}$, divided by the length of the segment MD.

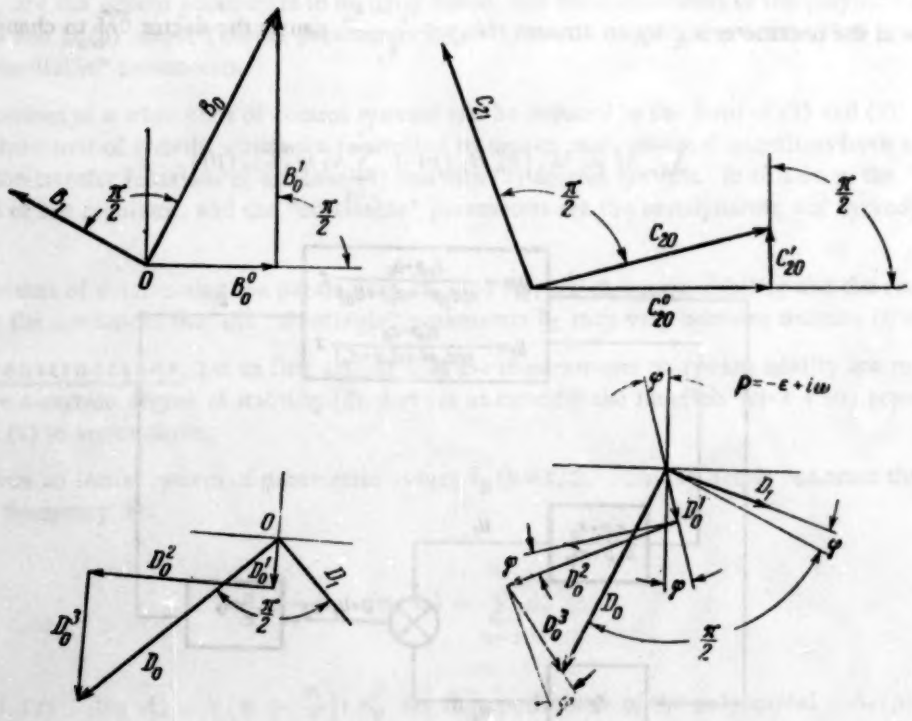

Fig. 2.

Example. Let us examine an automatic control system; the structure and transfer functions of the individual parts are shown in Fig. 1. The transfer function of this system has the form

$$W(p) = -\frac{(k_1 p + k_0)(b_1 p + b_0) + k_2 (m_1 p + m_0)(c_1 p + c_0)}{p (d_3 p^2 + d_2 p + d_1)(m_1 p + m_0)} e^{-pt_3}.$$

A diagram of the vectors

$$\overline{B_0(p)} = b_1 p + b_0,\ \overline{B_1(p)} = \overline{pB_0(p)},\ \overline{C_{20}(p)} = c_1 p + c_0,\ \overline{C_{21}(p)} = \overline{pC_{20}(p)},$$
$$\overline{D_0(p)} = d_3 p^3 + d_2 p^2 + d_1 p,\quad \overline{D_1(p)} = \overline{pD_0(p)},$$

where $p = i\omega$, is shown in Fig. 2. The diagram corresponds to a negative value of d_1 and to positive values of the remaining coefficients of the polynomials B(p), C(p), and D(p). A diagram of vectors $D_0(p)$ and $D_1(p)$, where $p = -\epsilon + i\omega$, is shown on the same figure for the sake of illustration. The diagram of vector $\overline{0D} = D(i\omega)$ and $\overline{0M} = -M(i\omega)e^{-i\omega t_3}$ is shown in Fig. 3 for the frequencies ω_0, ω_1, ω_2, and ω_3. Vectors $\overline{B_0}$, $\overline{B_1}$, $\overline{C_{20}}$ and $\overline{C_{21}}$ are rotated π radians in constructing the vectors $\overline{0M}$, and vectors $\overline{D_0}$ and $\overline{D_1}$ are rotated ωt_3 radians in constructing $\overline{0D}$. The amplitude-phase characteristic corresponding to this system of vectors is shown in the same figure (curve 1).

3. Analysis and Replotting of the Vector Diagrams with Fixed "Unreliable" Parameters.

We will assume that the "unreliable" parameters are fixed. Let us examine the basic methods for analyzing automatic control systems by means of vector diagrams.

1. The vector diagrams which have been plotted permit one to determine whether or not the system is stable with the given initial parameters, or whether it has a given degree of stability. This may be done on the basis of the Nyquist–Mikhailov criterion. The number of roots of the denominator with a positive real part (or with a real part greater than $-\epsilon$) may be found, for example, on the basis of the Mikhailov criterion from the be-

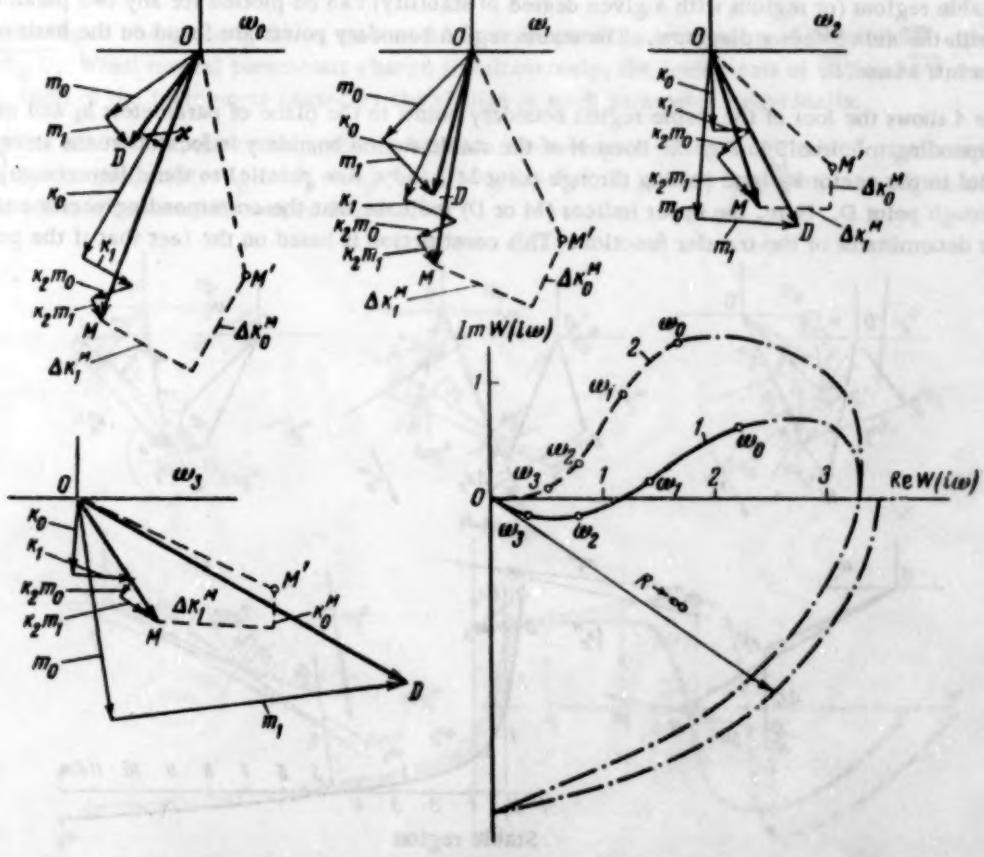

Fig. 3. Vector diagram and amplitude-phase characteristic of the open-loop system.

havior of vector $\overline{0D}$. Thus, the system of vectors plotted in Fig. 3 corresponds to an unstable system (the denominator of the transfer function has one root with a positive real part, since $d_1<0$).

2. The vector diagrams make it possible to evaluate the effect of parameters m_ν and k_λ on the shape of the amplitude–phase characteristic. Thus, for the system considered in the example, increasing k_1 at all frequencies causes angle χ to increase, that is, the argument of the amplitude–phase characteristic increases. A decrease in m_1 leads to the same result. Decreasing k_0 causes the modulus of the amplitude–phase characteristic to decrease, and a certain increase in its argument, etc.

3. The vector diagrams permit one to see the desirability of changing one or another of the parameters being examined as a group, and to determine which parameters should be changed and how, in order to shape the amplitude–phase characteristic into the desired form.

The amount of parametric change is limited, naturally, by the physical properties of each parameter. For example, the amplitude–phase characteristic of the system must be shaped so that it passes over the point (1, 0i), in order to ensure that it will be stable. The evaluations done in Section 2 permit one to determine what can be achieved, in particular, by increasing k_1 and decreasing k_0.

4. Having been given δm_ν and δk_λ on the basis of the evaluations done in Sections 2 and 3, the vectors $\overline{0D}$ and $\overline{0M}$, corresponding to a change in the parameters m_ν and k_λ, can be plotted. To do this, one need only find the increments of the respective vectors from formulas (6), (7), and (8), and plot them geometrically from points M and D. A number of such constructions must be done to find the optimum combination of parameters. Constructions corresponding to $\delta k_0=-0.5$ and $\delta k_1=2$ are shown in Fig. 3 by dashed lines. Curve 2 in this figure shows the amplitude–phase characteristic of the system altered in this manner.

5. The vector diagrams plotted make it possible to decide whether it is desirable to introduce corrective links into the control system (including differentiation and integration). The introduction of such links leads to an extension and rotation of the vectors proportional to the parameters which are coefficients for the quantities being corrected. Thus, for example, the derivative of Y_2 could be introduced into Fig. 3 to increase the angle χ. This would be a vector added to point M, perpendicular to the sum of the vectors proportional to k_2.

6. Stable regions (or regions with a given degree of stability) can be plotted for any two parameters, m_ν and k_λ, with the aid of vector diagrams. The stable region boundary points are found on the basis of a coincidence of points M and D.

Figure 4 shows the loci of the stable region boundary points in the plane of parameters k_0 and m_1 for the system corresponding to curve 2 in Fig. 3. Point N of the stable region boundary is located at the intersection of a line parallel to the vector k_0^M and passing through point M', and a line parallel to the difference $\overline{m}_1^D - \overline{m}_1^M$ and passing through point D. Here, the upper indices (M or D) indicate that the corresponding vector enters the numerator or denominator of the transfer function. This construction is based on the fact that if the position of point

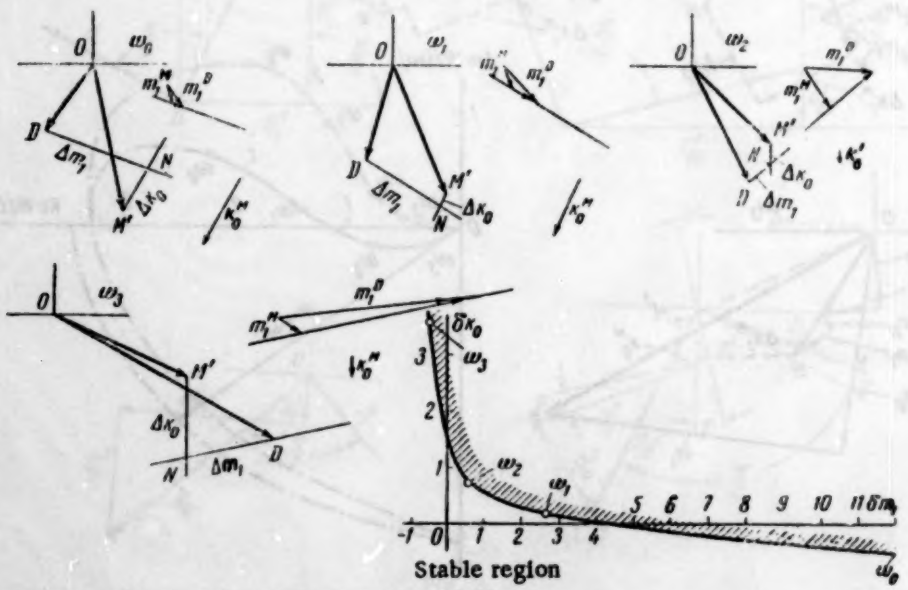

Fig. 4. Plot of the stable region.

M remains unchanged, the addition of vector $\bar{a}-\bar{b}$ to point D leads to the same change in the mutual position of points D and M as the addition of $\bar{a}$ to point D, and $\bar{b}$ to point M. The stable region in Fig. 4 is plotted on the coordinates $\delta k_0 = \Delta k_0/k_0^0$ and $\delta m_1 = \Delta m_1/m_1^0$, which are defined in terms of a ratio of the corresponding segments.

If both variants of the parameter enter expression (2) both linearly and in a product, then determining the stable region boundary points consists of solving a certain quadratic equation, whose coefficients are easily determined graphically (see Appendix).

7. By using vector diagrams, it is also possible to analyze control systems qualitatively by plotting the real part of the amplitude–phase characteristic of the closed-loop system with respect to the controlling input [4]. The construction consists of finding the ratio of the projection MP of vector $\overline{M0}$ on $\overline{MD}$ to the length of segment MD at each frequency ω. The effect of the system parameters on the shape of the amplitude–phase characteristic of the closed-loop system can be traced directly from the vector diagrams. A plot of the real part of the amplitude-phase characteristic of the system considered in the example is shown in Fig. 5 (curve 1). It follows from an examination of the vector diagram shown in Fig. 3 that it is sufficient to decrease m_0 in order to increase the positive region, for example. Corresponding constructions are shown in Fig. 5; the change in the position of points M, D, and P and the corresponding curve are designated by the index 2.

4. Construction of the Loci of the Ends of Vectors $\overline{0M}$ and $\overline{0D}$ as the "Unreliable" Parameters Change within Given Limits. Let the parameter l_μ assume an increment Δl_μ. Then the increment of A_0, in correspondence with (4) and (5), will equal

$$\overline{\Delta_\mu A_\nu} = \sum_{\gamma=1}^{n_\nu} \delta_\mu a_\nu^\gamma \overline{A_\nu^\gamma} \qquad \left(\delta_\mu a_\nu^\gamma = \left(\frac{1}{a_\nu^\gamma} \frac{\partial a_\nu^\gamma}{\partial l_\mu} \right)_0 \Delta l_\mu \right). \tag{9}$$

The increments $\overline{\Delta_\mu B_\lambda}$, $\overline{\Delta_\mu C_{\lambda\nu}}$ and $\overline{\Delta_\mu D_\nu}$, caused by the increment of l_μ, are found analogously. The increment of vectors $\overline{0M}$ and $\overline{0D}$, $\overline{\Delta_\mu M}$ and $\overline{\Delta_\mu D}$, can be found from expressions (2), in which A_ν, B_λ, $C_{\lambda\nu}$, and D_ν are replaced by their increments.

It is evident that a change in l_μ by an amount $n\Delta l_\mu$ corresponds to increments of $\overline{0M}$ and $\overline{0D}$ equal to $\overline{n\Delta_\mu M}$ and $\overline{n\Delta_\mu D}$. When several parameters change simultaneously, the increments of $\overline{0M}$ and $\overline{0D}$ are found as the geometric sums of the increments caused by the change in each parameter individually.

We will show how to find the correspondence between the subregion of the "unreliable" parameter space characterized by the inequalities $l_\mu' - \Delta l_\mu' \leq l_\mu \leq l_\mu' + \Delta_\mu'$ ($\mu = 1, 2, \ldots, t$) and the plane region within which the amplitude-phase characteristic can be located.

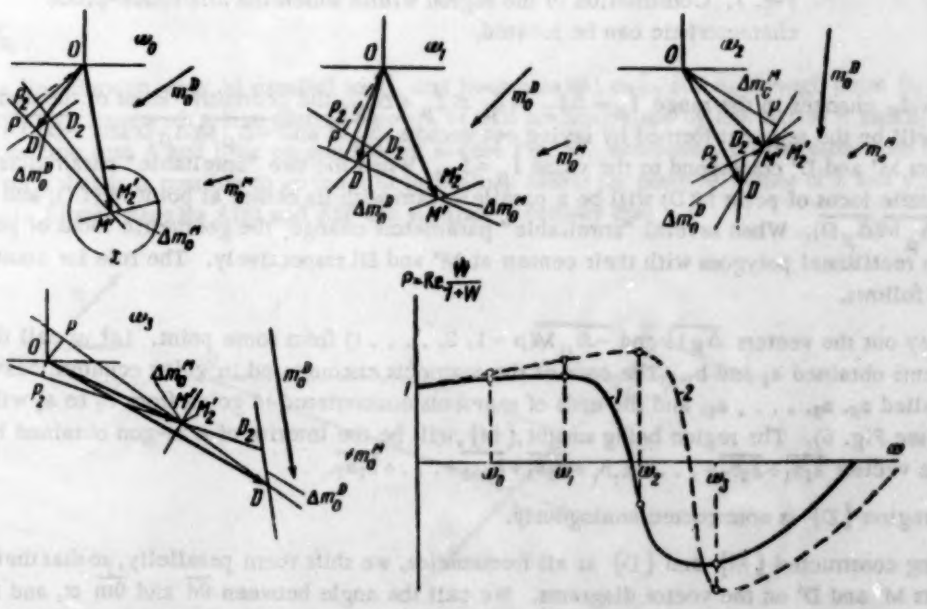

Fig. 5. Construction of the real part of the amplitude-phase characteristic of the closed-loop system.

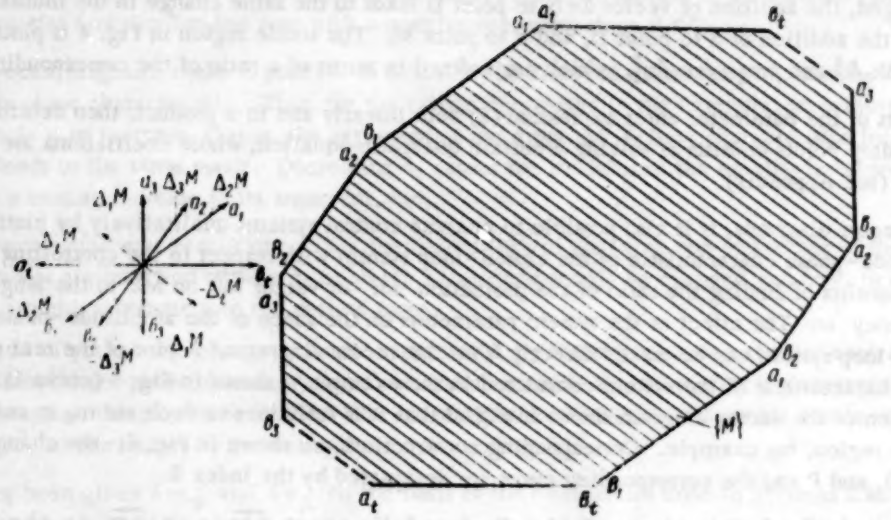

Fig. 6. Construction of the region $\{M\}$.

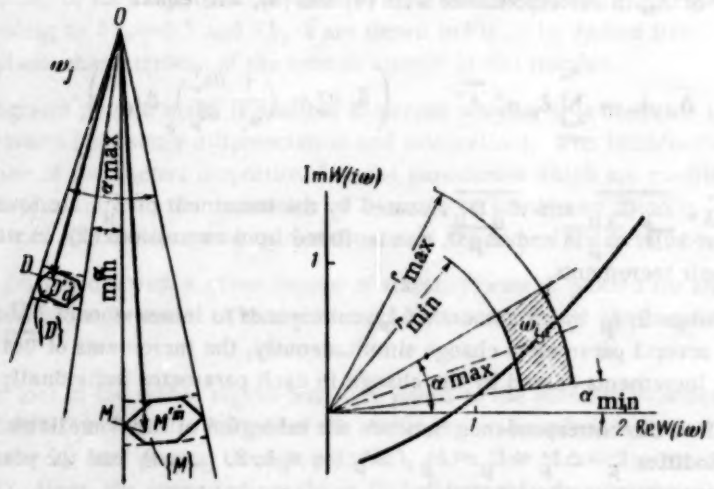

Fig. 7. Construction of the region within which the amplitude-phase characteristic can be located.

When l_μ changes in the range $\dot{l}_\mu - \Delta\dot{l}_\mu \le l_\mu \le \dot{l}_\mu + \Delta\dot{l}_\mu$, the geometric locus of the ends of the vector $\overline{0M}(\overline{0D})$ will be the segment formed by laying out vectors $\overline{\Delta_\mu M}$ and $\overline{-\Delta_\mu M}(\overline{\Delta_\mu D}$ and $\overline{-\Delta_\mu D})$ from point M(D). Here points M' and D' correspond to the value $l_\mu = \dot{l}_\mu$. When the two "unreliable" parameters ($\mu = s_1, s_2$) change, the geometric locus of point M(D) will be a parallelogram with its center at point M'(D'), and with its sides parallel to $\overline{\Delta_\mu M}(\overline{\Delta_\mu D})$. When several "unreliable" parameters change, the geometric locus of points M and D will be certain rectilineal polygons with their centers at M' and D', respectively. The rule for constructing these polygons is as follows.

We lay out the vectors $\overline{\Delta_\mu M}$ and $\overline{-\Delta_\mu M}(\mu = 1, 2, \ldots, t)$ from some point. Let us call the ends of one of the segments obtained a_1 and b_1. The ends of the segments encountered in going counterclockwise from a_1 to b_1 will be called $a_2, a_3, \ldots, a_t$, and the ends of segments encountered in going from b_1 to a_1 will be called $b_2, b_3, \ldots, b_t$ (see Fig. 6). The region being sought, $\{M\}$, will be the interior of a 2t-gon obtained by consecutively adding the vectors $\overline{a_1b_1} + \overline{a_2b_2} + \ldots + \overline{a_tb_t} + \overline{b_1a_1} + \overline{b_2a_2} + \ldots + \overline{b_ta_t}$.

The region $\{D\}$ is constructed analogously.

Having constructed $\{M\}$ and $\{D\}$ at all frequencies, we shift them parallelly, so that their centers coincide with points M' and D' on the vector diagrams. We call the angle between $\overline{0d}$ and $\overline{0m}$ α, and the ratio $0m/0d$ will be called r. The point d belongs to $\{D\}$, and point m belongs to $\{M\}$. The region within which the am-

plitude–phase characteristic can be located on plane W, where $\omega = \omega_j$, does not extend beyond the limits of the region characterized by the inequalities (see Fig. 7)

$$\min r(\omega_j) \leqslant |W(i\omega_j)| \leqslant \max r(\omega_j),$$
$$\min \alpha(\omega_j) \leqslant \arg W(i\omega_j) \leqslant \max \alpha(\omega_j).$$

Similar constructions can be done initially for all the given part of the "unreliable" parameter space. If the corresponding amplitude-phase characteristic location region does not provide sufficient bases for judging one or more properties of a system, the limits of this region can be made more precise by breaking up the "unreliable" parameter space into subspaces.

CONCLUSION

The method presented, based on the construction of vector diagrams, permits one to study a wide class of automatic control systems, and to solve stability and control quality problems.

The method permits one to evaluate the joint effect of both "reliable" and "unreliable" parameters on the shape of the amplitude-phase characteristic of an open-loop or closed-loop system.

The construction of vector diagrams can be used for determining the amplitude-phase characteristic of the linear part of nonlinear systems being studied, for example, by the methods given in [5, 6].

APPENDIX

Determining the Boundaries of the Stable Region in the Plane of the Parameters Entering the Numerator and Denominator Both Linearly and in the Form of a Product. Let us find a boundary point of the stable region at the frequency ω in the plane of parameters m_1 and k_1, assuming that $A_1(i\omega)$, $B_1(i\omega)$, $D_1(i\omega)$ and $C_{11}(i\omega)$ are not equal to zero [see formula (2)].

The increments of $\overline{0D}$ and $\overline{0M}$ caused by a change in these parameters can be written in the form

$$\overline{\Delta D} = \bar{h}_1 y, \qquad \overline{\Delta M} = \bar{n}_1 x + \bar{h}_2 y + \bar{n}_3 xy,$$

according to (7) and (8).

Here $\underline{x}$ and $\underline{y}$ are the relative increments of k_1 and m_1, respectively, and $\bar{n}_i$ and $\bar{h}_i$ are vectors corresponding to the initial values of these parameters. The problem consists of finding values of $\underline{x}$ and $\underline{y}$ which satisfy the equality

$$\overline{0D} - \overline{0M} = \bar{n}_1 x + \bar{n}_2 y + \bar{n}_3 xy,$$

where $\bar{n}_2 = \bar{h}_2 - \bar{h}_1$.

Let us draw a line through point M parallel to $\bar{n}_1$, and lines parallel to $\bar{n}_2$ and $\bar{n}_3$ through point D. The intersection of the latter two lines with a line passing through M will be designated by the letters A and B, respectively. We will initially assume that A and B lie on one side of M (see Fig. 8). Moreover, let the directions of vectors $\bar{n}_1$, $\bar{n}_2$, and $\bar{n}_3$ be such that it is possible to go from M to D along MEFD for positive values of $\underline{x}$ and $\underline{y}$ ($\overline{ME} = \bar{n}_1 x$, $\overline{EF} = \bar{n}_3 xy$, $\overline{FD} = \bar{n}_2 y$). Since triangles ABD and AEF are similar, it follows that

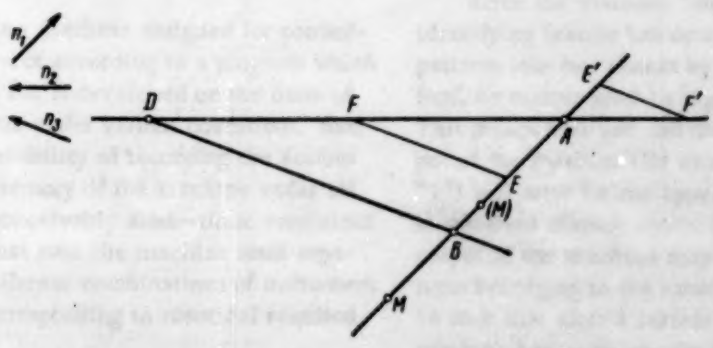

Fig. 8. Figure used in plotting the stable region.

$$\frac{b-n_1x}{b-d}=\frac{n_2xy}{c}=\frac{a-n_2y}{a}, \tag{10}$$

where a, b, c, and d are equal to the lengths of AD, AM, BD, and BM, respectively.

We get Equation (11) for finding $\underline{x}$ from proportion (10):

$$x^2+\left(\frac{cn_2}{an_3}-\frac{d}{n_1}\right)x-\frac{bcn_2}{an_1n_3}=0, \tag{11}$$

and after solving it, $\underline{y}$ is determined from the equality

$$y=a\frac{n_1x-d}{(b-d)n_3}. \tag{12}$$

We will assume that the directions of any two of the vectors $\bar{n}_1$, $\bar{n}_2$, and $\bar{n}_3$ are opposite to those of $\overline{ME}$, $\overline{EF}$, and $\overline{FD}$. Changing the sign of the relative increments ($\underline{x}$ and $\underline{y}$, if opposite to $\bar{n}_1$ and $\overline{ME}$, and $\bar{n}_2$ and $\overline{FD}$, or only $\underline{x}$, if opposite to $\bar{n}_1$ and $\overline{ME}$, and $\bar{n}_3$ and $\overline{EF}$, or only $\underline{y}$ if opposite to $\bar{n}_2$ and $\overline{FD}$, and $\bar{n}_3$ and $\overline{EF}$), we arrive at the same expression for (11) and (12).

If only $\bar{n}_3$ is directed opposite to $\overline{EF}$, we get expressions differing from (11) and (12) by the sign of the quantity $\underline{c}$, in a manner analogous to that already examined, from the similarity of triangles ABD and AE'F'. By appropriately choosing the signs of the relative increments, we can arrive at the same situation as when the directions of any one or all three of the vectors are opposite to those shown in Fig. 8.

When A and B lie on different sides of M, $\underline{x}$ and $\underline{y}$ are found from proportions differing from (10) only by the sign of $\underline{d}$, as is clear from Fig. 8. In this case, the relative increments of m_1 and k_1 defining the system at the boundary of the stable region are found in all cases from relations (11) and (12). The quantity $c>0$ if the directions of $\bar{n}_1$, $\bar{n}_2$, and $\bar{n}_3$ agree with the directions of $\overline{MA}$, $\overline{AD}$, and $\overline{BD}$; there are two different directions, and $c<0$ in the remaining cases. The quantity $d>0$ if points A and B are on one side of point M. The increment of k_1 is positive if the direction of $\bar{n}_1$ agrees with that of $\overline{MA}$; the increment of m_1 is positive if the direction of $\bar{n}_2$ agrees with that of $\overline{AD}$.

LITERATURE CITED

1. I. V. Ostoslavskii, The Aerodynamics of an Airplane [in Russian] (Oborongiz, 1957).
2. A. M. Basin, Theory of Stability on Course and Maneuverability of a Vessel [in Russian] (Gostekhizdat, 1949).
3. Ya. Z. Tsypkin and P. V. Bromberg, "On the degree of stability of linear systems," Izvest. Akad. Nauk SSSR, Otdel. Tekh. Nauk No. 12 (1945).
4. V. V. Solodovnikov, A Frequency Method for Analyzing the Quality of Automatic Control Systems [in Russian] (Mashgiz, 1950).
5. L. S. Gol'dfarb, "On certain nonlinearities in control systems," Avtomat. i Telemekh. 8, No. 5 (1947).
6. Ya. Z. Tsypkin, Theory of Automatic Control Relay Systems [in Russian] (Gostekhizdet, 1955).

CERTAIN PROBLEMS IN THE DESIGN OF MACHINES WHICH CLASSIFY OBJECTS ACCORDING TO AN IDENTIFYING FEATURE WHICH IS NOT SPECIFIED A PRIORI

É. M. Braverman

Moscow

Translated from Avtomatika i Telemekhanika, Vol. 21, No. 10,
pp. 1375-1386, October, 1959
Original article submitted February 17, 1960

The paper studies certain problems associated with the design of machines that can classify objects according to an indentifying feature which is not specified a priori. A number of general conditions are indicated for which this problem can be solved by machines with "stimulation" (machines which receive certain additional information from the operator). It is demonstrated that in a number of cases machines without stimulation can be used for the same purpose; a brief analysis is made of the capabilities of one machine of this type which has already been constructed (the "Perceptron").

1. Introduction

In designing various types of self-adaptive machines, the first problem is to design a machine that classifies input situations according to an identifying feature which is not known a priori. An example of this kind may be found in a high-speed computer which changes or formulates its program during the solution of the problem. After this machine has solved a number of problems, it will have accumulated experience which is manifested in the set of programs it has formulated. In solving a new problem the machine must first determine whether or not this problem is "similar" to some other problem it has solved previously; if this is so, then it must attempt to use a program which is already available. However, it is not known a priori which problems the machine must assume to be "similar." Thus, the experience of the machine must include not only a set of programs for solving specific problems, but also a program which is developed during the process of operation and makes it possible to separate the entire set of problems which are to be solved into classes of similar problems.

Another example is a machine designed for controlling a technological object according to a program which is not specified a priori but is developed on the basis of the actions of an operator under various conditions. But, as a rule, there is no possibility of recording the actions of the operator in the memory of the machine under all conditions that might conceivably arise—these conditions are too numerous. In that case the machine must separate the entire set of different combinations of instrument readings into classes corresponding to identical required control actions.

The basic features of the classification problem are often illustrated by the means of the following very clear example. Assume that photoelements, which act as the detectors in the machine, "scan" a certain field. The operator (human or machine) "shows" the machine geometric patterns in arbitrary sequence; these patterns have been subdivided by the operator into two classes according to some identifying feature. For example: 1) patterns located in the left and right sides of the field; 2) patterns located in the upper and lower parts of the field; 3) patterns with large and small areas; 4) squares and triangles; 5) patterns that are symmetrical relative to the horizontal and vertical axes, etc. Two situations are possible at the output of the machine (for example, the appearance of "0" or "1"). No separation of the input situations into two classes has been fed into the machine a priori. It is required that after a certain self-adaptive period the machine will be capable of producing a "1" at the output each time that the machine is shown a pattern belonging to some particular class, and of producing a "0" for the appearance of a pattern belonging to a different class.

Since the machine "does not know" a priori which identifying feature has determined the separation of the patterns into two classes by the operator, it will err at first, no matter what its algorithm for operation may be. This means that one and the same situation at the output of the machine (for example, the appearance of a "1") will arise for the appearance of patterns belonging to different classes; conversely, different situations at the output of the machine may correspond to different patterns belonging to the same class. The algorithm must be such that after a certain number of "viewings" the machine begins to operate without error, or at least in a

manner where the probability of error is small. We shall assume that when a self-adaptive machine has reached this quality of operation, it has developed a "comprehension" (in the example given here, the comprehensions that are developed are "right" and "left," "upper" and "lower," etc.).

Showing another pattern to the machine corresponds to the appearance of a certain situation at the input of the machine (the excitation of certain photoelements and the nonexcitation of other photoelements). Each specific sitation at the input will sometimes be called an "object."

In the general case, the machine develops a comprehension and then converts the set of input situations into a set of output situations. In our example, the set of output situations consists of two elements (0 and 1). The machine must have a series of variable parameters for which each value completely determines the transformation law carried out by the machine. We shall call each set of specific values for these variable parameters a "state" of the machine.

Initially we shall assume that the operator feeds the machine a specific signal each time the machine commits an error (i.e., the operator feeds additional information into the machine). The state of the machine may vary according to a definite law (in the general case it is not necessarily a deterministic law), depending on the input situations and on the additional information received from the operator. Such machines shall be called "adaptive machines with stimulation."

Below we shall demonstrate that machines with stimulation are not the only class of adaptive machine. Under certain definite conditions, machines can develop comprehensions without using the additional information from the operator.

2. Certain Conditions Which Assure the Development of Comprehensions by Machines

In the general case the operator can subdivide the set of input situations into arbitrary classes (comprehensions). In principle, the machine may err until all possible objects in the given experiment have appeared, and the operator has in some way informed the machine what output situation must correspond to each possible object. But the method of "total scanning," which is the only one that can solve the problem of developing comprehensions in this general case, is inexpedient if the number of objects is sufficiently great, and if it is necessary to solve the problem in a limited time with a limited memory.

Evidently, the only method by which total scanning can be avoided is to limit a priori the set of allowed classes into which the set of objects can be subdivided by the operator.

We shall examine certain examples of the limitations which can be imposed on the allowed classes of objects and shall examine certain concepts concerning the design of machines which develop comprehensions for these limitations. For simplicity we shall assume that all possible input situations are always subdivided into three classes by the operator: a) objects corresponding to one comprehension; b) objects corresponding to a different comprehension; c) objects which do not appear in the given experiment. In other words, the machine must develop two mutually complementary comprehensions for the condition that a portion of the objects does not appear.

Example 1. Assume that the input of the machine is formed by r detectors whose state is described by the vector $(u_1, u_2, \ldots, u_r)$; assume further that n arbitrary functions of the state of the detectors are known:

$$x_i = f_i(u_1, u_2, \ldots, u_r) \quad (i = 1, 2, \ldots, n). \qquad (1)$$

Each object corresponds to a definite point with the coordinates $x_1, x_2, \ldots, x_n$ in the space $\{x\}$. We shall impose the following limitation on the allowed classes of objects. In the space $\{x\}$ it is possible to select two regions E and E' such that: a) points corresponding to objects associated with one comprehension are confined to one, and only one, region, and points corresponding to objects associated with different comprehensions are confined to different regions; b) there exists a set of hyperplanes such that the regions E and E' lie on different sides of any hyperplane in this set.

We shall turn our attention to the fact that the regions E and E' are not fixed a priori and may be different for different classes of objects.

Assume the equation for a hyperplane in $\{x\}$ is written as

$$\sigma = \sum_{i=1}^{n} \lambda_i x_i + \lambda_{n+1} = 0. \qquad (2)$$

If the hyperplane $\sigma = 0$ passes between the regions E and E', it follows that the linear function

$$\sigma = \sum_{i=1}^{n} \lambda_i x_i + \lambda_{n+1}$$

acquires positive values in one of the regions and negative values in the other region.

We shall study the $(n+1)$-dimensional space $\{\lambda\}$ with the coordinates $\lambda_1, \lambda_2, \ldots, \lambda_{n+1}$. We note that if a certain point $(\tilde{\lambda}_1, \tilde{\lambda}_2, \ldots, \tilde{\lambda}_{n+1})$ in this space defines the hyperplane

$$\sigma = \sum_{i=1}^{n} \tilde{\lambda}_i x_i + \tilde{\lambda}_{n+1} = 0$$

in the space $\{x\}$, it follows that any point in $\{\lambda\}$

lying on the straight line connecting the origin with the point $(\tilde{\lambda}_1, \tilde{\lambda}_2, \ldots, \tilde{\lambda}_{n+1})$ will define the same hyperplane. Therefore, the set of separating hyperplanes in the space $\{x\}$ will correspond to the set of straight lines in the space $\{\lambda\}$ emanating from the origin and filling a certain hypercone. The problem of developing comprehensions reduces to transferring the current value of the vector $\lambda = (\lambda_1, \lambda_2, \ldots, \lambda_{n+1})$ into the indicated hypercone. The number of errors during a series of trials (a series of "scans" of different objects) can serve as the criterion of the distance between λ and the hypercone. For example a machine classifying objects at its input for the condition that the corresponding regions E and E' can be separated by a hyperplane can operate according to the following algorithm. When a new object appears the machine determines the values of all x_i from (1) (all x_i are known functions); then the value of the linear function σ is determined for the current value $(\lambda_1, \lambda_2, \ldots, \lambda_{n+1})$, and a signal 0 or 1 appears at the output of the machine, depending of the sign of σ. From additional signals received from the operator the machine counts up the number of errors for the series of trials and alters (for example, randomly or in some other fashion) the value of $(\lambda_1, \lambda_2, \ldots, \lambda_{n+1})$; then it again determines the number of errors during the series of trials, etc., until the number of errors becomes minimal.

An algorithm of this type is the basis for a machine designed by O. Selfridge [1] and called "Pandemonium." The machine consists of several computer (or converter) stages (Fig. 1)*. The first stage consists of detectors D which perceive the objects. The detector outputs supply the computer devices C of the second stage that form certain functions $x_1, x_2, \ldots, x_n$ for the state of the detectors which are known a priori. The output from the ith computer device is applied to the corresponding amplifier A with a variable gain λ_i. The outputs from all the amplifiers are summed, and the sum

$$\sigma = \sum_{i=1}^{n} \lambda_i x_i$$

is applied to the decision block DB which produces 1 or 0 depending on the sign of σ. If "Pandemonium" errs, then the output applies a signal to the control unit CU. The number of errors in the operation of Pandemonium over a sufficiently long series of trials $F(\lambda_1, \lambda_2, \ldots, \lambda_n)$ is a function of the coefficients λ_i. The control unit varies λ in such a way as to minimize the number of errors during a series of trials; the variation is performed according to the method of steepest descent. Thus, the control unit is essentially an external controller with "regulating organs" $\lambda_1, \lambda_2, \ldots, \lambda_n$, that minimize the function $F(\lambda_1, \lambda_2, \ldots, \lambda_n)$.

In the example involving a machine which must classify geometric patterns projected onto the photoelement field x_i may describe the state of ith photoelement. Assume that when the photoelement is excited the corresponding coordinate acquires the value 1, and that the value 0 is acquired when it is not excited. Then the act of "showing" any pattern to the machine corresponds to a point in the space $\{x\}$ lying on one of the vertices of a unit n-dimensional hypercube (n is the number of photoelements). It is easy to see that when the machine develops such comprehensions as "left" and "right," "upper" and "lower," "large" and "small," we can find corresponding regions E and E'. However, in this space it is impossible to develop such comprehensions as a "square" or a "triangle," "a pattern symmetrical with respect to the vertical axis," and "a pattern symmetrical with respect to the horizontal axis."

Example 2. It was assumed above that only one space for performing the separation was known to us a priori. However, it is also possible to encounter the following case. Several spaces are specified (several sets of functions for the state of detectors) along with the following limitation on the allowed classes of objects: two regions E and E' having the properties indicated in the first example are found in at least one of these spaces.

The problem of developing comprehensions reduces to a search for the required vector in the spaces which are successively formed. The following condition may be used to govern the transition to trials in the next space: the absence of a variation in a certain current value of the vector λ in the sampled space such that the number of errors during the series of trials will be reduced. Since the desired variation in the vector λ must be determined each time on the basis of a finite number of steps, it follows that there may exist a certain probability that transition to trials in the next space will be performed erroneously. Thus, in the case under study the machine may develop a comprehension only with a certain probability.

As we have already noted, in our example the photoelement field cannot develop the comprehensions: a "square" and a "triangle," a "pattern symmetrical with respect to the horizontal axis," and a "pattern symmetrical with respect to the vertical axis," if the search for the separating hyperplane is performed in a space where each coordinate corresponds to the state of one photoelement. However, it is possible to organize another space $\{x\}$ in the following fashion. Assume that the field of the photoelements forms a matrix and that the excitation of each photoelement causes the appearance of a pair of numbers (j, k) at the input of the machine; here j and k respectively denote the numbers of the row and column which locate the particular

*The Pandemonium can develop several comprehensions simultaneously. In this paper we will describe a simplified Pandemonium network designed for developing just two mutually complementary comprehensions.

photoelement. In each row we take the excited photoelement with the smallest column number $k(j)_{min}$ and the excited photoelement with the largest column number $k(j)_{max}$, and then form the following half-sum for each j:

$$\bar{k}(j) = \frac{1}{2}[k(j)_{max} + k(j)_{min}]$$

Then we find the maximum half-sum with respect to j: $\max_j \bar{k}(j)$, and choose $f_j = \frac{\bar{k}(j)}{\max_j \bar{k}(j)}$ as function of the input situation. If not a single pair of numbers with any $\tilde{j}$ appears at the input of the machine when a certain object is "shown," then we shall assume that the value of the corresponding function is $f_{\tilde{j}} = 1$.

If the photoelements form a matrix with n rows and m columns, we shall have n functions

$$f_j = \frac{\bar{k}(j)}{\max_j \bar{k}(j)} \qquad (j = 1, 2, \ldots, n). \tag{3a}$$

Analogously, we form m functions

$$f_{n+k} = \frac{\bar{j}(k)}{\max_k \bar{j}(k)} \qquad (k = 1, 2, \ldots, m). \tag{3b}$$

We shall study the space $\{x\}$ with the coordinates $x_i = f_i$ $(i=1, 2, \ldots, n+m)$. In this space it is already possible to isolate patterns which are symmetrical with respect to the horizontal axis, patterns which are symmetrical with respect to the vertical axis, squares†, and triangles.

These examples demonstrate that the manner in which a machine with stimulation must operate is determined by the limitation imposed on the allowed classes of objects.‡

3. Machines Without Stimulation

Recently it has been determined that when certain additional limitations are imposed on the allowed classes of objects (these limitations are based on the statistics which govern the appearance of the object), it is possible to design machines which separate objects into classes without stimulation.

Up to now we have studied the following problem: the operator subdivides the entire set of objects into two classes; the machine, after a certain adaptive process, is required to subdivide these very objects into classes which coincide more or less exactly with the classes specified by the operator. Here we noted that the classes into which the operator subdivides the set of objects must satisfy certain limitations.

Now we shall study a different problem. A set of objects appears at the input of the machine; these objects are objectively (independently of the desires of the operator) subdivided into classes which satisfy the same limitations as those given in the preceding problem. The machine must subdivide the objects into these classes and provide the operator with information on objectively existing classes which were not known to the operator.

Both of these problems can be posed with respect to a machine without stimulation. And, although in principle the second problem is of greater interest, it is true that essentially the same machine can be used for solving both the first and second problems.

In order to clarify how either of these problems can be solved, we shall study the following simplest example. Assume that each object is made to correspond to a certain number x; assume also that on the x axis it is possible to find two nonintersecting segments $[x_1, x_2]$ and $[x_1', x_2']$ such that the numbers corresponding to objects of the same class belong to only one segment, and the numbers corresponding to objects of different classes belong to different segments.

† It is assumed that the axes of symmetry for a square coincide with one of the rows and one of the columns of the photoelement matrix.

‡ It should be noted that the general problem of developing comprehensions is closely associated with the far more difficult problem of formulating the space proper, as well as with the problem of separating two sets in a specified space, which is treated in this paper. This problem has evidently not been posed or solved in any acceptable form as yet.

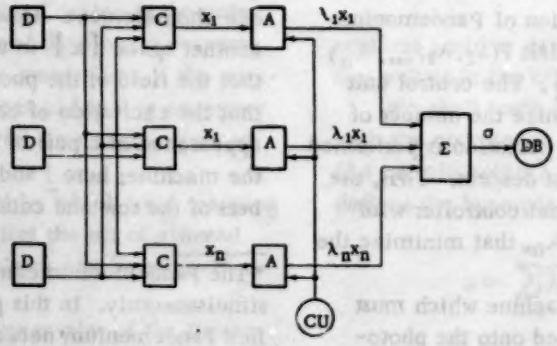

Fig. 1.

Assume further that the probability-density distribution f(x) for the appearance of objects with the coordinate $\underline{x}$ is specified. Then it is possible to establish relationships between the numbers x_1, x_2, x_1', x_2' (Fig. 2) and the properties of the probability-density function f(x), which are sufficiently general so that when the machine operates by comparing the average value $\bar{x}$ with the current value $\underline{x}$ (Fig. 3), it is capable of developing the specified comprehensions without any additional information from the operator.** This principle can be generalized to apply to multidimensional spaces.

The first to propose a self-adaptive machine without stimulation was F. Rosenblatt [2]. His machine (which he called the "Perceptron"††) operates according to a principle that differs from the one cited above. The shortcoming of the principle proposed by F. Rosenblatt is that the limitations imposed on the allowed classes of objects for which the Perceptron can operate are not natural ones and cannot be interpreted in convenient terms. However, since the Perceptron is the first constructed machine without stimulation, the subsequent sections of this paper will analyze the principle of operation of the Perceptron and certain problems in the theory of this operation.

4. The Perceptron Network‡‡

A Perceptron (Fig. 4) consists of a set of identical elements which are conditionally called neurons. A certain function $\underline{x}$ of the state of the detectors is applied to the input of each neuron at discrete instants n=0, 1, 2, . . ., corresponding to the instants at which the objects appear. Each neuron is an amplifier with a variable gain λ that changes at these same discrete instants. The increment of gain during one cycle is determined from the formula***

$$\Delta\lambda^n = \lambda^{n+1} - \lambda^n = (x^n - k\lambda^n)\, p^n, \qquad (4)$$

where $\underline{p}$ is the signal produced at the output of the next Perceptron stage, and $\underline{k}$ is a certain constant. The output of the neuron at the $\underline{n}$th instant is the quantity $\lambda^n x^n$.

All neurons are subdivided into two groups. Assume that there are l neurons in the first group and $\underline{m}$ neurons in the second group. We shall prime those quantities which refer to neurons of the second group. The variable p is the same for all neurons in one group. Thus, we obtain l + m relationships:

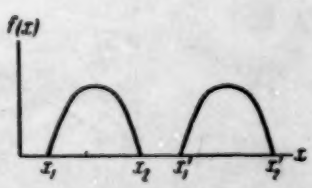

Fig. 2.

$$\Delta\lambda_i^n = (x_i^n - k_i\lambda_i^n)\, p^n \qquad (i = 1, 2, \ldots, l),$$

$$\Delta\lambda_j'^n = (x_j'^n - k_j'\lambda_j'^n)\, p'^n \qquad (j = 1, 2, \ldots, m). \qquad (4a)$$

The outputs of all the neurons are summed; the outputs of the neurons in the first group are taken with a plus sign, while the neurons in the second group are taken with a minus sign. The resulting sum

$$\sigma^n = \sum_{i=1}^{l} \lambda_i^n x_i^n - \sum_{j=1}^{m} \lambda_j'^n x_j'^n$$

is applied to the input of the decision element DE at each instant; the decision element has two outputs $\underline{p}$ and p' and operates according to the law

$$p^n = \begin{cases} 1 & \sigma^n \geqslant 0 \\ 0 & \sigma^n < 0, \end{cases} \qquad (4b)$$

$$p'^n = 1 - p^n.$$

Note that if the sequence of values acquired by the vector $x^n = (x_1^n, x_2^n, \ldots, x_l^n, x_1'^n, \ldots, \bar{x}_m'^n)$ and the initial value of the vector $\lambda^0 = (\lambda_1^0, \lambda_2^0, \ldots, \lambda_l^0, \lambda_1'^0, \ldots, \lambda_m'^0)$ are known, then Eqs. (4a) and (4b) completely define the value of the vector λ^n and the outputs p^n and p'^n of the decision element at all instants n = 0, 1, 2, ...

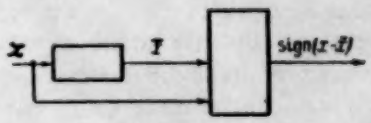

Fig. 3.

**For example, a sufficient condition is the validity of the inequalities

$$x_1 \int_{x_1}^{x_2} f(x)\,dx + x_1' \int_{x_1'}^{x_2'} f(x)\,dx > x_2,$$

$$x_2 \int_{x_1}^{x_2} f(x)\,dx + x_2' \int_{x_1'}^{x_2'} f(x)\,dx < x_1'.$$

Here $\int_{x_1}^{x_2} f(x)\,dx$ is the probability that an object belonging to the first class will appear, and $\int_{x_1'}^{x_2'} f(x)\,dx$ is the probability that an object belonging to the second class will appear.

††From the English word "perception"—perception, recognition.

‡‡The presentation of the Perceptron properties in this and subsequent sections differs from the corresponding treatment in [2].

***Here and throughout, the superscripts n, n+1, etc., indicate a corresponding instant; they are not exponents.

We shall study the $l + m$)-dimensional space $\{x\}$ with the coordinates $x_1, x_2, \ldots, x_l, x'_1, \ldots, x'_m$). Each object appearing at the input corresponds to a point in $\{x\}$. At each instant the equation

$$\sigma = \sum_{i=1}^{l} \lambda_i^n x_i - \sum_{j=1}^{m} \lambda_j'^n x'_j = 0$$

specifies a hyperplane in $\{x\}$ whose directional cosines are determined by the neuron gains (i.e., by the value of the vector λ^n). Since during the process involved in the appearance of the object at the Perceptron input λ^n varies in accordance with (4a) and (4b), it follows that the hyperplane $\sigma=0$ is "rotated" in some fashion.

At each instant n the appearance of $p^n=1$ at the Perceptron output corresponds to the appearance of an object whose coordinates lie on one side of the hyperplane; the appearance of $p'^n=1$ at the Perceptron output corresponds to the appearance of an object whose coordinates lie on the other side of the hyperplane. If, after a sufficiently large number of objects appear, the position of the hyperplane is stabilized (i.e., it merely "rocks" near a certain position), then the appearance of p=1 or p=0 at the output of the machine will determine the subdivision of the output into two classes in a more or less stable fashion; only objects whose coordinates are located in the "rocking" region will correspond first to p=1, then to p=0. Assume (as we have done throughout this paper) that the objective difference between the classes of objects resides in the fact that each class corresponds to a region in the space $\{x\}$; here these regions are governed by the limitations in Section 2. If

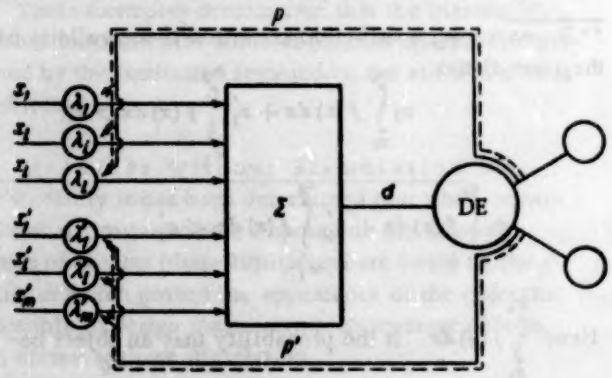

Fig. 4.

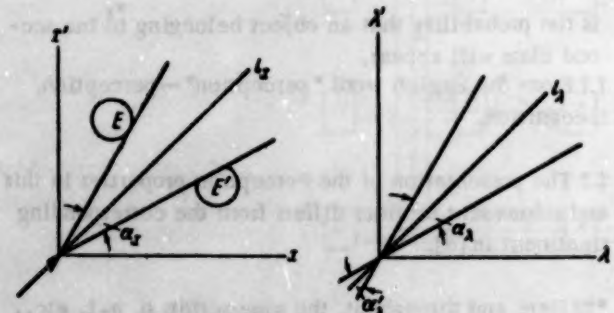

Fig. 5.

the subdivision of objects into two classes by the Perceptron corresponds to the separation of these regions, then this will indicate that the machine has developed a comprehension.

In the analysis below we shall demonstrate that the Perceptron is far from being able to develop a comprehension in this sense for all cases.

5. Certain Problems in the Theory of a Perceptron

We shall derive certain relationships which determine the process involved in the time variation of the vector λ. For simplicity we shall assume that there are two neurons with the gains λ and λ' and the inputs x and x'. However, it is obvious that if we treat x, x', λ, λ' as vectors, then the basic results remain valid.

Assume that the plane $\{x\}$ contains two regions E and E' which can be separated by the straight line l_x passing through the origin; then the set of these separating straight lines form the angle α_x (Fig. 5). As we have already noted in Section 2, each separating straight line l_x in the plane $\{\lambda\}$ corresponds to a straight line l_x passing through the origin; the set of separating lines which fills the angle α_x on the plane $\{x\}$ corresponds to the set of straight lines in the plane $\{\lambda\}$ that fills the two opposing angles α_λ and α'_λ (a "two-dimensional cone").

The problem which the machine must solve reduces to separating objects whose coordinates lie in the regions E and E'. Since all of the straight lines which separate these regions lie within the angle α_x on the plane $\{x\}$, it follows that the machine develops a comprehension only if the values of the neuron gains λ and λ' lie either solely within the angle α_λ or solely within the angle α'_λ on the plane $\{\lambda\}$ for most of the time after the adaptive process has been completed. Under these conditions the point (λ, λ') must not pass from α_λ into α'_λ (or vice versa after the adaptive process has been completed; this holds because if such a transition were to occur, the sign of σ would be changed, and on the basis of (4b) the alternate values p=1 and p=0 would correspond to the same region E (or E'); this is inadmissible.

Before we pass on to further derivations we shall study the simplest example which will show that in certain cases the Perceptron is actually capable of developing a comprehension (i.e., it is capable of performing

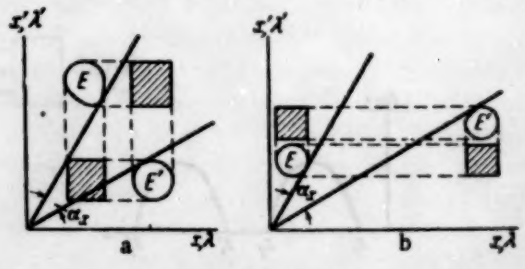

Fig. 6.

the necessary separation); it is also possible to encounter cases when the Perceptron is not capable of developing a comprehension.

Example. We shall study a Perceptron in which $k = k' = 1$. In accordance with (1), $\lambda = \tilde{x}$ and $\lambda' = \tilde{x}'$ at each instant; here $\tilde{x}$ is the x coordinate of the nearest preceding object for which $\sigma \geq 0$, and $\tilde{x}'$ is the x coordinate of the nearest preceding object for which $\sigma < 0$.

We shall superimpose the planes $\{x\}$ and $\{\lambda\}$ and shall assume for simplicity that the angle α_x is symmetrical relative to the bisectrix of the first quadrant. Then it is not difficult to see from the equation $\sigma = \lambda x - \lambda' x' = 0$ that the angle α_λ coincides with the angle α_x when the planes are superimposed (Fig. 6a). If the separation has been performed, then the point (λ, λ') must lie only in one of the shaded rectangles. It is obvious that if we shift the regions E and E' in such a way that the angles α_x and α_λ are not altered, it is possible to obtain shaded rectangles both inside and outside the angle α_λ (Fig. 6, a and b). However, if no rectangle lies inside the angle α_λ, then it is certain that separation is impossible.

We shall now continue our study of the general case. We shall assume that the sequence in which objects appear is random and that we know only the probability-density function $\varphi(x, x')$ for the appearance of an object with the coordinates (x, x'); the probability that a certain object will appear at a certain specified instant is not dependent on what has appeared previously.

Note that in this case the probabilities that the point (λ^n, λ'^n) will be shifted to the point $(\lambda^{n+1}, \lambda'^{n+1})$ depend solely on the current value of (λ^n, λ'^n) and are determined by the function $\varphi(x, x')$; i.e., the process consisting of the variation of (λ, λ') is a random Markov process.

Assume that we know how to determine $f_n(\lambda, \lambda')$ [this function is the probability-density function for (λ, λ') after n instants].

For each appearance of a new object a variation can occur either for λ only or for λ' only, since either $p = 0$ or $p = 1$ is mandatory. Therefore, only those points (λ, λ') for which either $\lambda = \tilde{\lambda}$ or $\lambda' = \tilde{\lambda}'$ can arrive at the point $(\tilde{\lambda}, \tilde{\lambda}')$ during one step. Here the point $(\lambda, \tilde{\lambda}')$ is transferred to the point $(\tilde{\lambda}, \tilde{\lambda}')$ if an object appears with the coordinates (x, x') satisfying the condition $\sigma = \lambda x - \tilde{\lambda}' x' \geq 0$ $(p = 1)$ and $x = \tilde{\lambda} - (1 - k)\lambda$; this result is valid on the basis of Eq. (4a). Analogously, the point $(\tilde{\lambda}, \lambda')$ is transferred to the point $(\tilde{\lambda}, \tilde{\lambda}')$ if an object appears with the coordinates (x, x') which satisfy the condition $\sigma = \tilde{\lambda} x - \lambda' x' < 0$ $(p = 0)$ and $x' = \tilde{\lambda}' - (1 - k')\lambda'$. The probability density for transfer from the point $(\lambda, \tilde{\lambda}')$ to the point $(\tilde{\lambda}, \tilde{\lambda}')$ is therefore equal to

$$\psi_1(\lambda, \tilde{\lambda}, \tilde{\lambda}') = \int \varphi(\tilde{\lambda} - (1 - k)\lambda, x')\, dx',$$

$$x'\tilde{\lambda}' \leqslant [\tilde{\lambda} - (1 - k)\lambda]\lambda,$$

where the integral is taken over all x' satisfying the condition

$$x'\tilde{\lambda}' \leqslant [\tilde{\lambda} - (1 - k)\lambda]\lambda.$$

The probability density for transfer from the point $(\tilde{\lambda}, \lambda')$ to the point $(\tilde{\lambda}, \tilde{\lambda}')$ is equal to

$$\psi_2(\lambda', \tilde{\lambda}, \tilde{\lambda}') = \int \varphi(x, \tilde{\lambda}' - (1 - k')\lambda')\, dx,$$

$$x\tilde{\lambda} < [\tilde{\lambda}' - (1 - k')\lambda']\lambda',$$

where the integral is taken over all x satisfying the condition

$$x\tilde{\lambda} < [\tilde{\lambda}' - (1 - k')\lambda']\lambda'.$$

The recursion relationship which determines the Markov process in the case under study is written as

$$f_{n+1}(\tilde{\lambda}, \tilde{\lambda}') = \int_{\lambda} f_n(\lambda, \tilde{\lambda}')\, \psi_1(\lambda, \tilde{\lambda}, \tilde{\lambda}')\, d\lambda + \int_{\lambda'} f_n(\tilde{\lambda}, \lambda')\, \psi_2(\lambda', \tilde{\lambda}, \tilde{\lambda}')\, d\lambda',$$

where the integrals are taken over all possible values of λ and λ', and the functions ψ_1 and ψ_2 are determined according to the expressions cited above.

The probability that the point (λ, λ') will be located within the angle α_λ after the nth instant is equal to

$$P_n((\lambda, \lambda') \in \alpha_\lambda) = \iint_{\alpha_\lambda} f_n(\lambda, \lambda')\, d\lambda\, d\lambda'. \qquad (6a)$$

The corresponding probability that the point will be located within the angle α'_λ is equal to

$$P'_n((\lambda, \lambda') \in \alpha'_\lambda) = \iint_{\alpha'_\lambda} f_n(\lambda, \lambda')\, d\lambda\, d\lambda'. \qquad (6b)$$

Here the integrals are taken over the regions belonging to the angles α_λ and α'_λ, respectively.

It is evident that the Perceptron develops the required comprehensions if after a sufficiently large number of different objects have appeared, there is established a sequence of distributions $f_n(\lambda, \lambda')$ such that either the value of P_n or the value of P'_n is close to 1 in the predominant number of cases. Quantitatively this condition can be expressed as follows: for each initial value (λ^0, λ'^0) we find a value of N such that for all $n > N$ either the inequality

$$\frac{\sum_N^n P_n}{n - N + 1} \geqslant 1 - \varepsilon, \qquad (7a)$$

or the inequality

$$\frac{\sum_N^n P'_n}{n - N + 1} \geqslant 1 - \varepsilon \qquad (7b)$$

will be satisfied.

It is possible to require that a more rigorous condition be satisfied: for each (λ^0, λ'^0) we must find an N such that for all $n > N$ we have either

$$P_n = 1 \qquad (8a)$$

or

$$P'_n = 1. \qquad (8b)$$

The validity of one of these conditions means that in the final analysis a sequence of probability-density functions $f_n(\lambda, \lambda')$ is established such that the point (λ, λ') never emerges beyond the limits of either the angle α_λ or the angle α'_λ; therefore the probability of error in the Perceptron becomes equal to zero.

It is considerably simpler to predetermine the ability of the Perceptron to satisfy one of the conditions (8a) or (8b) rather than one of the conditions (7a) or (7b). Assume that the adaptive process has been completed and that one of the conditions (8a), (8b) is satisfied. This means that the straight line $\sigma = 0$ passes rigorously between the regions E and E'. Therefore, in view of (4a), the value of λ can change only at those instants when $(x, x') \in E$, and that of λ', only at those instants when $(x, x') \in E'$; or conversely, the change is dependent on whether the point (λ, λ') is within the angle α_λ or within the angle α'_λ [i.e., whether condition (8a) or (8b) is satisfied]. Assume, for example, that condition (8a) is satisfied, and that λ changes in those cases when $(x, x') \in E$ (the remaining cases are treated analogously).

We shall now study only those instants $s = 0, 1, 2, \ldots$, at which an object with the coordinates (x, x') appears, instead of studying all instants; therefore, we assume that the value of λ changes. We shall choose some instant after the adaptive process has been completed as the initial instant; under these conditions the point (λ, λ') is already within the angle α_λ.

In accordance with the difference equation (4a),

$$\lambda^s = \sum_{j=0}^{s-1} (1-k)^{s-j-1} x^j + (1-k)^s \lambda^0. \dagger\dagger\dagger \quad (9)$$

The variables x^j are independent random quantities with identical probability-density functions that are equal to the conditional probability-density function for the condition $(x, x') \in E$:

$$\frac{\int_E \varphi(x, x')\, dx'}{\iint_E \varphi(x, x')\, dx\, dx'},$$

since the instants $s = 0, 1, 2, \ldots$ are by definition $(x, x') \in E$ at these instants.

Since λ^s is a linear function of independent random variables, it follows that

$$\bar{\lambda}^s = \sum_{j=0}^{s-1} (1-k)^{s-j-1} \bar{x}^j + (1-k)^s \lambda^0, \quad (10)$$

where the bar above a quantity denotes mathematical expectation. The series (10) converges only for the condition $0 < k < 2$; here

$$\lim_{s\to\infty} \bar{\lambda}^s = \bar{\lambda} = \frac{1}{k} \bar{x}. \quad (11)$$

From (9) it is also easy to derive the expression for the dispersion of the limiting probability-density function:

$$\lim_{s\to\infty} D(\lambda^s) = D(\lambda) = \frac{1}{2k - k^2} D(x). \quad (12)$$

Thus, knowing the arrangement of the regions E and E', it is possible to find the angles α_λ and α'_λ; knowing $\varphi(x, x')$, it is possible to determine λ, $D(\lambda)$ and to estimate whether λ^s is located solely within the angle α_λ.

mate whether λ^s is located solely within the angle α_λ.

We should pay attention to the fact that the dispersion D(x) in (12) is computed only for the region E. Equation (12) illustrates the part played by the feedback loops for the quantities p and p' (Fig. 4). If these relationships do not exist, then the quantity λ will change for the appearance of objects from both the region E and the region E'; the dispersion D(x) will then be computed over both regions. This will cause a pronounced increase in the dispersion of the limiting distribution and will mean that the probability of the emergence of the point (λ, λ') beyond the limits of the bounded angle α_λ will have increased.

We shall now pose the following problem: the operator has a priori subdivided the objects into two classes which satisfy the limitations cited in Section 2. Is it possible always to choose the statistic involved in the appearance of the objects in such a way that the Perceptron will perform the separation conceived of by the operator?

An analysis of the Perceptron operation shows that for certain additional conditions the Perceptron is capable of performing the separation conceived of by the operator (i.e., it is able to develop the required comprehensions). However, these conditions are not obvious.

The example cited above demonstrates the possibility that there may be no statistics of object appearance for which the Perceptron can perform the required separation.

In the general case the capacity of the Perceptron for developing the required comprehensions is determined by its structure (the value of the quantity k and the specific form of the function x), by the nature of the objects which are "shown" to the machine (the arrangement of the regions E and E'), and by the statistics governing the "showing" process (the form of the probability-density function for the appearance of the objects). In order to determine this capacity a priori for a specified structure and specified "showing" statistics, it is necessary to perform a computation using formulas (5), (6), (7); this process in itself requires the use of mathematical machines.

LITERATURE CITED

1. O. G. Selfridge, Pandemonium: A Paradigm for Learning. Symposium on the Mechanization of Thought Processes (England, November, 1958).
2. F. Rosenblatt, Two Theorems of Statistical Separability in the Perceptron. Symposium on the Mechanization of Thought Processes (England, November, 1958).

†††Here and throughout, $(1-k)^j$ denotes the jth power of (1-k).

CONTROLLING A SERVODRIVE USING ONE NULL INDICATOR WHICH PERFORMS THE FUNCTIONS OF TWO NULL INDICATORS

V. D. Vershinin

Moscow

Translated from Avtomatika i Telemekhanika, Vol. 21, No. 10,
pp. 1387-1392, October, 1960
Original article submitted April 4, 1960

The paper studies a network for summing the fine and coarse control signals; this network can be used to control a servodrive while simultaneously monitoring the accuracy of automatic tracking with only one null indicator.

In existing servodrives semiautomatic control and monitoring of the automatic tracking accuracy are achieved with two null indicators that are connected in parallel with the selsyn receivers (or other detecting elements).

The null indicators have different sensitivities with respect to the mismatch angle, and their pointers deviate in direct proportion to the envelope corresponding to the voltages from the fine and coarse detector elements:

$$\alpha_c = S\frac{U_m \sin\theta}{R_1}, \quad \alpha_f = S\frac{U_m \sin k\theta}{R_2},$$

where α_c, α_f are the deviation angles for the pointers on the null indicators for coarse and fine control, respectively; U_m is the maximum output voltage of the detector element; θ is the mismatch angle; R_1 and R_2 are the resistances in the signal-winding circuit of the null indicators; S is the slope of the characteristic for the null indicators; k is the transfer number between the detector elements for fine and coarse control.

The semiautomatic control of a servodrive using two null indicators is based on using an appropriate device (a semiautomatic control device) to achieve a constant alignment of the pointers of both null indicators with their zero positions. The basic difficulty in control of this type and in monitoring the tracking accuracy resides in the necessity for simultaneous observation of the pointers of two meters. In the analysis below we study a network for summing the fine and coarse signals; this network makes it possible to control the servodrive and to monitor the accuracy of the automatic tracking using a single null indicator.

The operation of the network (Fig. 1) is based on a nonlinear volt-ampere resistance characteristic; the fine control signal and a portion of the coarse control signal are limited by the nonlinear resistor NR formed by two solid-state rectifiers at the input of the null indicator. For a small mismatch angle the pointer of the null indicator is deflected basically by the fine control signal; for a large mismatch angle it is reflected basically by the coarse control signal. In order to avoid reverse deflection of the null indicator pointer when the phase of the fine control signal changes [i.e., when the value of the mismatch angle is in the range $\pi/k - 2\pi/k$ ($i = 1, 2, 3, \ldots$)], a branch with the resistor r_5 is introduced into the network. The resistor r_5 applies a voltage to the nonlinear resistance for maintaining the phase of the mismatch.

The Dependence of the Deflection Angle of the Null Indicator Pointer on the Mismatch Angle

The dependence of the deflection angle α of the null indicator pointer on the mismatch angle θ can be derived by making use of the mesh current method. In order to facilitate the derivation of this relationship, we neglect the inductive reactance of the null indicator signal winding, since it is small compared to the resistances of the loops; we shall assume that the shape of the current sinusoid (at the carrier frequency ω) is not distorted by the mismatch angle. Then

$$U_f = I_1(r_{i1} + r_1 + r_2 + r_3) + I_2(r_{i1} + r_1) - I_4(r_{i1} + r_1) + I_3 r_3,$$
$$U_f = I_1(r_{i1} + r_1) + I_2(r_{i1} + r_1 + r) - I_4(r_{i1} + r_1),$$
$$U_c = I_1 r_3 + I_3(r_{i2} + r_4 + r_3) + I_4 r_{i2},$$
$$U_c - U_f = -I_1(r_{i1} + r_1) - I_2(r_{i1} + r_1) + I_3 r_{i2} + I_4(r_{i1} + r_{i2} + r_5 + r_1),$$

where r is the static resistance of the NR and is determined from the volt-ampere characteristic; r_{i1}, r_{i2} are the resistances of the output windings in the detector elements.

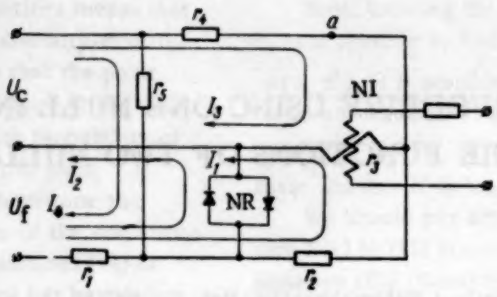

Fig. 1.

The determinant for the system of equations is

$$\Delta = \begin{vmatrix} A & C & r_3 & -C \\ C & B & 0 & -C \\ r_3 & 0 & D & r_{i2} \\ -C & -C & r_{i2} & F \end{vmatrix} = AB(DF - r_{i2}^2) - BFr_3^2 -$$

$$-C^2(AD + DF + BD - r_3^2 - r_{i2}^2 - 2r_3r_{i2}) + 2DC^3 - 2Br_3r_{i2}C,$$

where

$$A = r_{i1} + r_1 + r_2 + r_3, \qquad B = r_{i1} + r_1 + r,$$
$$C = r_{i1} + r_1, \quad D = r_{i2} + r_3 + r_4, \quad F = r_{i1} + r_{i2} + r_5 + r_1.$$

The current flowing through the signal winding of the null indicator is equal to $I = I_1 + I_3$, where $I_1 = \Delta_1/\Delta$, $I_3 = \Delta_3/\Delta$,

$$\Delta_1 = \begin{vmatrix} U_f & C & r_3 & -C \\ U_f & B & 0 & -C \\ U_c & 0 & D & r_{i2} \\ U_c - U_f & -C & r_{i2} & F \end{vmatrix} =$$

$$= U_f(BDF - Br_{i2}^2 - CDF + Cr_3r_{i2} + Cr_{i2}^2 - BDC + C^2D - Br_3r_{i2}) +$$
$$+ U_c(-Br_3F - BCr_{i2} + C^2r_{i2} + C^2r_3 + BDC - C^2D + Br_3r_{i2}),$$

$$\Delta_3 = \begin{vmatrix} A & C & U_f & -C \\ C & B & U_f & -C \\ r_3 & 0 & U_c & r_{i2} \\ -C & -C & U_c - U_f & F \end{vmatrix} =$$

$$= U_f(ABr_{i2} - BCr_{i2} + C^2r_{i2} - BFr_3 - ACr_{i2} + CFr_3 - C^2r_3 + BCr_3) +$$
$$+ U_c(ABF + 2C^3 - C^2B - AC^2 - C^2F - ABr_{i2} + r_3C^2 - BCr_3 + C^2r_{i2}).$$

Turning our attention to the deflection angle of the null indicator pointer instead of the current, we obtain

$$\alpha = SI, \qquad \text{or} \qquad \alpha = S\frac{U_f(Bm + N) + U_c(Bm_1 + N_1)}{Bm_2 + N_2},$$

where

$$m = DF - r_{i2}^2 - DC - r_3r_{i2} + Ar_{i2} - Cr_{i2} - Fr_3 + Cr_3,$$
$$N = -CDF + Cr_3r_{i2} + Cr_{i2}^2 + C^2D + C^2r_{i2} - ACr_{i2} + CFr_3 - C^2r_3,$$
$$m_1 = -r_3F - Cr_{i2} + DC + r_3r_{i2} + AF - C^2 - Ar_{i2} - Cr_3,$$
$$N_1 = C^2r_{i2} + C^2r_3 - C^2D + 2C^3 - AC^2 - C^2F + r_3C^2 + C^2r_{i2},$$
$$m_2 = ADF - Ar_{i2}^2 - Fr_3^2 - C^2D - 2r_3r_{i2}C,$$
$$N_2 = -C^2AD - C^2DF + C^2r_3^2 + C^2r_{i2}^2 + 2DC^3 + 2r_3r_{i2}C^2.$$

Here m_i, N_i are constant coefficients ($i = 0, 1, 2$).

The expression for the coefficient B includes $\underline{r}$ (the static resistance of the nonlinear element).

After replacing B with the expression $R_1 + \underline{r}$ (where $R_1 = r_{i1} + r_1$) and replacing U_c and U_f with the expressions $U_m \sin\theta$ and $U_m \sin k\theta$, we obtain

$$\alpha = SU_m \frac{\sin k\theta\,[(R_1 + r)\,m + N] + \sin\theta\,[(R_1 + r)\,m_1 + N_1]}{(R_1 + r)\,m_2 + N_2}. \quad (1)$$

This formula describes the dependence of the deflection angle of the pointer on the mismatch angle between the receiving and transmitting devices. The formula is inconvenient because it includes three variables: the mismatch angle θ, the deflection angle α of the pointer, and the static resistance r of the nonlinear element.

In formulating the function $\alpha = f(\theta)$ we shall assume that the shape of the current sinusoid flowing through the movable winding of the null indicator is not distorted by the variation of the mismatch angle (or by the variation in the position of the operating point on the volt-ampere characteristic of the nonlinear element).

In order to eliminate one of the variables from the latter formula, we must determine the function $r = f_1(\theta)$ or $r = f_2(\alpha)$. Obtaining either of these functions in explicit form presents a complex mathematical problem. However, it is not mandatory to have these functions in explicit form to formulate the function $\alpha = f(\theta)$. In order to find $r = f_1(\theta)$, we shall make use of a function that expresses the current I_2 through the nonlinear resistance in terms of the mismatch angle θ:

$$I_2 = \frac{\Delta_2}{\Delta},$$

where

$$\Delta_2 = \begin{vmatrix} A & U_f & r_3 - C \\ C & U_f & 0 - C \\ r_3 & U_c & D \quad r_{i2} \\ -C & U_c - U_f & r_{i2} \quad F \end{vmatrix} =$$

$$= U_f(-CDF + Cr_{i2}^2 + ADF - Ar_{i2}^2 - Fr_3^2 + C^2D + Cr_3^2 - ADC) +$$
$$+ U_c(C^2r_{i2} - C^2r_3 - ACr_{i2} + CFr_3 - C^2D - Cr_3^2 + ADC - Cr_3r_{i2}) =$$
$$= U_f Q + U_c w.$$

Then

$$I_2 = \frac{U_f Q + U_c w}{(R_1 + r)\,m_2 + N_2}. \quad (2)$$

As we know, the relationship between the current and voltage for nonlinear solid-state rectifiers is given by the formula

$$U_a = U_{an}\left(\frac{i_a}{I_{an}}\right)^{\beta_1},$$

where U_a, i_a are the instantaneous values of the forward voltage and current for the rectifier; U_{an}, I_{an} are the forward voltage and current for the rectifier when its class is specified [1].

Turning from the voltage to the static resistance of the rectifier in the forward direction, we obtain

$$\frac{U_a}{i_a} = \frac{U_{an}}{(I_{an})^{\beta_1}} \frac{i_a^{\beta_1}}{i_a} \quad \text{or} \quad r = Mi_a^{\beta_1 - 1},$$

where

$$M = \frac{U_{an}}{(I_{an})^{\beta_1}}.$$

In the case under study, $I_2 = \sqrt[P]{\frac{r}{M}}$, where $P = \beta_1 - 1$.

Substituting into Formula (2), we obtain

$$\sqrt[P]{\frac{r}{M}} = \frac{U_r Q + U_c w}{(R_1 + r)\,m_2 + N_2}$$

or

$$\lambda r\sqrt[P]{r} + l\sqrt[P]{r} = U_m(Q\sin kQ + w\sin\theta),$$

where

$$\lambda = \frac{m_2}{\sqrt[P]{M}}, \quad l = \frac{1}{\sqrt[P]{M}}(R_1 m_2 + N_2).$$

Specifying the value of r, we find the value of θ; then these two values are used in conjunction with Formula (1) to determine the deflection angle α of the pointer.

In Fig. 2 we have shown the dependence of the deflection angle α on the mismatch angle θ for two different cases (for a closed circuit and an open circuit at the point a in Fig. 1).

A Simplified Method for Computing the Network

In performing the computation (selecting the parameters), we assume the following parameters are known:

1. The maximum voltages applied to the detector elements, and the transfer number between detector elements.
2. The null indicator sensitivity and the resistance r_3 of the signal winding.
3. The volt-ampere characteristic of the nonlinear element.
4. The resistances of the output windings in the detector elements.
5. The mismatch angle θ within whose limits the null indicator pointer is deflected predominantly by the fine control signal.
6. The mismatch angle $\theta_2 - \theta_1$, within whose limits the pointer is deflected predominantly by the coarse control signal.
7. The deflection angles α_1 and α_2 of the pointer which correspond to the angles θ_1 and θ_2.

The angle θ_2 must be equal to the deflection angle of the pointer up to the pointer stop.

The voltage drop ΔU across the nonlinear resistance is made equal to or greater than the null indicator voltage drop corresponding to a pointer deflection angle α_1.

The resistance r_2 is computed from the formula $r_2 = S\frac{\Delta U}{\alpha_1} - r_3$. The derivation of the formulas for determining the resistors r_1 and r_5 is achieved on the basis of the following conditions:

$$\frac{U_m \sin k\theta_1 - \Delta U}{r_1 + r_{i1}} + \frac{U_m \sin \theta_1 - \Delta U}{r_5 + r_{i2}} = \frac{\Delta U}{r_{eq}}, \quad (3)$$

$$\frac{U_m \sin \theta_3}{r_5 + r_{i2}} = 2\frac{U_m}{r_1 + r_{i1}}. \quad (4)$$

Formula (3) is the condition for deflection of the pointer through the angle α_1 when the mismatch angle is θ_1 (excluding the effect of the current I_3). Formula (4) is the condition for elimination of the possibility of reverse deflection of the pointer when the fine-control detector element is rotated through approximately 270° from the matched position.

In Formulas (3) and (4),

$$\theta_3 = \sim \frac{270^\circ}{k}, \quad r_{eq} = \frac{(r_3 + r_2)r'}{r_2 + r_3 + r'},$$

where r' is the resistance of the nonlinear element at the knee of the volt-ampere characteristic.

After a series of simple transformations we obtain

$$r_1 = \frac{2B_1U_m - \varepsilon d r_{i1} + A_1\varepsilon}{\varepsilon d}, \quad r_5 = \frac{B_1}{d - \frac{A_1}{C_1}} - r_{i2},$$

where

$$A_1 = U_m \sin k\theta_1 - \Delta U, \quad B_1 = U_m \sin \theta_1 - \Delta U, \quad C_1 = r_1 + r_{i1},$$
$$\varepsilon = U_m \sin \theta_3, \quad d = \frac{\Delta U}{r_{eq}}.$$

The resistance r_4 is obtained from the formula

$$r_4 = \frac{U_m \sin \theta_2 - U_m \sin \theta_1}{\frac{\alpha_2 - \alpha_1}{S}}.$$

The network described above was checked under laboratory conditions. Here the network parameters were as follows: $r_1 = 100$ kohm, $r_2 = 1$ kohm, $r_4 = 20$ kohm, $r_5 = 10$ kohm.

The null indicator was a ferrodynamic instrument of the type "IF-2"; the nonlinear resistance was a selenium bar of the type "AVS-18-18" with shorted outer leads (the voltage drop across it was ~1.1 v). The signals were generated by a receiving device with "SS-405" selsyns. The transfer number between the selsyns was $k = 20$. The deflection angle of the null indicator pointer was $\alpha_1 = \sim 25°$ and corresponded to a mismatch angle of ~3°; the deflection angle $\alpha_2 = 45°$ corresponded to the mismatch angle $\theta_2 = 12°$.

Thus, our network for summing the signals permits automatic assurance of a high sensitivity to small mismatch angles (this is the function of a fine-control null indicator) and a low sensitivity to large mismatch angles (this is the part played by a coarse-control null indicator

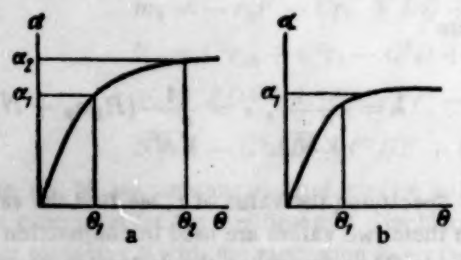

Fig. 2.

The fact that it is not necessary for the operator to shift his eyes from one null indicator to the other permits an improvement in the quality of semiautomatic control and makes it more convenient to monitor the accuracy of the automatic tracking. In addition, the construction of the mounting of the device is simplified, and more advantageous conditions are created for its protection from shock.

LITERATURE CITED

1. V. G. Komar, The Operation of Semiconductor Rectifiers in Control Circuits [in Russian] (Gosénergoizdat, 1952).

TAKING THE WEAK SURFACE EFFECT INTO ACCOUNT IN SWITCHING THE MAGNETIC STATE OF A FERROMAGNETIC PLATE

M. G. Vitkov

Moscow

Translated from Avtomatika i Telemekhanika, Vol. 21, No. 10,
pp. 1393-1400, October, 1960
Original article submitted March 25, 1960

The paper performs a quantitative investigation of the process involved in switching the magnetic state of sufficiently thin plane cores with rectangular hysteresis loops (for example, magnetic ribbons with a thickness of up to 3-5 μ). For thicker ribbons the qualitative picture is described. A criterion is established for the intensity of the magnetic skin effect; this criterion is a relative increase in the switching coefficient for the core. The results of the computations are compared with known experimental data on the magnetic switching of ribbon cores.

In various fields of automation and computing engineering, magnetic elements in the form of ribbon and sheet cores are widely used. Such cores are used, for example, in registers, in logic and memory cells, in decoders, etc. It is of interest to analyze the physical processes and the electrical computation method for the various types of pulsed magnetic circuits, while taking into account the effect of certain basic factors (the magneto-viscous properties of the core material, and eddy currents) which lead to closer coincidence between the computed results and the observed phenomena.

The problem of studying the effect of eddy currents for switching the magnetic state of cores with a rectangular hysteresis loop requires the solution of nonlinear differential equations.

For particular cases involving ribbon cores we use numerical integration methods [1]. The results are in good agreement with experimental data. In this paper we obtain an analytical solution of the problem. In general form such a solution may be obtained for the case of a weak surface effect, which is of special practical interest.

The presence of the surface effect leads to a prolongation of the magnetic switching process and to a change in its form. We derive an expression which is convenient for determining the prolongation time. The paper shows the dependence of this time on thickness and properties of the ribbon core material.

The problem is solved by the method of successive approximations used earlier for an analysis of the surface effect in ferrite ring cores. We shall cite the basic assumptions of this method and shall apply them to cores shaped in the form of a plate (Fig. 1). At the initial instant $t = 0$ the plate is magnetized in the direction of the y axis to an amount equal to the remanent flux density B_r. The magnetic switching is performed by an external magnetic field $H = H_e(t)$ which is applied along the y axis.

The magnetic switching process in the surface layers of the plate is determined exclusively by the magneto-viscous properties of the ferromagnetic. The change in magnetic state can be expressed in terms of a pulse Q of the switching magnetic field [2]:

$$Q = \int_0^t (H - H_0)\, dt, \tag{1}$$

$$\frac{\partial B}{\partial Q} = r_m\left(1 - \frac{B^2}{B_s^2}\right), \tag{2}$$

$$B = B_s \operatorname{th}\left(\frac{r_m}{B_s} Q - \varphi\right). \tag{3}$$

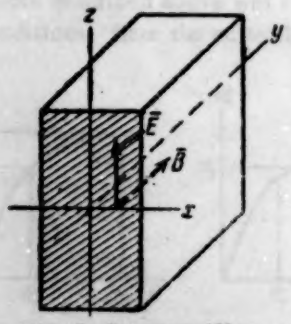

Fig. 1. Diagram illustrating the problem.

Here B_s is the saturation flux density; r_m and H_0 are experimentally determined parameters that characterize the dynamic magnetic properties of the core material; $\varphi = \mathrm{Arth}\frac{B_r}{B_s}$.

For the surface layers ($H = H_e$, $Q = Q_e$),

$$Q_e = \int_0^t (H_e - H_0)\,dt.$$

The graphs corresponding to Expressions (2) and (3) are plotted in Fig. 2, where the quantities B and Q_e are given in relative units. They describe the magnetic switching process $B = B_e(t)$ in the surface layers of the plate exactly. Analogous assumptions are also the basis of the computation performed in the widely known paper [3]; however, the authors of this paper made use of a coarser approximation of expression (2) in analyzing the surface effect: $\partial B/\partial Q = \mathrm{const}^*$. Such an assumption can be justified for a strong surface effect (in cores with a ribbon thickness of the order of 100 microns).

The magnetic switching in the inner layers is related to the external magnetic field pulse in a more complex fashion. It is necessary to take into account the screening effect of the eddy currents. The eddy currents induced during the magnetic switching of the plate produce an additional pulse Q_{in} for the inner layers, and thus, $Q = Q_e + Q_{in}$.

In order to take the eddy currents into account we make use of the integral form of the electrodynamics equations. Assuming that in a first approximation the value of the flux density B is constant over the cross section for the case of a weak surface effect, we proceed to solve the problem in the following approximation. From the first Maxwell equation we obtain the first approximation for the intensity of the induced electric field:

$$E = x\frac{\partial B}{\partial t}.$$

The induced field is directed along the z axis. It causes eddy currents whose density J (taking the displacement currents into account) is determined by the electrical properties of the material: the conductivity σ and the permittivity ϵ:

$$J = x\left(\sigma + \varepsilon\varepsilon_0\frac{\partial}{\partial t}\right)\frac{\partial B}{\partial t}.$$

The magnetic field is computed from the total-current law, while taking the boundary conditions ($H = H_e$) at the surface of the plate into account:

$$H = H_e - \frac{1}{2}(b^2 - x^2)\left(\sigma + \varepsilon\varepsilon_0\frac{\partial}{\partial t}\right)\frac{\partial B}{\partial t},$$

where b is one-half the thickness of the plate whose magnetic state is switched.

Thus, in a first approximation the magnetic switching pulse produced by the field depends on the depth of the layer in the plate. The magnitude of the pulse can be derived on the basis of (1) by integrating the expression above for H with respect to t:

$$Q_{in} = -\frac{1}{2}(b^2 - x^2)\left(\sigma + \varepsilon\varepsilon_0\frac{\partial}{\partial t}\right)(B + B_r). \quad (4)$$

The correction for the first approximation consists of a correction proportional to the conductivity of the ferromagnetic:

$$Q_\sigma = -\frac{1}{2}(b^2 - x^2)\sigma(B + B_r), \quad (5)$$

and a correction which depends on the permittivity. The latter component can be written in the following form if we take (2) into account:

$$Q_\varepsilon = -\frac{1}{2}(b^2 - x^2)\,\varepsilon\varepsilon_0 r_m\left(1 - \frac{B^2}{B_s^2}\right)(H - H_0). \quad (6)$$

* In terms of the notation used in [3], $\partial B/dQ \equiv f(B)$.

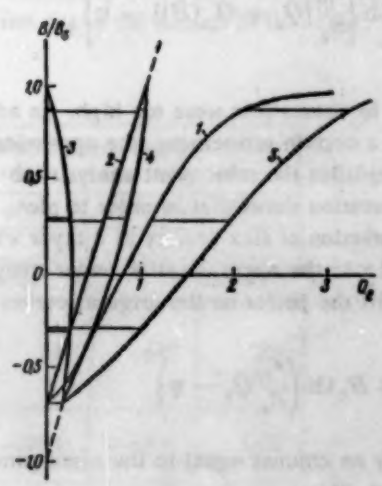

Fig. 2. Basic graphs:

$1 - B_e = B_s\,\mathrm{th}\left(\frac{r_m}{B_s}Q_e - \varphi\right)$,

$2 - Q_\sigma = Q_\sigma(B)$,

$3 - Q_\varepsilon = Q_\varepsilon(B)$,

$4 - Q_{in} = Q_\sigma + Q_\varepsilon$,

$5 - B = B_s\,\mathrm{th}\left\{\frac{r_m}{B_s}(Q_e + Q_{in}) - \varphi\right\}$

Thus, both corrections to the pulse are expressed as a function of the flux density B. Expression (5) in Fig. 2 corresponds to the straight line 2 whose angle with the flux density axis is proportional to the conductivity of the ferromagnetic, and increases as the layer under study is further removed from the surface of the plate. For the surface layer the angle which the straight line 2 makes with the B axis is equal to zero ($x^2 = b^2$). For the axial layer of the plate it is a maximum ($x^2 = 0$).

The graph of the function (6) is a quadratic parabola (Curve 3 in Fig. 2) which intersects the axis of ordinates at the points ±1. The maximum value of this correction increases with the intensity of the magnetic switching field. An interesting feature of this correction is its rapid tendency toward zero at the beginning and end of the magnetic switching process. This explains the fact that the effect of the permittivity on the time required for completing the magnetic switching process is weakened.

The simplicity of expressions (5) and (6) permits easy plotting of the corresponding graphs for the chosen value of $\underline{x}$. By the same token it is easy to plot the graph of the total correction (4) for a definite value of $\underline{x}$ (Curve 4 in Fig. 2).

An important problem is the appropriate choice of the values of flux density in Formulas (4), (5), and (6). The simplest approach is to choose this value equal to the magnitude of the surface flux density $B = B_e$.

Since the magnitude of the flux density actually decreases with the depth of the layer, such a computation in a first approximation yields values of flux density that are too low. The computation will be somewhat more exact if we choose a value of flux density equal to the flux density in the axial layer for use in Formulas (4), (5), and (6). Here the result obtained in the first approximation will yield values of flux density that are too high for the individual layers.

We chose a somewhat improved form of the approximation:

$$B = B_s \operatorname{th}\left\{\frac{r_m}{B_s}[Q_e + Q_{in}(B)] - \varphi\right\},$$

which also resulted in values that were too high. In addition to achieving a certain refinement, the approximation form above simplifies the subsequent analysis substantially. The expression shows that in order to plot the graph for the variation of flux density in a layer with a specified value of $\underline{x}$ in the approximation under study, it is sufficient to shift the points on the original curve:

$$B_e = B_s \operatorname{th}\left(\frac{r_m}{B_s} Q_e - \varphi\right)$$

along the Q_e axis by an amount equal to the corresponding value of Q_{in} (Fig. 2).

The error of the approximation can easily be estimated. It does not exceed the value $50\left(\frac{B_e - B}{B_e - B_r}\right)^2$ %, where the values of the flux densities B and B_e are taken for one value of time (Fig. 2).

Figure 3 shows the corresponding computation for the case of surface effect in a thin Permalloy sheet of the type "79-NM" which was 5 μ thick. [See Appendix for "79-NM" characteristics.] In that case the surface effect is sufficiently weak, and the approximation under study assures an accuracy of approximately 10%.

The analysis of the surface effect is simplified for the case of metal ferromagnetics in which the displacement currents can be neglected compared to the conductivity currents, right up to frequencies in the optical spectrum [4]. In that case the correction of the pulse is determined basically by the linear component of (5). This case also includes the example of a Permalloy plate cited above. The magnetic switching curves for different layers in a metallic ferromagnetic (as obtained in the approximation under study) have an interesting property. The tangents to these curves always intersect at one point lying on the straight line $B = -B_r$ (Fig. 3) when they are drawn to points with an arbitrary fixed value of flux density. A definite point corresponds to each value of flux density $B(-B_r \leq B \leq B_s)$. This property makes it possible to compute the magnetic switching rate $\partial B_x / \partial Q_e$ for a layer with the coordinate x in terms of the known function of the magnetic switching rate in the surface layer $\partial B_e / \partial Q_e$.

For a flux density B_x in the layer $\underline{x}$,

$$\frac{\partial B_x}{\partial Q_e} = \frac{\partial B_e}{\partial Q_e}\left(1 + \frac{\partial B_e}{\partial Q_e}\frac{b^2 - x^2}{3}\sigma\right)^{-1}, \qquad (7)$$

where the quantity $\partial B_e / \partial Q_e$ is determined by substituting $B_e = B_x$ into expression (2).

In order to compare the computations above with experimental data, it is necessary to make the transition

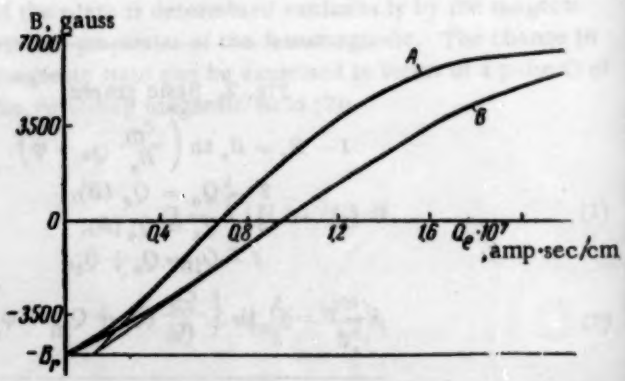

Fig. 3. Surface effect in a Permalloy ribbon. A) Magnetic switching of the surface layer; B) magnetic switching of the central layer.

to the experimentally observed average values of flux density, since the emf in the metering winding is proportional to the rate of change of the average flux density. In the approximation under study we have

$$\max\left(\frac{\partial B_{av}}{\partial Q_e}\right) = \frac{r_m}{1 + r_m\sigma\frac{b^2}{3}}, \qquad (8)$$

with an accuracy of no less than 12.5 $(r_m\sigma b^2)^2\%$; i.e., the maximum rate of change of the average flux density is

$$\max\left(\frac{\partial B_{av}}{\partial t}\right) = \frac{r_m}{1 + r_m\sigma\frac{b^2}{3}}(H_e - H_0). \qquad (8a)$$

The maximum value of the magnetic switching rate is achieved for an average core flux density

$$B_{av.m} = -\frac{r_m\sigma b^2 B_r}{3}\cdot\frac{1}{1 + r_m\sigma\frac{b^2}{3}}. \qquad (9)$$

The approximate expressions (8) and (9) can be used for the independent determination of the parameter r_m from the experimental data for $(\partial B_{av}/\partial Q_e)$ or $B_{av.m}$ that are obtained when a plate made of a known metallic magnetic material is subjected to magnetic switching.

In order to check expressions (8) and (9) we make use of the results obtained from an investigation of ribbon cores made of Permalloy "79-NM" ribbon 10 and 20 μ thick [1]. The surface effect in such cores is quite pronounced. Nevertheless, as we shall demonstrate below, Formulas (8) and (9) are in good agreement with experimental results. We shall write the known characteristics for "79-NM" Permalloy:

B_s = 7000 gauss; B_r = 4900 gauss; $\sigma = 1.8\cdot10^4$ 1/ohm·cm.

In order to select the value of r_m we shall make use of the results obtained by V. L. Dyatlov, who performed an exact numerical integration for the problem. In [1] the value r_m = 950 ohm/cm was obtained. The results of the experiments and computations are cited in the table.

In conclusion we shall estimate the most important characteristic of ribbon cores – the duration of the magnetic switching – in the approximation used above. When there is no surface effect, this duration is determined completely by the magnetoviscous properties of the core. The theoretical duration of the magnetic switching given by expression (3) is infinite. Therefore in practice we use the concept of the duration required to reach a steady state at some level. We often choose the average value of the flux density over the cross section $B_{av} = B_r$ as this level. The time t_r required for the magnetic switching process to reach this level is assumed to be the duration of the process. Expression (3) permits easy determination of the field pulse Q_r corresponding to this time (on the assumption that there is no surface effect):

$$Q_r = 2\frac{B_s\varphi}{r_m}.$$

When the surface effect is present, the magnetic switching process in the core terminates at the level $B_{av} = B_r$ for a field pulse which is increased by the amount $-Q_{in}(B_r)$:

$$Q_{in} \approx -\frac{2}{3}b^2\sigma B_r.$$

Thus, the relative increase in the pulse required for reaching completion of the magnetic switching at the specified level is

$$\frac{|Q_{in}|}{Q_r} \approx \frac{b^2}{3}\frac{B_r}{B_s}\frac{r_m\sigma}{\varphi}. \qquad (10)$$

Expression (10) determines the relative increase in the switching coefficient for the core. For magnetic switching of a core by means of rectangular current pulses (here it is possible to assume that $H_e - H_0 \approx$ const), relationship (10) also determines the relative prolongation Δt_r of the pulse. In that case,

Compared quantity	Ribbon core with thickness 2b			
	2b=10 μ		2b=20 μ	
	computed	experiment	computed	experiment
$\max\left(\frac{\partial B_{av}}{\partial Q_e}\right)$, ohm/cm	400	500	140	280
$B_{av.m}$, gauss	—2860	—2000	—4200	—3500

$$\frac{\Delta t_r}{t_r} \approx \frac{b^2}{3} \frac{B_r}{B_s} \frac{r_m \sigma}{\varphi}. \quad (11)$$

Expression (11) shows that the relative prolongation of the switching time due to eddy currents is in a first approximation independent of the magnetic switching rate and directly proportional to the square of the plate thickness.

For the case of ribbon cores with the parameters cited above, computation according to Formula (11) leads to the following values for the relative prolongation of the magnetic switching time: 28% for a thickness of 5 μ; 110% for a thickness of 10 μ.

These results can be used in designing magnetic elements for computer-decision units.

Expression (11) permits us to compute the allowable thickness of ribbon cores which assure the maximum rate of recording and readout of information.

The recommended plotting of the graph for the dependence of the average magnetic flux density in the core on the magnetic switching pulse can be made the basis of the electrical design for pulse networks with ribbon cores (for example, magnetic registers).

APPENDIX

We shall prove certain propositions cited in the paper.

1. We shall derive Formula (7). Assume that the curve $B_e = B_e(Q_e)$ is given. We shall study a new curve $B = B(Q_e)$ which is obtained from the first curve by shifting its points along the axis Q_e by the amount $f = f(B)$. Here $f(B)$ is a specified function of B. The curve $B(Q_e)$ is obtained by replacing the argument Q_e by the argument $Q = Q_e - f(B)$ in the curve $B_e(Q_e)$:

$$B(Q_e) = B_e[Q_e - f(B)].$$

Differentiating this equation, we obtain

$$\frac{\partial B(Q_e)}{\partial Q_e} = \frac{\partial B_e[Q_e - f(B)]}{\partial [Q_e - f(B)]} \frac{\partial [Q_e - f(B)]}{\partial Q_e}.$$

Thus,

$$\frac{\partial B}{\partial Q_e} = \left[1 - \frac{\partial f(B)}{\partial B} \frac{\partial B}{\partial Q_e}\right] \frac{\partial B_e}{\partial Q_e}\bigg|_{Q_e - f(B)}.$$

From the equation above we obtain

$$\frac{\partial B}{\partial Q_e} = \frac{\partial B_e}{\partial Q_e} \left[1 + \frac{\partial f(B)}{\partial B} \frac{\partial B_e}{\partial Q_e}\right]^{-1},$$

where the derivatives are taken for the identical fixed value $B = B_e$. The substitution $f(B) = -Q_\sigma \equiv \frac{b^2 - x^2}{2} \times \sigma (B + B_r)$ leads to (7).

2. We shall show that for a weak surface effect the the flux density, averaged over the cross section of the core, is approximately equal to the flux density in a certain layer—the layer located at a distance $x = b/\sqrt{3}$ from the axis. In a linear approximation,

$$B(Q_2) = B(Q_1) + (Q_2 - Q_1) \frac{\partial B}{\partial Q},$$

where Q_1 and Q_2 are the values of the external field pulse at any instants which are sufficiently close together. Assuming $Q_1 = Q_e - Q_{in}$ and $Q_2 = Q_e$, we arrive at a convenient expression which relates the values of the flux density in the surface layer and in the layer corresponding to the specified value of the eddy current field pulse:

$$B(Q_e) = B(Q_e - Q_{in}) + Q_{in} \frac{\partial B_e}{\partial Q_e} = B_e(Q_e) + Q_{in} \frac{\partial B_e}{\partial Q_e}. \quad (12)$$

Equation (12) can easily be averaged if we keep in mind the face that only the term Q_{in}, which is proportional to $(b^2 - x^2)/2$ according to (4), is dependent on x:

$$B_{av}(Q_e) = \frac{1}{b} \int_0^B \left[B_e(Q_e) + Q_{in} \frac{\partial B_e}{\partial Q_e}\right] dx =$$

$$= B_e(Q_e) - \frac{b^2}{3} \left(\sigma + \varepsilon\varepsilon_0 \frac{\partial}{\partial t}\right)(B_e + B_r). \quad (13)$$

Expression (13) is equal to (12) for $Q_{in} = Q_{in}(x)$ when $x = b/\sqrt{3}$; this is what we set out to prove.

Assuming $B_e = 0$ and $Q_{in} = Q\sigma$ in (13), we arrive at the approximate expression (9).

TRANSLATOR'S APPENDIX

The characteristics of the permalloy "79-NM" are the following: thickness 0.01 mm; initial permeability μ_0 (in gauss/oe) not less than 15,000; maximum permeability μ_{max} (in gauss/oe) not less than 65,000; coercive force H_c (in oe) 0.07; saturation flux density B_s (in gauss) not less than 7,500. (See also "Characteristics of Magneto Materials for Use in Magnetic Amplifiers Operating at Audio-frequencies," Automation and Remote Control, Vol. 18, No. 10, pp. 927-933.)

LITERATURE CITED

1. V. L. Dyatlov, "Consideration of the eddy currents and viscosity for magnetic switching of ribbon cores in large fields," Nauchnye Doklady Vysshei Shkoly, Élektromekhanika i Avtomatika No. 2 (1959).
2. Yu. M. Shamaev, V. L. Dyatlov and A. I. Pirogov, "Dynamic characteristics of ferrites," Nauchnye Doklady Vysshei Shkoly, Élektromekhanika i Avtomatika No. 1 (1959).
3. T. C. Chen and A. Papoulis, "Terminal properties of magnetic cores," Proc. IRE 46, I No. 5 (1958).
4. L. Landau and E. Lifshits, Electrodynamics of Solid Media [in Russian] (Gostekhizdat, 1957).

SELECTION OF THE MOST SUITABLE CIRCUIT FOR A PHOTOELECTRIC FLUXMETER

I. G. Gutovskii

Moscow

Translated from Avtomatika i Telemekhanika, Vol. 21, No. 10, pp. 1401-1409, October, 1960
Original article submitted March 10, 1960

This article presents the theory of photoelectric fluxmeters (PEF), i.e., amplifiers with photoelectric optical amplification. Various types of PEF with and without feedback are compared. It is shown that the greatest accuracy of integration and the greatest speed can be achieved with a PEF circuit with negative feedback with respect to the derivative with the smallest time constants in the open circuit. The proposed theory makes it possible to determine the integration accuracy in dependence on the signal shape directly with respect to the curves recorded at the output.

At the present time, the so-called photoelectric optical amplifiers (PEOA)* [1] are being used to an ever increasing extent as dc amplifiers in various measuring and automation circuits.

The principle of photoelectrical optical amplification consists in using the galvanometer of the magnetoelectric system at the input and in converting the displacement of the galvanometer light spot into voltage by means of an optical system and a photocell bridge [2].

The extremely low input noise level ($\sim 10^{-9}$–10^{-10} v) and the large amplification factor (up to 10^8 for voltage) make it possible to use PEOA in devices where ordinary electronic amplifiers cannot be utilized.

A particular example of such a device is the photoelectric fluxmeter (PEF) [3]–an integrating amplifier based on PEOA–for measuring magnetic fluxes or electric charges. The considerably greater sensitivity and accuracy, as well as a longer allowable measurement time in comparison with ordinary fluxmeters, render the PEF a valuable instrument in scientific-research work and automation.

The face that different PEF circuits are recommended in literature (see survey [3]) and a lack of comparative evaluations of their efficiency create a pressing problem, which is to be solved by theoretical analysis of the existing variants for the purpose of selecting the variant most suitable for practical application.

The PEF theory presented in this article is a development of the method described in [4], which is based on operational calculus [5].

PEF Circuits and Their Relation to Integrating Amplifier Circuits

The block diagrams of PEF are identical with the basic integrating amplifier circuits [6], which have been developed independently and mainly before the PEF circuits†.

Figure 1 shows an integrator circuit with a negative series feedback with respect to the derivative. This integrator pertains to the overwhelming majority of the PEF circuits described in literature. The wiring diagram of such PEF is given in Fig. 2 and has been described in [3] and [7]. The time constants of the amplification circuit (without taking into account the feedback) of this PEF variant are rather small [8], and, in the first approximation, this circuit can be considered as an ideal amplifier

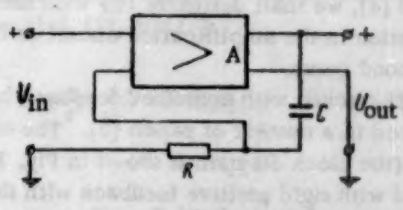

Fig. 1. Circuit of the RC-integrator with a negative series feedback.

* There are now greater opportunities for the application of PEOA, since the industry has started the mass production of amplifiers of this kind (F17 and F117).

† The actual differentiating circuit in the feedback loop is of no importance. For the sake of clarity, we shall use an RC circuit throughout.

The R_kC_k circuit mainly serves for ensuring stability.

The "+" and "–" signs in Figs. 1–5 conventionally indicate the presence or absence of a 180 deg phase shift of the output voltage with respect to the input voltage in the amplification circuit of the open-loop system.

with a constant amplification factor [9]. In [3] and [4], PEF of this type were called PEF of the first group.

The prototype of a PEF without feedback, which has been proposed by S. P. Kapitsa [10], has an integrating amplifier (Fig. 3). This device uses the principle of integration by means of a RC_k circuit with a decoupling amplifier A, where the usual resistance is replaced by a higher-the dynamic resistance R of the amplifier A_1 output tube. The introduction of a dynamic resistance increases the time constant $T_0 = RC_k$ of the integrating circuit and brings the operating conditions of the circuit section, which is the input section with respect to the C_k capacitor, closer to the operating conditions of the current generator. In Kapitsa's PEF, PEOA plays the role of the A_1 amplifier, and the dynamic resistance of vacuum photocells ($\rho \approx 10^9$ ohm, $T_0 \approx \rho C_k \approx 1000$ sec) plays the role of the tube dynamic resistance.

The application of negative feedback with respect to the derivative in Kapitsa's model leads to a circuit which is identical to circuits of PEF of the first group (Fig. 2), but is characterized by a larger capacitance C_k (almost by three orders of magnitude).

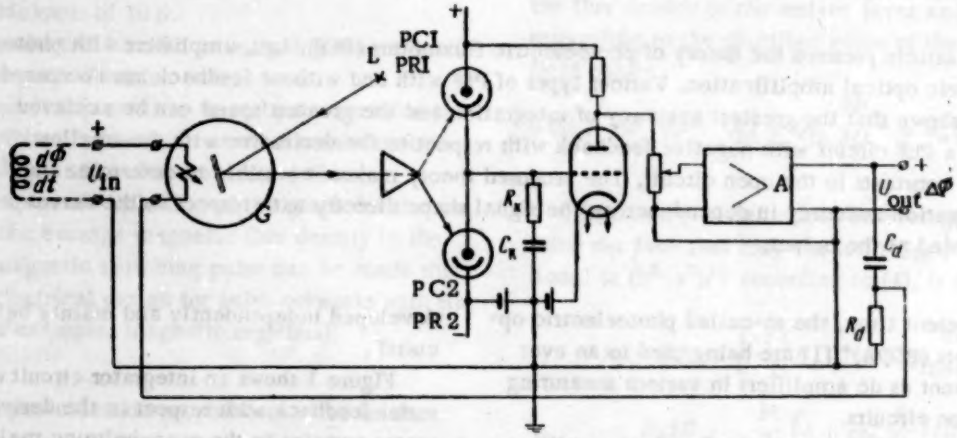

Fig. 2. PEF wiring diagram which is similar to that in Fig. 1. G) Galvanometer; L) illuminator which projects the light spot image on the photocells (PC) or the photoresistors (PR); A) electronic power amplifier; Φ) magnetic flux to be measured.

The integrating regime in the amplification circuit can also be secured by other means [11]. According to [3] and [4], we shall designate PEF with feedback and integration in the amplification circuit as fluxmeters of the second group.

PEF circuits with combined feedback have been described in a number of papers [3]. The circuit in Fig. 2 (the block diagram is shown in Fig. 1) is supplemented with rigid positive feedback with the coefficient $A_0 = r_2/(r_1 + r_2)$ (Fig. 4).

The most widely used circuit for analog computer integrators is the circuit with parallel feedback (Fig. 5). By using Kirchhoff's laws, it can be readily shown that, in contrast to the circuit in Fig. 1, the feedback of Fig. 5 does not reduce the input load current. Since this current lowers the magnetic measurement accuracy, the circuit given in Fig. 5 is not used in PEF designs.

The circuit shown in Fig. 2, supplemented with positive feedback in the general case (Fig. 4), will be used as the basis hereafter. All particular circuit variants can be obtained by eliminating some of the circuit elements‡ or by changing the numerical value of individual parameters.

Basic Approximations of the PEF Theory

In the proposed PEF theory, it is assumed that all directional elements, as well as amplitude distortions and loads, are absent. In particular, it is assumed that the

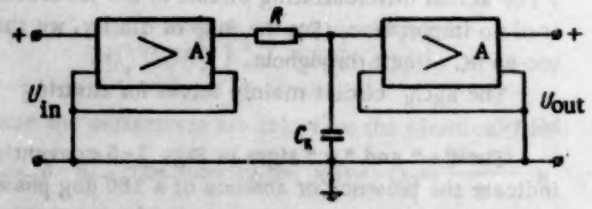

Fig. 3. Circuit of a RC-integrator using the dynamic resistance R of the amplifier A_1 output stage.

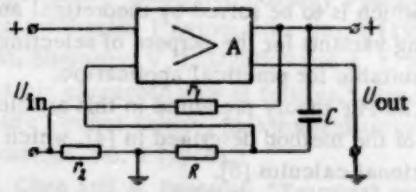

Fig. 4. Wiring diagram of a RC-integrator with combined feedback.

‡ Thus, for instance, Kapitsa's circuit without feedback is obtained by eliminating the feedback circuit.

connection of a measuring coil and an output instrument does not affect the PEF operation.

The conditions which the parameters of the loads to be connected must satisfy if the presented theory is to remain valid, as well as the justification of the other assumptions, will have to be treated in a separate paper.

Notation and the Basic Equations

The practical system of units is used throughout.

The electromotive force U_{in} induced in the measuring circuit or any voltage supplied to the instrument input is taken as the PEF input. The output voltage U of the amplifier A is at the same time the PEF output; f is the difference of light fluxes incident on the photocells of the photocell bridge; v is the bridge diagonal voltage; v_r is the feedback voltage; v_d is the same voltage without feedback and without taking into account the capacitor C_d leakage; t and θ are time; s is the differentiation operator.

The operator conductances (transfer functions) of the elements are given below.

1. Mirror galvanometer with an optical lever (see [11] and [12]). If we take into account the inductance of the measuring circuit,

$$W_g(s) = \frac{NS_u}{(\tau_0 s + 1)(Hs^2 + Gs + 1)}, \qquad f = W_g U_{in} \quad (1)$$

In practice, the τ_0, H, and G parameters are close to the measuring circuit time constant ($\tau_0 \approx L/R$, where L is the inductance, and R is the resistance), to $1/\omega_0^2$, and to $2\beta/\omega_0$ (ω_0 is the galvanometer natural frequency, and β is the damping coefficient), respectively. Moreover, in Eq. (1), N is the optical system conversion factor in lumens per radian; S_u is the galvanometer sensitivity in radians per volt for the chosen operating conditions.

As a rule, the galvanometer is overdamped**, and the measuring circuit inductance is neglected. Then

$$W_g(s) = \frac{NS_u}{(\tau_1 s + 1)(\tau_2 s + 1)}, \qquad \tau_1\tau_2 = H, \quad \tau_1 + \tau_2 = G, \quad \tau_1 > \tau_2. \quad (1a)$$

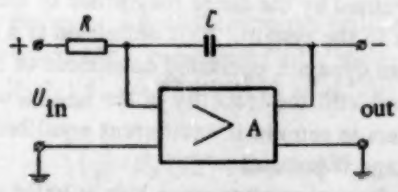

Fig. 5. Wiring diagram of a RC-integrator with parallel negative feedback.

2. Photocell bridge (vacuum photocells FE or photoresistors FS [7]). A stabilizing (correcting) R_kC_k circuit is connected to the bridge circuit:

$$W_m(s) = \alpha\rho\frac{\tau_4 s + 1}{\tau_3 s + 1}, \qquad v = W_m f. \quad (2)$$

Here, α is the FE sensitivity (amp/lu), ρ is their dynamic resistance,

$$\tau_3 = \tau_4 + \tau_5, \qquad \tau_4 = R_kC_k, \qquad \tau_5 = \rho C_k.$$

3. Direct current amplifier (the amplifier inertness is neglected):

$$W_a = k = \text{const}, \quad U = W_a v. \quad (3)$$

4. Differentiating element (without leakage and without taking into account the load [13]):

$$W_d(s) = \frac{\tau_d s}{\tau_d s + 1}, \qquad v_d = W_d U, \quad (4)$$

where $\tau_d = R_dC_d$, R_d is the circuit resistance, and C_d is its capacitance.

5. The feedback operator (Fig. 4):

$$W_r(s) = W_d + \frac{R_d}{R_{du}} - A_0 = W_d - A, \quad (5)$$

where R_{du} is the resistance of the C_d capacitor leakage, and $A_0 = r_2/(r_1 + r_2)$ is the positive feedback coefficient. Equation (5) follows from Fig. 4.

The open-circuit operator (without feedback) is obtained from (1a), (2), and (3):

$$W_0(s) = W_g W_m W_a = K_0 w_0(s), \qquad U = W_0 U_{in} \quad (6)$$

Here,

$$K_0 = S_u N \alpha \rho k = \text{const}, \qquad w_0(s) = \frac{\tau_4 s + 1}{(\tau_1 s + 1)(\tau_2 s + 1)(\tau_3 s + 1)}. \quad (7)$$

We shall introduce the PEF constants C_{φ_0} and C_φ so that, with an accuracy to the basic errors, $\int_0^t U_{in}\, d\theta = C_{\varphi_0} U$ for PEF without feedback (including PEF of the first group with an open circuit, for which the integration error exceeds $C_{\varphi_0}U$); also $\int_0^t U_{in}\, d\theta = C_\varphi U$ when feedback is

** This is mainly connected with the requirement for greater vibration stability of the instrument during zero adjustment (with the C_d capacitor short-circuited).

present.

We shall also introduce the creep time constants†† T and T_r for PEF with feedback and T_0 for PEF without feedback. It will become clear later on that

$$T = K_0 C_\varphi, \qquad C_\varphi = \tau_d + C_{\varphi_0}. \tag{8}$$

$$T_r = \frac{T}{1 - AK_0}, \tag{9}$$

$$T_0 = \tau_3 + \tau_2, \tag{10}$$

$$C_{\varphi_0} = \frac{T_0}{K_0}. \tag{11}$$

By T_e, we shall denote the time interval during which integration is performed.

PEF Theory

A. PEF without Feedback

In this case, $U = W_0 U_{in}$. On the basis of (6) and (7),

$$W_0(s) = \frac{K_0}{\tau_2 s + 1} \frac{\tau_4 s + 1}{\tau_1 s + 1} \frac{1}{\tau_3 s + 1}. \tag{12}$$

If the galvanometer is overdamped, it can be considered that $\tau_2 = 0$ in the first approximation. The circuit parameters R_k and C_k can be so chosen that [10]

$$\tau_4 = \tau_1. \tag{13}$$

The first factor, to which the expression for $W_0(s)$ is now reduced, coincides with the operator of the integrating RC_k circuit with an amplifier (cf. Fig. 3; in the given case, $R = \rho + R_k$):

$$W_0(s) = \frac{K_0}{\tau_3 s + 1}. \tag{14}$$

Hence [6],

$$U = \frac{K_0}{\tau_3} \int_0^t U_{in}\, d\theta \tag{15}$$

with the error in percentages [6]

$$p = 50 \frac{T_e}{\tau_3}. \tag{16}$$

Here, τ_3 is the creep time constant.

For a more complete theory, we shall seek the relation between the observed output voltage U and the voltage U_{id} of an ideal integrator of the same sensitivity as that of the actual one under consideration. For this purpose, we shall multiply every term of the identity

$$\frac{K_0}{T_0 s} \frac{1}{W_0} \equiv \frac{1}{T_0 s} + \frac{1}{T_0 s}\left(\frac{1}{w_0} - 1\right) \tag{17}$$

by U after the preliminary transformations‡‡

$$\frac{1}{s}\left(\frac{1}{w_0} - 1\right) U = (\tau_3 + \tau_2)\, U' + \left[\frac{B_1 U''' + B_2 U'' + B_3 U'}{\tau_4 s + 1} + B_4 U''\right] = T_0 U + P$$

or

$$\frac{1}{s}\left(\frac{1}{w_0} - 1\right) U \approx (\tau_3 + \tau_2)\, U' + [B_1 U''' + (B_2 + B_4)\, U'' + \tau_1 U'] = T_0 U + P. \tag{18}$$

Here, P is the portion of expression (18) in square brackets,

$$B_1 = \tau_2 \tau_3 (\tau_1 - \tau_4), \qquad B_2 = (\tau_2 + \tau_3)(\tau_1 - \tau_4),$$

$$B_3 = \tau_1 - \tau_4, \quad B_4 = \tau_2 \tau_3.$$

As a result, we shall find that the ideal integrator output voltage is

$$U_{id} = \frac{K_0}{T_0} \int_0^t U_{in}\, d\theta = U + \frac{\int_0^t U\, d\theta}{T_0} + \frac{P}{T_0}. \tag{19}$$

The second term in (19) is the creep, and the third term represents the error which is due to the fact that the second and the third factor in (12) differ from unity ("structural" error).

B. PEF with Series Feedback

A circuit with combined feedback represents the most general case. By substituting operators for figures in the well-known expression for the amplification factor of an amplifier with feedback, we obtain

$$W(s) = \frac{W_0}{1 + W_0 W_r}, \qquad U = W U_{in}. \tag{20}$$

---

†† Creep is the instrument reading deviation at any instant of time from the readings of an ideal integrator; it is determined by the finite magnitude of the largest time constant in the system. This definition is a natural extension to dynamic operating conditions of the concept connected with the inability of the needle of ordinary fluxmeters to remain in indifferent equilibrium if no input voltage is present.

‡‡ Transformation after the ≈ sign is valid only if $\tau_4 \ll 1$. For the evaluation of the error due to the $\tau_4 s + 1 \approx 1$ substitution, see [4].

By using the identity

$$\frac{1}{\tau_d s}\frac{1}{W} \equiv \tag{21}$$

$$\equiv 1+\frac{1}{s}\left[\frac{1}{K_0\tau_d}+\left(\frac{1}{W_0\tau_d}-\frac{1}{K_0\tau_d}\right)+\left(\frac{W_r}{\tau_d}-s\right)\right],$$

we obtain, in a manner similar to that used in deriving (19) after a number of transformations [including (18)],

$$U_{id}=\frac{1}{C_\varphi}\int_0^t U_{in}\,d\theta = U+Er_1+Er_2+Er_3, \tag{22}$$

where

$$Er_1=\frac{\int_0^t U d\theta}{T_r} \tag{23}$$

is the creep, and

$$Er_2=\frac{P}{T} \tag{24}$$

is the error due to the difference between the amplification circuit and the ideal circuit (when $w_0 \equiv 1$); this error will be called the "structural" error. The quantity

$$Er_3=\frac{\tau_d}{\tau_d+C_{\varphi_0}}\int_0^t\left(\frac{W_d}{\tau_d}U-U'\right)d\theta \approx -\tau_d U' \tag{25}$$

is the error caused by the differentiation error in the feedback circuit; this will be called the "differential" error.

C. Effect of Disturbances and Distortions

Let a disturbance, equivalent to the U_b voltage, arise at the output of the element (circuit with feedback) whose output signal U_1 is related to the input signal by the equation

$$U_1 = W_1(s)\,U_{in}.$$

By finding the equation relating U_b and U (for $U_{in}=0$), we obtain the instrument output error

$$Er_b = U = \frac{W_2}{1+W_0W_r}U_b, \qquad W_1W_2 = W_0. \tag{26}$$

The transformation

$$\frac{W_2}{1+W_0W_r} \equiv \frac{W_0}{1+W_0W_r}\frac{1}{W_1}$$

reduces the theory of disturbances to the utilization of the results obtained in Subsection B [if $(1/W_1)U_b$ is substituted for U_{in}], i.e., to a variant of Eq. (22):

$$\frac{1}{C_\varphi}\int_0^t\left(\frac{1}{W_1}U_b\right)d\theta = Er_b+\Sigma Er, \tag{27}$$

where analogs (23)–(25) enter ΣEr after substituting Er_b for U.

Due to the possibility of zero setting between individual measurements and the limitation of the output instrument transmission band, the frequency spectra for the disturbances to be registered and for the useful signals are comparable***. Hence, $\Sigma Er \ll Er_b$ [since $\Sigma Er \ll U$ in (22)], and the term ΣEr in (27) can subsequently be neglected.

By applying transformations similar to (17) and (18) to the left-hand side of Eq. (27), we can readily obtain a sufficiently accurate expression for Er_b in developed form. In particular, for $W_1 = W_0$, it follows from (19), after substitution of U_b for U, that

$$Er_b = \frac{T_0}{T}U_b + \frac{\int_0^t U_b d\theta}{T} + \frac{P(U_b)}{T}. \tag{28}$$

The last two terms differ from (23) and (24) only by the fact that U_b was substituted for U, and, therefore, they are small simultaneously with (23) and (24) if only $U_b \leq U$. For $T_e > 1$ sec, the first term is smaller than the other terms for PEF of the first group and is considerably larger for PEF of the second group. Thus, approximately,

$$\frac{\tau_3}{T}U_b < Er_b < \frac{T_e}{T}U_{b\max} \tag{29a}$$

for PEF of the first group, and

$$Er \approx \frac{\tau_3}{T}U_b \tag{29b}$$

for PEF of the second group. The right-hand side of (29a) was obtained from (28) by replacing the integral by its maximum value for $U_b = U_{b\max} = \text{const}$ and $t = T_e$, under the assumption that the basic errors are of the same order of magnitude.

Equation (27), including its variants (28), (29a), and (29b), should be considered as the initial equation for determining the parameters characterizing the quality of individual elements and of the entire instrument: the optimum sensitivity, the maximum allowable line current and the amplifier drift, the required feed stability, etc.

The amplitude distortions of the open circuit are formally equivalent to disturbances, and their effect can be taken into account by using the derived equations.

The above concerns only circuits with feedback. In circuits without feedback, the disturbance level is not lowered, which constitutes their main efficiency.

Operational Stability of PEF

The Mikhailov stability criteria [13] were found for the most general case of a circuit with combined feed-

*** The operation of zero setting unavoidably cuts the output signal frequency spectrum from below without discrimination between the useful signal and the disturbance; the same holds for the output instrument (for instance, a self-recorder), which can be considered as a barrier filter in the high-frequency region.

Polynomial roots (ω_2 and ω_4 are roots of the real, and ω_1, ω_3, and ω_5 are roots of the imaginary part of the characteristic equation)	Approximate expressions for the roots	General stability criteria	Stability criteria for PEF with a galvanometer under aperiodic conditions
ω_1^2	0		
ω_2^2	$\frac{1}{T_r\tau_4}$		
ω_3^2	$\frac{T}{H(\tau_3+\tau_0+\tau_d)}$	$\frac{T}{H(\tau_3+\tau_0+\tau_d)} > \frac{1}{T_r\tau_4}$	
ω_4^2	$\frac{T\tau_4+G\tau_3}{\tau_3(\tau_0+\tau_d)H}$	$\tau_4 > \frac{\tau_d+\tau_0}{1+\frac{\tau_0+\tau_d}{\tau_3}}$	$\tau_4 > \tau_d+\tau_0$
ω_5^2	$\frac{\tau_3+\tau_0+\tau_d}{\tau_3\tau_0\tau_d}$	$T < \frac{H\tau_3\frac{\tau_0+\tau_d}{\tau_4}\left(1+\frac{\tau_0}{\tau_3}\right)}{\tau_0\tau_d}$	
		$T < \frac{H\tau_3\left(1+\frac{\tau_0}{\tau_3}\right)^2}{4\tau_0\tau_d}$	$T < \frac{\tau_1\tau_2\tau_3}{4\tau_0\tau_d}$

back. The galvanometer operator was taken in the form given by (1). A variant of the Mikhailov criterion, according to which the conditions for the sequence of roots of the real and imaginary parts are found from the equation $1+W_0(i\omega)W_r(i\omega)=0$ (ω is the angular frequency of signal harmonics), was used. The problem is solved exactly, since it is reduced to the solution of two quadratic equations. It is sufficient to use the approximate solution (see table).

The basic stability criteria follow from the requirement that the roots be real:

$$T < \frac{\tau_3\left(1+\frac{\tau_0}{\tau_3}\right)^2}{4\tau_0\tau_d\omega_0^2}, \qquad (30)\dagger\dagger\dagger$$

and from their sequence conditions:

$$\tau_4 > \tau_d + \tau_0. \qquad (31)$$

The other conditions (not shown completely in the table) cannot be disturbed, and they do not have to be considered separately.

It follows from (30) and (31) that the measuring circuit inductance, the galvanometer natural frequency, the feedback circuit constant τ_d, and the value of $T(K_0$, accordingly restrict each other. It is also obvious that the τ_3 and τ_4 constants cannot be reduced below the determined level (30)–(31).

It should be noted that stability can be secured also if the galvanometer operates under periodic conditions and in the presence of positive feedback.

In contrast to the method used in [7], the system behavior can be determined with respect to the equations derived for the general case, and, thus, the stability margin can be determined beforehand [13].

Discussion of the Results

A. Creep and the Role of Rigid Feedback

The determination and nature of creep follow from expressions (19), (22), and (23). Assuming that the structural and differential errors are equal to zero (this is equivalent to $W_0=\text{const}$ and $W_d=\tau_d s$), we find that creep characterizes those properties of the instrument which permit the simulation of PEF by an integrating circuit of the RC type, which is described by an equation of the type (14). The creep is caused by incomplete compensation of the input signal by the feedback signal with re-

†††It was indicated in [7] that the stability of PEF does not depend on the restoring moment W_m of the galvanometer tension wires. This is due to the fact that T, as well as $1/\omega_0^2$, are proportional to $1/W_m$.

spect to the derivative or its formal analog (in PEF without feedback). If additional rigid feedback is present, the input quantity compensation can be increased by using the feedback signal portion which is proportional to dU/dt. Thus, it follows from Eq. (9) that this occurs for $A > 0$ and $A \to 1/K_0$. In this case, creep will be at the minimum. This compensation can also be reduced, which takes place for $A < 0$, for instance, due to R_{du} leakage. In this case, according to (5), creep becomes larger.

Thus, the reduction of leakage through R_{du} and the introduction of a rigid positive feedback are effective means for reducing creep.

The necessary condition for applying the other method is a sufficient smallness of amplitude distortions in the open-loop system‡‡‡. In the opposite case, due to the instability of K_0 in (9), the $0 < 1 - AK_0 = \text{const} \ll 1$ relation cannot be maintained throughout the entire measurement cycle.

B. Justification of Securing Integrating Conditions in the Amplification Circuit (in Circuits with Feedback)

The reduction of creep in the open circuit (in the amplification circuit), i.e., the operation of this circuit under integrating conditions (as recommended in [10] and [11]), is not justifiable.

In the first place, the expedients whereby T is augmented due to an increase in T_0 are of little effectiveness when they are not accompanied by an increase in K_0[1], since they are reduced only to an increase in $K_0\tau_d$, which is considerably smaller than T_0. This is clear from an analysis of Eqs. (8) and (11) if we take into account that the use of feedback is justified only if $C_{\varphi_0} < C_\varphi$.

Considering the effect of integration conditions in the amplification circuit on the structural error (24), we can readily see by taking into account (18) that such a regime tends to increase the error determined by the rate of change in the magnetic flux to be measured, i.e., the allowable speed of operation of PEF is reduced for a certain given accuracy (due to the increase in τ_3). At the same time, this regime sharply reduces the efficiency of feedback with respect to noise suppression [see (29a) and (29b)].

The (24) and (29a) errors are the smallest for $w_0(s) \equiv 1$. In practice, this is realized (approximately) in PEF of the first group if we provide elements with the smallest time constants in the amplification circuit, or if we correct the amplification circuit with respect to an ideal amplifier with $W_0 = \text{const}$. In this, the restrictions imposed by stability conditions must be taken into account.

C. Role of the PEF Theory in Design Calculations and in Developing Methods for Estimating the Measurement Accuracy

The given PEF theory relates in the most direct way the basic instrument errors, which are expressed in terms of the output quantity, to its parameters, eliminating the necessity of double spectral resolution, as is the case when Fourier transformation or a step function is used. This makes it easy, for instance, to calculate beforehand the allowable shape and duration of pulses for a certain assigned accuracy and parameters, or to solve any reverse problem.

SUMMARY

1. The simplest, and at the same time sufficiently perfect, PEF variant (also with the greatest operating speed) is the instrument with a negative series feedback with respect to the output derivative, and with the maximum approximation (as far as the stability conditions allow) to the ideal character of amplification in the open circuit.

2. The PEF variant with combined feedback, including rigid positive feedback, secures a considerable reduction of creep; however, it can be effectively used only in the case of sufficiently small nonlinear distortions in the amplification circuit.

3. In PEF theory, along with frequency methods, it is convenient to use the method where the basic errors are expressed in terms of integrals and derivatives of the output quantity. This method provides the simplest solution in analyzing the instrument operation, in design, and in error determination.

The method can also be useful in analyzing the operation of integrators of different types.

The author extends his thanks to S. P. Kapitsa, R. R. Kharchenko, S. G. Rabinovich, and M. I. Levin for their help in clarifying a number of principles stated in the present article.

LITERATURE CITED

1. A. N. Kasperovich, "Photoelectric amplifiers F17," Izmeritel'naya Tekh. No. 5 (1959).[2]
2. B. A. Seliber and S. G. Rabinovich, "Photocompensation dc amplifiers," Avtomat. i Telemekh. 17, No. 8 (1956).[2]
3. I. G. Gutovskii, "Photoelectric fluxmeters (survey)," Izmeritel'naya Tekh. No. 1 (1960).[2]
4. I. G. Gutovskii, "Photoelectric fluxmeter theory," Doklady Akad. Nauk SSSR 116, No. 2 (1957).
5. Ya. Mikusinskii, Operator Calculus [Russian translation] (IL, 1956).
6. G. Korn and T. Korn, Electronic Simulating Devices [Russian translation] (IL, 1955).

‡‡‡ This requirement was not fulfilled in any of the proposed circuits with combined feedback [3]. It is understandable that the expected lowering of creep did not take place.

[1] This situation occurs, for instance, when T_0 increases due to an increase in C_k in the operation model in [10]. In [11], T increases proportionally with T_0 due to the simultaneous increase in the tube amplifier amplification factor. This can be brought about also without an increase in T_0.

[2] See English translation.

7. S. G. Rabinovich and A. N. Tkachenko, "On the design of photoelectric fluxmeters," Izmeritel'naya Tekh. No.5 (1959).[2]
8. R. F. Edgar, "A new photoelectric hysteresigraph," Trans. AIEE 56 (1937).
9. F. G. Brockman and W. G. Steneck, "A new automatic hysteresis curve recorder," Philips Techn. Rev. 16, No.3 (1954).
10. S. P. Kapitsa, "On photoelectric fluxmeters," Zhur. Tekh. Fiz. 25, No.7 (1955).
11. R. R. Kharchenko, Special Problems in the Dynamics of Magnetoelectric Instruments, Doctoral Dissertation (MÉI, 1956).
12. V. O. Arutyunov, Electric Measurements and Measuring Instruments [in Russian] (Gosénergoizdat, 1958).
13. A. A. Voronov, Automatic Control Fundamentals [in Russian] (Oborongiz, 1954) 2nd ed.

[2]See English translation.

SYNTHESIS OF CIRCUITS WHOSE OPERATION IS DESCRIBED BY BOOLEAN TIME FUNCTIONS

D. A. Pospelov

Moscow

Translated from Avtomatika i Telemekhanika, Vol. 21, No. 10,
pp. 1410-1413, October, 1960
Original article submitted May 5, 1960

This article describes methods for the synthesis of circuits whose operation can be described by means of a certain special class of time functions. The determination of this class of functions and methods for their investigation are given.

Great interest was shown lately in problems connected with the synthesis and analysis of circuits and devices whose operation can be completely described by means of a certain functional time relation between the input and output parameters. For the solution of such problems in the case where the circuit under investigation can be reduced to its equivalent trigger circuit, various methods have been proposed (see, for instance, [1], [2], and [5]). Problems in the analysis and synthesis of a certain special class of circuits, not reducible to trigger circuits, will be considered in the present article.

We shall consider the totality of sets

$$(x_1, x_2, \ldots, x_n, t), \tag{1}$$

where x_i ($i = 1, 2, \ldots, n$) can be equal to either 0 or 1, and t can assume the value of any integer from 0 to $s-1$, inclusively. It is obvious that the total number of different sets (1) for a certain fixed value of n is equal to $s \cdot 2^n$

Determination. A function determined by sets of the form (1), and assuming one of the two possible values 0 or 1, is called a Boolean time function.

The statement that there is a finite number of different sets (1) is equivalent to the statement that any Boolean time function can be represented in the form of a finite table.

Example 1.

x_1	x_2	t	$\varphi(x_1, x_2, t)$
0	0	0	1
0	1	0	1
1	0	0	1
1	1	0	1
0	0	1	1
0	1	1	1
1	0	1	0
1	1	1	0
$(0 \leqslant t \leqslant 1)$			

Despite its "clarity of presentation," such a table determination is unsuitable in the majority of practical cases because it is cumbersome. When written in analytical form, the function under investigation is more suitable for practical work.

Consider a certain Boolean time function

$$y = \varphi(x_1, x_2, \ldots, x_n, t) \qquad (0 \leqslant t \leqslant s-1). \tag{2}$$

If t is now assigned a certain fixed value $t = k$ where $0 \leq k \leq s-1$, function (2) assumes the form

$$y_k = \varphi_k(x_1, x_2, \ldots, x_n). \tag{3}$$

Function (3) is now an ordinary logic algebra function [2 and 6]. If we let t assume all the allowable values, we obtain the sequence of logic algebra functions

$$\varphi_0, \varphi_1, \ldots, \varphi_{s-1}. \tag{4}$$

Thus, for any Boolean time function, we can obtain a corresponding sequence of logic algebra functions.

Example 2. For the Boolean time function from example 1, we have

$$\varphi_0 = \bar{x}_1\bar{x}_2 \vee \bar{x}_1 x_2 \vee x_1\bar{x}_2 \vee x_1 x_2 = 1,$$
$$\varphi_1 = \bar{x}_1\bar{x}_2 \vee \bar{x}_1 x_2 = \bar{x}_1.$$

Let us now introduce the function τ_α, which is determined by the relation

$$\tau_\alpha = \begin{cases} 0, & t \neq \alpha \\ 1, & t = \alpha \end{cases} \qquad (0 \leqslant \alpha \leqslant s-1). \tag{5}$$

For any $s-1$, the following equalities hold:

$$\bigvee_{i=0}^{s-1} \tau_i = 1, \qquad \bigvee_{i \neq j} \tau_i \tau_j = 0, \tag{6}$$

which signify that at the instant of time $t = \alpha$, the τ_α func-

tion, and only τ_α, is equal to 1, while all other $\tau_i (i \neq \alpha)$ functions are equal to 0 at this moment.

By taking into account relation (5), any Boolean time function can be written in the following manner:

$$\varphi(x_1, x_2, \ldots, x_n, t) = \varphi_0\tau_0 \vee \varphi_1\tau_1 \vee \cdots \vee \varphi_{s-1}\tau_{s-1}. \quad (7)$$

Formula (7) provides means for writing any Boolean time function in convenient analytical form.

Example 3. By writing the function from example 1 in analytical form, we obtain

$$\varphi(x_1, x_2, t) = \tau_0 \vee \bar{x}_1\tau_1.$$

Determination. If in relation (7) all $\varphi_i (i = 1, 2, \ldots, s-1)$ functions are represented in disjunctive (conjunctive, accordingly) perfect normal form, we shall say that the given Boolean time function is represented in a disjunctive (conjunctive) perfect normal form.

From the theory of logic algebra functions [6], it is well known that any logic algebra function can be written in one of the two perfect normal forms. This justifies us in stating that any Boolean time function can be written in one of the possible perfect normal forms.

Relation (7) and the above-formulated determination indicate that the nature of Boolean time functions is close to that of ordinary logic algebra functions. In solving problems in the analysis and synthesis of circuits whose operation is described by such functions, this makes it possible to use an apparatus similar to that already available for logic algebra functions.

One of the most important problems in the logic algebra method of circuit synthesis is the problem of minimizing the given function. In the case of Boolean time functions, this problem can be solved by using any of the methods described in [2], [4], and [6] after certain preliminary modifications. For an illustration of this statement, we shall consider the example of minimization of the Boolean time function from example 1 by means of the modified method of minimizing charts.

Example 4. The disjunctive perfect normal form for our function is

$$\varphi = (\bar{x}_1\bar{x}_2 \vee \bar{x}_1 x_2 \vee x_1\bar{x}_2 \vee x_1 x_2)\tau_0 \vee (\bar{x}_1\bar{x}_2 \vee \bar{x}_1 x_2)\tau_1.$$

Let us apply the method of minimizing charts to this function:

~~$\bar{x}_1\bar{x}_2\tau_0$~~	$\bar{x}_1\bar{x}_2$	$\bar{x}_1\tau_0$	$\bar{x}_2\tau_0$	$\bar{x}_1$	~~$\bar{x}_2$~~	τ_0
~~$\bar{x}_1 x_2\tau_0$~~	$\bar{x}_1 x_2$	$\bar{x}_1\tau_0$	$x_2\tau_0$	$\bar{x}_1$	~~x_2~~	τ_0
~~$x_1\bar{x}_2\tau_0$~~	$x_1\bar{x}_2$	$x_1\tau_0$	$\bar{x}_2\tau_0$	~~x_1~~	~~$\bar{x}_2$~~	τ_0
~~$x_1 x_2\tau_0$~~	$x_1 x_2$	$x_1\tau_0$	$x_2\tau_0$	~~x_1~~	~~x_2~~	τ_0
~~$\bar{x}_1\bar{x}_2\tau_1$~~	$\bar{x}_1\bar{x}_2$	$\bar{x}_1\tau_1$	~~$\bar{x}_2\tau_1$~~	$\bar{x}_1$	~~$\bar{x}_2$~~	~~τ_1~~
~~$\bar{x}_1 x_2\tau_1$~~	$\bar{x}_1 x_2$	$\bar{x}_1\tau_1$	~~$x_2\tau_1$~~	$\bar{x}_1$	~~x_2~~	~~τ_1~~
~~$x_1\bar{x}_2\tau_1$~~	~~$x_1\bar{x}_2$~~	~~$x_1\tau_1$~~	~~$\bar{x}_2\tau_1$~~	~~x_1~~	~~$\bar{x}_2$~~	~~τ_1~~
~~$x_1 x_2\tau_1$~~	~~$x_1 x_2$~~	~~$x_1\tau_1$~~	~~$x_2\tau_1$~~	~~x_1~~	~~x_2~~	~~τ_1~~

According to this minimizing chart, the minimum form for our function is given by $\varphi = \bar{x}_1 \vee \tau_0$.

As can be seen from this example, the proposed minimization method makes it possible to eliminate in the given function the terms which do not depend on time, which is useful in the synthesis of time circuits. However, for large values of n or s, the corresponding minimizing charts become too cumbersome and impractical. In these cases, the method of approximate minimization can be recommended. According to this method, minimization is performed separately for all φ_i functions in expression (7). This method is especially efficient for small n and large s values.

Example 5. For the function of example 1, the approximate minimization yields the following expression:

$$\varphi = \tau_0 \vee \bar{x}_1\tau_1.$$

Determination. A Boolean time function is said to be periodic with the period q if, for any t, the following condition holds:

$$\varphi_{t+q} = \varphi_t. \quad (8)$$

It can be readily seen that any Boolean time function

$$y = \varphi(x_1, x_2, \ldots, x_n, t) \quad (0 \leqslant t \leqslant s-1)$$

can be additionally determined until a periodic function with the period $q \geq s$ is obtained. On the basis of this and relation (7), we can state that, in synthesizing any circuit whose operation is described by a certain Boolean time function, we obtain a circuit of the type shown in Fig. 1. In this circuit, switch S successively connects circuits which process the $\varphi_0, \ldots, \varphi_{s-1}$ functions. After s units of time, the cycle will be repeated. For the time unit in the operation of switch S, we can take any quantity (for instance, the physical time in which one cycle in the operation of a certain device is performed).

In such a diagramatic realization of Boolean time functions, the elimination of terms that do not contain τ_α in the function to be synthesized corresponds to the case where the circuits processing these terms are con-

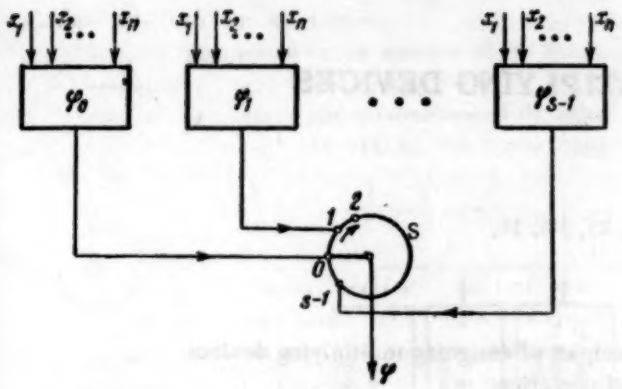

Fig. 1.

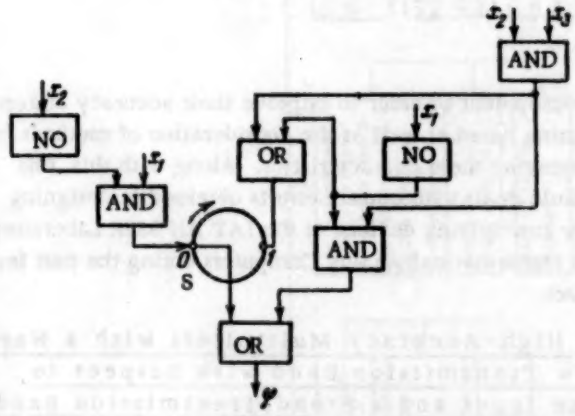

Fig. 2.

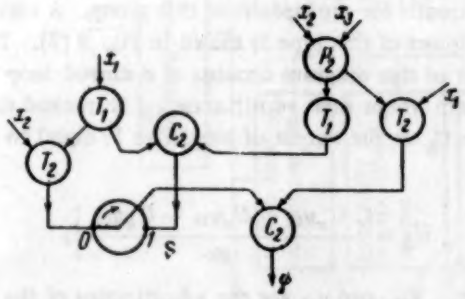

Fig. 3.

nected to the circuit output, bypassing the switch S. The presence of terms consisting only of τ_α in the function minimum form corresponds to the case where, at the instant of time $t=\alpha$, a voltage comparable to unity is supplied to the circuit output.

In conclusion, let us consider the synthesis of a circuit that processes an assigned Boolean time function.

Example 6.

x_1	x_2	x_3	t	$\varphi(x_1, x_2, x_3, t)$
0	0	0	0	0
0	0	1	0	0
0	1	0	0	0
0	1	1	0	1
1	0	0	0	1
1	0	1	0	1
1	1	0	0	0
1	1	1	0	0
0	0	0	1	1
0	0	1	1	1
0	1	0	1	1
0	1	1	1	1
1	0	0	1	0
1	0	1	1	0
1	1	0	1	0
1	1	1	1	1

The disjunctive perfect normal form for this function is

$$\varphi = (\bar{x}_1 x_2 x_3 \vee x_1 \bar{x}_2 \bar{x}_3 \vee x_1 \bar{x}_2 x_3)$$

$$\tau_0 \vee (\bar{x}_1 \bar{x}_2 \bar{x}_3 \vee \bar{x}_1 \bar{x}_2 x_3 \vee \bar{x}_1 x_2 \bar{x}_3 \vee \bar{x}_1 x_2 x_3 \vee x_1 x_2 x_3)\,\tau_1.$$

As a result of applying the method of minimizing charts, we obtain

$$\varphi = \bar{x}_1 x_2 x_3 \vee x_1 \bar{x}_2 \tau_0 \vee (\bar{x}_1 \vee x_2 x_3)\,\tau_1.$$

The corresponding functional diagram is given in Fig. 2. Its realization by means of electronic tubes yields the functional diagram shown in Fig. 3. The notation in this diagram is the same as in [4].

LITERATURE CITED

1. Yu. Ya. Bazilevskii, "Problems in the theory of logic time functions," Collection: Problems in the Theory of Mathematical Machines [in Russian] (Fizmatgiz, 1958) Vol. 1.
2. M. A. Gavrilov, Theory of Relay Contact Circuits [in Russian] (Izd. AN SSSR, 1950).
3. G. N. Povarov, "On the logical synthesis of electronic computer and control circuits," Collection: Logical Investigations [in Russian] (Izd. AN SSSR, 1959).
4. V. I. Shestakov (ed.), Synthesis of Electronic Computer and Control Circuits, [Russian translation] (IL, 1954).
5. M. L. Tsetlin, "On nonprimitive circuits," Problems in Cybernetics [in Russian] (Fizmatgiz, 1958) Vol. 1.
6. S. V. Yablonskii, "Functional constructions in k-unit logic," Trudy Matem. Inst. im. V. A. Steklov [in Russian] (Izd. AN SSSR, 1958) Vol. 51.

SURVEY AND CLASSIFICATION OF MULTIPLYING DEVICES

A. A. Maslov

Moscow

Translated from Avtomatika i Telemekhanika, Vol. 21, No. 10,
pp. 1414-1432, October, 1960
Original article submitted May 7, 1960

The paper deals with systematization of various principles of designing multiplying devices with regard to increasing their accuracy and speed of operation.

It contains some results of development of new multiplying devices carried out in the Laboratory of Analog Computers in the Institute of Automation and Remote Control of the Academy of Sciences of the USSR.

Introduction

In solving many scientific and technical problems, it is now more often necessary to use computers which perform nonlinear mathematical operations, in particular, multiplication and division.

The design of an analog multiplying (or dividing) device which would satisfy modern technological standards is a very complicated problem. This is indicated by the great diversity of the proposed principles on which the multiplication and division operations are to be based. However, regardless of the great attention paid to this problem, even the most perfect designs of multiplying devices are inferior to linear computer components with respect to the basic technical specifications, accuracy and speed.

The contradiction between the accuracy and the speed requirements, which is especially pronounced in nonlinear computer components, makes it possible to classify the multiplying devices according to the scheme given in Fig. 1. Although such a classification is somewhat arbitrary, since it is impossible to make sharp distinctions with respect to errors and the frequency passband for each group, it is very convenient in selecting the most suitable multiplying device design for a certain problem, in developing new designs, and, especially, in combining new and old designs in systems where high accuracy and good dynamic properties are required.

The classification (Fig. 1) is based on principles which make it possible to determine the limits of technical characteristics of the devices in each group. These limits are ultimately determined by the principles used in different designs, and, therefore, the diagram in Fig. 1 in many ways reflects the chart composed with respect to the characteristics determining the method of obtaining the product [1].

The aim of the present article is the systematization of the various principles used in the design of multiplying devices with respect to possibilities of their further development in order to improve their accuracy and operating speed, as well as the consideration of methods for improving these characteristics. Along with this, this article deals with certain results obtained in designing new multiplying devices at the IAT AN SSSR Laboratory for Mathematical Analog Computers during the past few years.

1. High-Accuracy Multipliers with a Narrow Transmission Band with Respect to One Input and a Broad Transmission Band with Respect to the Other Input

With respect to dynamic properties, circuits where the transfer constant changes stepwise are the most promising circuits for multipliers of this group. A circuit for a multiplier of this type is shown in Fig. 2 [2]. The upper part of this diagram consists of a closed-loop follow-up system where such admittance y_{12} is tracked that the voltage U_δ at the output of amplifier 1, equal to

$$U_\delta = \left[\frac{U_x y_{11} + U_c y_{13} - U_k y_{12}}{y_1}\right], \qquad (1)$$

where y_{11}, y_{12}, and y_{13} are the admittances of the amplifier input circuit, y_1 is the admittance of the circuit parallel to the amplifier, U_X is the input signal, and U_C and U_k are constant stabilized voltages, does not exceed the absolute value of the actuation voltage $U_{\delta 0}$ of the command supply device 5. For $U_{\delta 0} y_1 \to 0$, under steady-state conditions, the admittance y_{12} is equal to

$$y_{12} = \frac{U_k y_{11}}{U_k} + \frac{U_c y_{13}}{U_k}. \qquad (2)$$

In order to obtain the product, an additional admittance y_{21}, equal to y_{12}, is formed in the circuit (Fig. 2), and this admittance is commutated by means of an additional system of relay contacts or electronic switches,

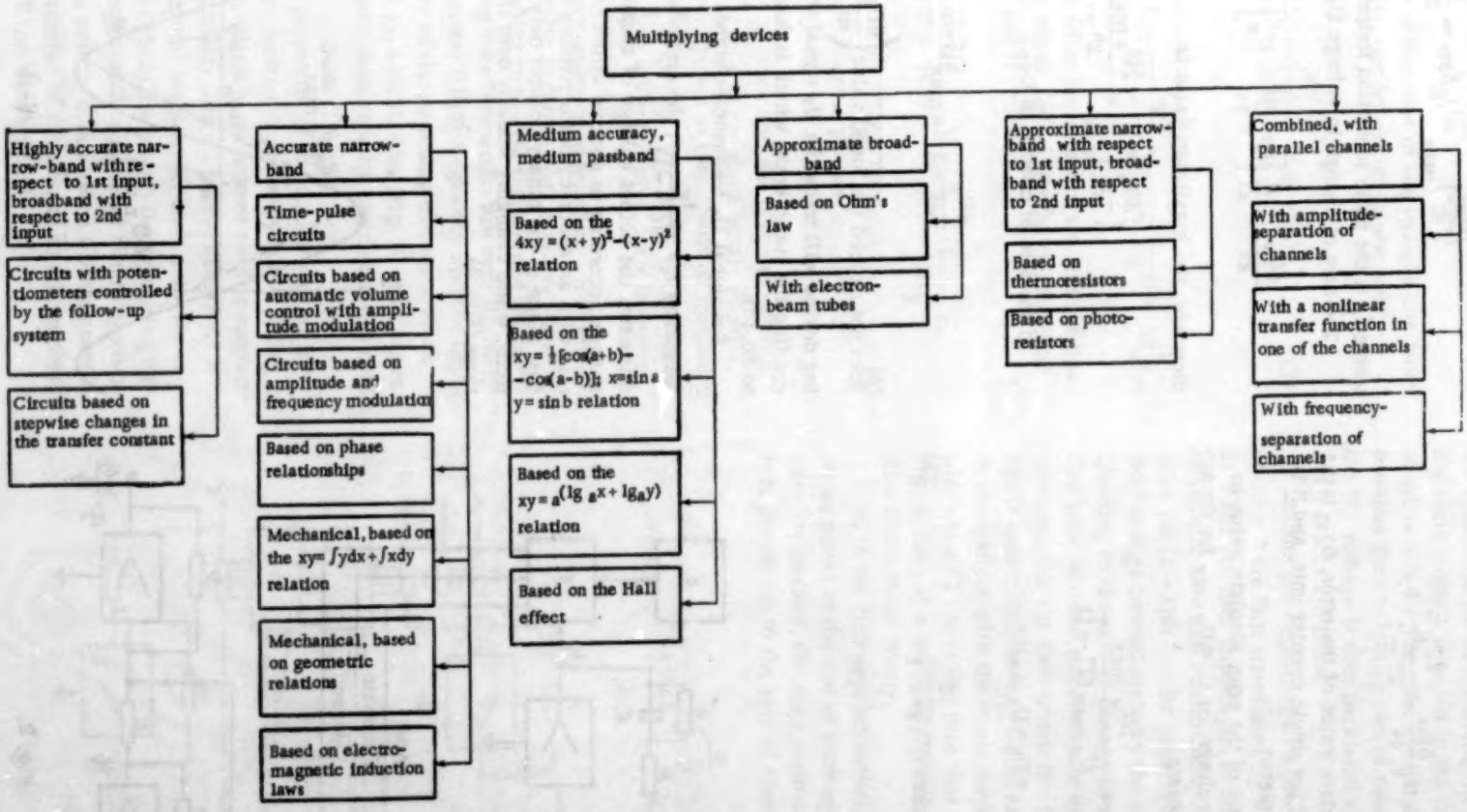
Multiplying devices
Highly accurate narrow-band with respect to 1st input, broadband with respect to 2nd input
Circuits with potentiometers controlled by the follow-up system
Circuits based on stepwise changes in the transfer constant
Accurate narrow-band
Time-pulse circuits
Circuits based on automatic volume control with amplitude modulation
Circuits based on amplitude and frequency modulation
Based on phase relationships
Mechanical, based on the $xy=\int ydx+\int xdy$ relation
Mechanical, based on geometric relations
Based on electromagnetic induction laws
Medium accuracy, medium passband
Based on the $4xy=(x+y)^2-(x-y)^2$ relation
Based on the $xy=\frac{1}{2}[\cos(a+b)-\cos(a-b)]$; $x=\sin a$ $y=\sin b$ relation
Based on the $xy=a^{(\lg_a x+\lg_a y)}$ relation
Based on the Hall effect
Approximate broadband
Based on Ohm's law
With electron-beam tubes
Approximate narrow-band with respect to 1st input, broadband with respect to 2nd input
Based on thermoresistors
Based on photoresistors
Combined, with parallel channels
With amplitude-separation of channels
With a nonlinear transfer function in one of the channels
With frequency-separation of channels

Fig. 1.

which are controlled by means of counter 4. If the binary counter 4 has a sufficiently large number of places, and if $y_{11} = y_{12} = y_2$, the voltage U_Z at the output of amplifier 2 in Fig. 2 will be approximately equal to $\frac{U_X U_Y}{U_k}$.

The deviation of voltage U_Z from the voltage equal to the ideal product value under steady-state conditions, if all other conditions are ideal, obviously depends on the number of places in counter 4:

$$\Delta U_z = U_y \frac{\Delta y_{12}}{y_2} = \frac{2U_y}{2^n - 1},$$

where ΔU_Z is the absolute value of the error, Δy_{12} is the admittance increment per single counter unit, and n is the number of binary places.

If we take the ratio of the error absolute value to the maximum output voltage for $U_y = U_{y\,max}$ for the accuracy criterion, we obtain

$$\delta U_{max} = \frac{2U_{y\,max}}{U_{z\,max}(2^n - 1)};$$

or, for $U_{x\,max} = U_{y\,max} = U_k = U_{z\,max}$,

$$\delta U_{z\,max\,1} = \frac{2}{2^n - 1}. \qquad (3)$$

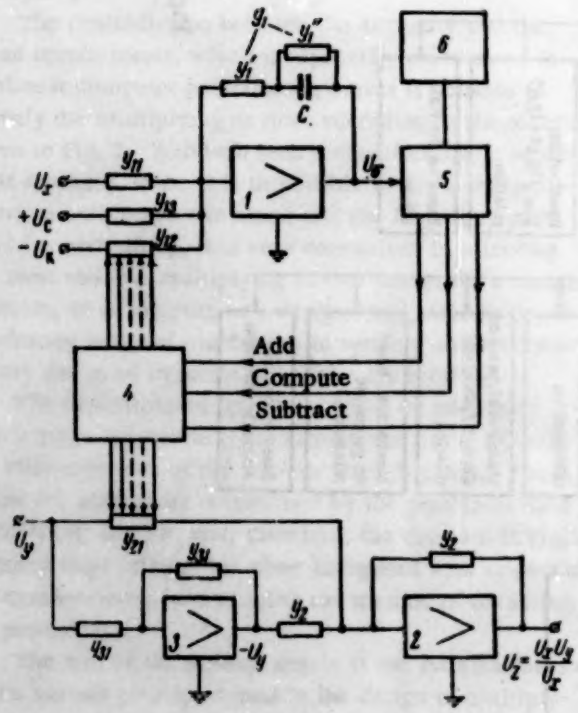

Fig. 2.

For a qualitative estimate of the dynamic properties of the circuit under consideration, we shall calculate the error in multiplying the sinusoidal voltage $U_X = U_{X\,max} \times \sin \omega t$ by the constant voltage $U_y = U_{y\,max}$ as a function of the frequency $f = \omega/2\pi$ of signal U_X for n places of counter 4. If we consider that the command supply device 5 is practically inertialess, we find the maximum rate of change in admittance $y_{12} = y_{21}$:

$$\left(\frac{dy_{12}}{dt}\right)_{max} = f_g \Delta y_{12} = \frac{2 f_g y_{11}}{2^n - 1},$$

where f_g is the pulse repetition frequency of generator 6.

The rate of change in voltage U_Z for $U_y = \text{const}$ is

$$\frac{dU_z}{dt} = \frac{d}{dt}\left[U_y \frac{y_{12}}{y_2} - U_y\right] = \frac{U_y}{y_2}\frac{dy_{12}}{dt};$$

therefore, the maximum value is

$$\left(\frac{dU_z}{dt}\right)_{max} = \frac{2U_{x\,max} f_g}{2^n - 1}. \qquad (4)$$

If the rate of change in U_X,

$$\frac{dU_x}{dt} = U_{x\,max}\,\omega \cos \omega t, \qquad (5)$$

does not exceed the found value $\left(\frac{dU_Z}{dt}\right)_{max}$, the multiplying device will track the U_X signal with an error not exceeding the static error, which is determined according to Eq. (3).

For signal U_X frequencies higher than the limiting frequency $f_1 = \frac{f_g}{\pi(2^n - 1)}$, the error sharply increases. In this case, the output voltage of amplifier (2) (Fig. 2) will change according to a curve which coincides with a sinusoid with an accuracy corresponding to the unit of the first place of the binary counter only over certain portions, while changing linearly over the remaining portions (Fig. 3).

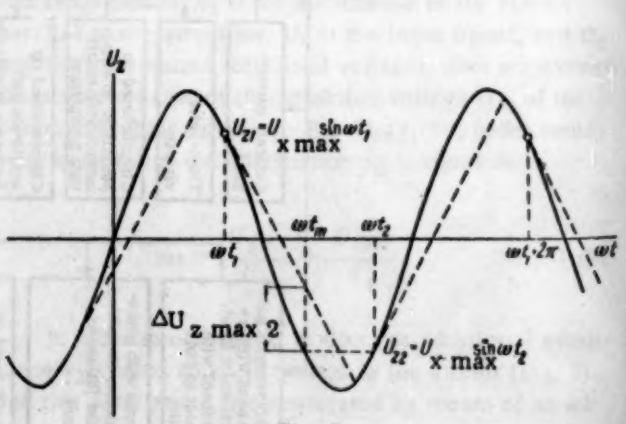

Fig. 3.

The sinusoid and the straight line begin to diverge at the instances of time $t_1+\frac{2\pi k}{\omega}$ and $t_2+\frac{2\pi k}{\omega}$, when the sinusoid slope is equal to the maximum rate of change in the output voltage.

From Eqs. (4) and (5), we find

$$\omega t_1 = \arccos\left[-\frac{2f_g}{(2^n-1)\,\omega}\right]. \qquad (6)$$

If we know t_1, the equation of the straight line issuing from the point U_{z1} can be written in the form

$$U_z = U_{z1} - \left(\frac{dU_z}{dt}\right)_{\max}(t-t_1) \qquad (7)$$

or

$$U_z = U_{x\max}\left[\sqrt{1-\frac{4f_g^2}{(2^n-1)^2\omega^2}} - \frac{2f_g}{2^n-1}(t-t_1)\right].$$

At the moment when the slopes of the straight line and the sinusoid are equal, for $t_m=(2\pi/\omega)-t_1$, the error is at the maximum and is equal to

$$\delta U_{z\max_2} = \frac{2f_g}{(2^n-1)\,\pi f}\arccos\frac{f_g}{(2^n-1)\,\pi f_g} - 2\sqrt{1-\frac{f_g^2}{(2^n-1)^2\pi^2 f^2}}. \qquad (8)$$

Figure 6 (curve a) represents the diagram of error variations $\delta U_Z(f)$ for an eleven-place binary counter, which is supplied with pulses at the repetition frequency $f_g=1$ kc. Up to the frequency $f=f_1\approx 0.16$ cps, the error is somewhat lower than 0.1%; however, for a frequency of 3 cps, it already attains 60%.

Thus, the circuit under consideration, while securing a rather high static accuracy, has very low dynamic properties (with respect to the U_X signal), and the possibilities of improving these properties are very limited, since the binary counter filling frequency and the upper operating frequency of the switching elements which control the y_{12} and y_{21} admittances (Fig. 2) must exceed the multiplier transmission band by more than two orders of magnitude.

The dynamic properties of the circuit can be improved by using the method of place-by-place filling of the binary counter, which is sometimes used in converting a continuous quantity into a discrete quantity. A variant of the structural diagram for such a device is shown in Fig. 4. In comparison with the preceding circuit, this circuit contains an additional binary counter 8, and a command switch 4, for which a binary counter with scaling to a number of units equal to the number of places of counter 7 can also be used.

In the initial position, the command switch 4 does not transmit a pulse from generator 6 to the first place of counter 7 as usual, but to its upper nth place, whereby it is transferred from position 0 to position 1. After this, the error voltage U_δ at the output of amplifier 1 is measured by the command supply device, and, in dependence on the magnitude and sign of the error, either the command for switching the nth place to position 0 or the command for its remaining in position 1 is given. At the same time, 1 is added in the counter of the command switch 4. The next cyclic pulse from generator 6 transfers the (n−1)th place of counter 7 into position 1; the U_δ voltage is then measured again, etc., until all of the n places are filled.

Before the beginning of a new cycle, the contents of counter 7 are first transferred by a cyclic pulse to counter 8 and are then tripped out to zero. Thus, the contents of counter 8, which controls admittance y_{21}, change only after the (n + 1)th cyclic pulse from generator 6, but they change immediately by the number of units corresponding to the rate of change in signal U_X. In connection with this, also, the character of the dynamic error changes. For the case where the $U_X = U_{X\max}\sin\omega t$ voltage is multiplied by $U_Y = U_{Y\max}$, the increase in error in comparison with the static error begins at a frequency which is n + 1 times less than that used in the circuit in Fig. 2, i.e., at a frequency of only 0.15 cps; however, it rises much more slowly.

If, in the first approximation, we assume that the nodal points at the end of each operating cycle are accurately tracked, the maximum error will change in direct proportion to the rate of change in U_X, i.e.,

$$\delta U_{z\max} = \frac{2\pi f\,(n+1)}{f_g}. \qquad (9)$$

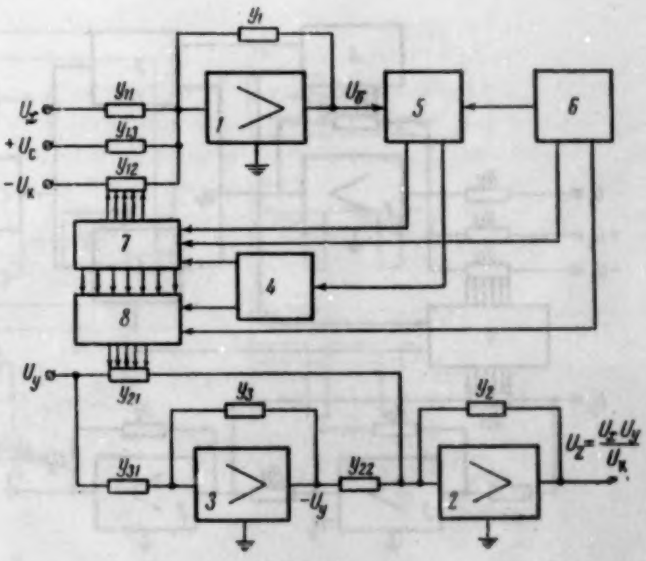

Fig. 4.

In this case, a 10% error will occur only at the 1.35 cps frequency, while in the preceding case, such an error occurred at the 0.18 cps frequency (see curve b in Fig. 6).

The deficiencies of the described method are: a considerable amount of additional equipment and more stringent requirements imposed on the transmission band of amplifier 1, which must transmit a rectangular signal with the frequency of the cyclic pulses from generator 6.

A more perfect method for increasing the operating speed of circuits where the transfer constant changes stepwise is the method of automatically changing the number of places in the counter. The essence of this method becomes clear if we consider the circuit in Fig. 2. Actually, if, for n places in the counter in this circuit, a considerable increase in the dynamic error begins with the signal U_X frequency equal to f_1, then for the (n−1)th place, this increase starts at the $2f_1$ frequency, while the error before attaining the $2f_1$ frequency also increases twofold. In the successive disconnection of lower counter places in the circuit, for U_X change rates equal to the maximum rate of change in U_Z (4), the maximum dynamic error in following the sinusoidal voltage will vary in jumps at the limiting frequencies

$$f_i = \frac{f_g}{\pi (2^{n-i+1} - 1)} \quad (i = 1, 2, \ldots, n-1).$$

In the frequency range from f_i to f_{i+1}, it will remain constant and equal to

$$\delta U_{z\max} = \frac{2}{2^{n-i} - 1}. \qquad (10)$$

The rate of change in voltage U_X in the circuit shown in Fig. 2 can be perhaps most suitably estimated with respect to the magnitude of the error voltage U_δ, which is demonstrated by the structural diagram shown in Fig. 5. For the disconnection of lower places in counter 4, the circuit is provided with an additional command supply device. 7, and a reversive counter 8, with a number of places securing the storage of a number of units equal to the number of places to be disconnected.

The command supply device 7 starts to fill counter 8 when the error voltage U_δ is somewhat larger than $|2U_{\delta_0}|$, and to subtract units from it when $|U_\delta| < |U_{\delta_0}|$. For each addition of a unit to counter 8, the admittance y_1 increases twofold, and the supply of commands is switched to a higher place of counter 4.

The automatic variation of the admittance y_1 secures the correspondence between the actuation voltages of the command supply devices 5 and 7 (which remain constant during operation) and the number of places in counter 4 (Fig. 5).

The described method ensures the multiplication of the sinusoidal signal U_X by a constant quantity at f_g=1 kc and n=11, with an error less than 6.4% at frequencies of up to 10 cps, and with an error of less than 12.8% at frequencies of up to 20 cps, etc. (Fig. 6c). Moreover, the application of this method does not involve more stringent requirements for the quality of amplifier 1, and the use of two multiplace counters is not necessary.

Finally, another way of improving dynamic properties of the circuit in Fig. 2 is the use of the time-pulse interpolation effect [2].

When the circuit in Fig. 2 operates under self-oscillation conditions, and the number contained in the binary counter alternately increases or decreases by unity, the $y_{12} = y_{21}$ admittances change linearly, and not in steps, as functions of U_X; therefore, the over-all number of counter places can be reduced without diminishing the accuracy. However, in this case, pulsations with the fre-

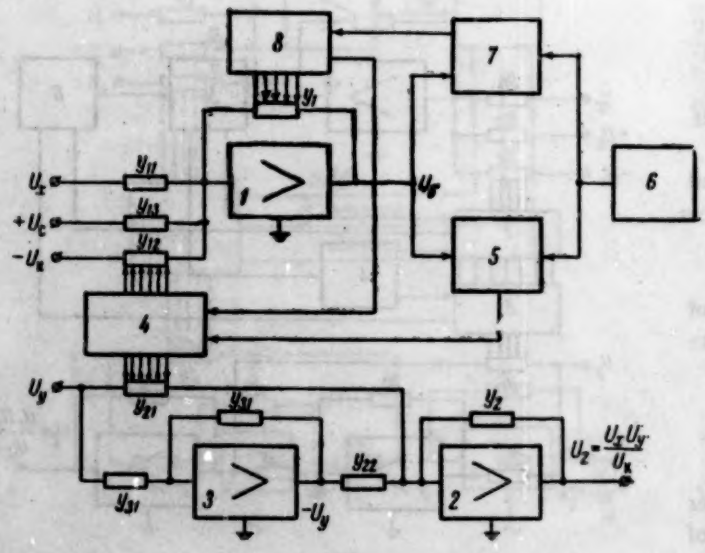

Fig. 5.

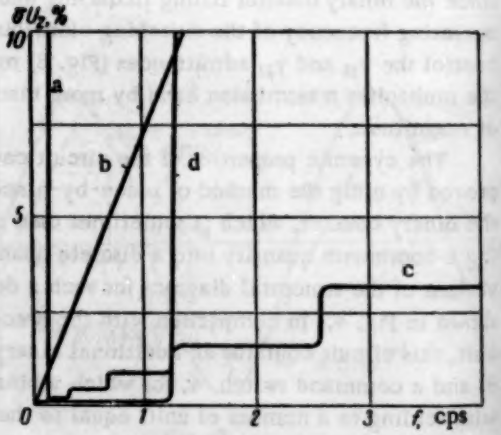

Fig. 6.

quency of self-oscillations whose amplitude sharply increases with a decrease in the number of places arise at the device output; therefore, the possibilities of broadening the transmission band by this method are limited. The frequency-response curve of the circuit in Fig. 2 under self-oscillation conditions for $n=8$ and $f_g=1$ kc is shown in Fig. 6d.

2. Accurate Narrow-Band Multipliers

The most effective method for eliminating the influence of intrinsic tube parameters in linear decision elements is the application of circuits with deep negative feedback.

Multipliers based on the negative feedback principle also secure a comparatively high accuracy; however, at the present time, the application of this principle is possible only in circuits where the output signals are first transformed into the amplitude or duty ratio of rectangular oscillations [14 and 13], in circuits where different methods of signal modulation by sinusoidal voltage are used [14 and 22], and also in certain circuits with special electron-beam tubes [56 and 61].

As a rule, in replacing input voltages by signals of different shapes and higher frequencies, the production of final results requires also reverse transformation, which necessitates the use of detectors, frequency or phase discriminators, circuits for producing the average voltage, etc; therefore, the transmission band of multipliers with preliminary transformation of signals is essentially limited to the region of audio-frequencies and, in many cases, to regions of considerably lower frequencies.

Up to now, the best technical characteristics of time-pulse devices have been secured by using circuits with stabilized electronic keys [7], for which, according to the data provided by the authors, the accuracy was 0.1% for a transmission band of up to 200 cps. However, such circuits are extremely complicated, and they require a large number of decision amplifiers. In connection with this, an investigation with the aim of finding ways for improving the quality of time-pulse devices by using simpler means has been conducted at the Institute of Automation and Remote Control, Academy of Sciences, USSR. Figure 7a shows the block diagram of a multiplier with combined connection of time-pulse dividers. The structure of this circuit is similar to the circuit proposed by A. A. Fel'dbaum and A. I. Manukhin [6]; however, the electronic keys are connected simultaneously to the input circuits and to the circuits parallel to amplifiers 1 and 2. The upper part of the circuit in Fig. 7a consists of a closed-loop follow-up system where the factor U_x is transformed into relative operation times of keys K_1 and K_2. Trigger Tr is switched from one steady state to another with a frequency equal to the frequency f_{sg} of sawtooth oscillations. The relation between times t_1 and t_2 (Fig. 7b) for each of the trigger states depends linearly on voltage U_1, due to changes in the duration of the total U_1+U_{sg} voltage, which is smaller than the trigger switching voltage U_{s1}, and larger than U_{s2}.

The keys are controlled by the trigger in phase opposition in such a manner that, when key K_1 is open, K_2 is closed, and conversely. The average value of the U_{k2} voltage at the key K_2 output, to which voltage U_0 is supplied, is proportional to its relative open-state time $\alpha=t_1/T$ (Fig. 7b), i.e., $U_{k2\,av}=-U_0\alpha$. Correspondingly, $U_{k1\,av}=U_x(1-\alpha)$.

For a sufficiently large amplification factor of amplifier 1, such a voltage U_1 is obtained at its output that

$$\frac{U_x(1-\alpha)}{R_1+R_{f1}}=-\frac{U_0\alpha}{R_2+R_{f2}}$$

or

$$\frac{\alpha}{1-\alpha}=U_x\frac{R_2+R_{f2}}{U_0(R_1+R_{f1})}. \qquad (11)$$

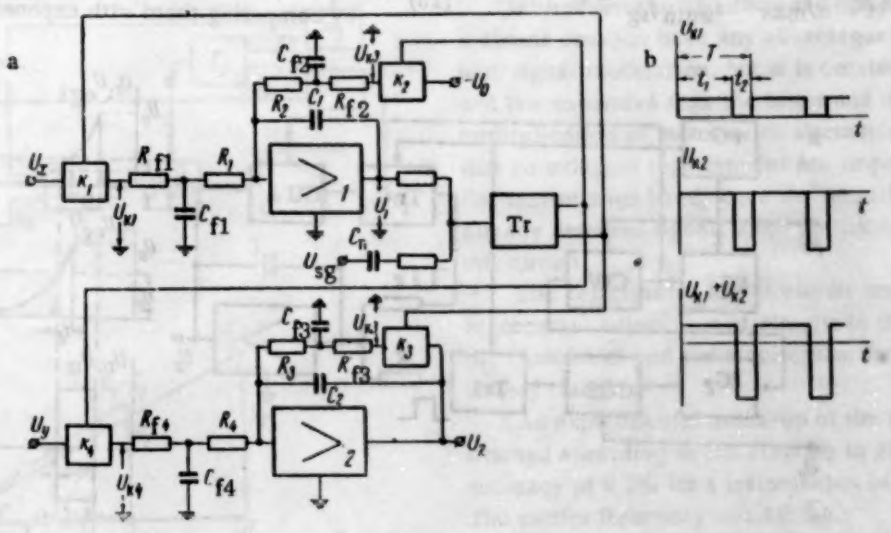

Fig. 7.

For the lower portion of the circuit, the following relation holds:

$$U_z = -\frac{\alpha}{1-\alpha} U_y \frac{R_{f1} + R_1}{R_{f2} + R_3}.$$

By substituting here the $\frac{\alpha}{1-\alpha}$ value from (11), we have

$$U_z = -\frac{U_x U_y}{U_0}.$$

Instead of obtaining the duty ratio ξ of rectangular pulses, which is usually determined by the equation $\xi = \frac{t_1 - t_2}{T}$, the voltage U_X is here transformed into the value of the fraction $\frac{\alpha}{1-\alpha} = \frac{t_1}{t_2}$. If the range in which the duty ratio ξ changes is limited by definition by a number less than 1, the fraction $\frac{\alpha}{1-\alpha}$ can change from zero to infinity. In practice, the duty ratio maximum value ξ_{max} is limited by a number less than 1, and the value of the fraction $\frac{\alpha}{1-\alpha}$ is limited by a finite quantity, since the time (Fig. 7b) cannot change smoothly if it becomes smaller than the sum of the leading and trailing trigger front times $t_l + t_t$. If t_l and t_t are given, ξ_{max} will linearly decrease with an increase in the sawtooth oscillation frequency f_{sg}, since

$$\xi = \frac{t_{1max} - t_{2min}}{T} = 1 - 2t_{2min} f_{sg} \qquad (12)$$

and the upper limit of changes in $\frac{\alpha}{1-\alpha}$ is related to the f_{sg} frequency by the equation

$$\left(\frac{\alpha}{1-\alpha}\right)_{max} = \frac{1}{t_{2min} f_{sg}} - 1. \qquad (13)$$

By comparing (12) and (13), we can readily see that the value of $\left(\frac{\alpha}{1-\alpha}\right)_{max}$ can be chosen to be considerably greater greater than ξ_{max} for a large f_{sg} frequency. For equal product scales, this makes it possible to reduce the transfer constant of the output decision amplifier, by means of which the error caused by the keys can be considerably reduced. If the f_{sg} frequency is increased, filters for a broader transmission band can be designed. The simultaneous connection of filters in input circuits and circuits parallel to amplifiers 1 and 2 (Fig. 7) also contributes to the improvement of the circuit dynamic properties due to the forcing action of filters R_{f2}, C_{f2}, R_2, and R_{f3}, C_{f3}, R_3.

An experimental check of the mock-up of a multiplier circuit with combined connection of pulse dividers, which was based on EMU-8 decision amplifiers, indicated the possibility of securing the following characteristics after careful circuit adjustment:

1) a maximum static error of 0.2 v if the factor voltages U_X and U_Y and the output voltages U_Z change in the interval from 0 to 100 v;

2) drift of less than 40 mv over a period of 10 min when $U_y = 100$ v is multiplied by $U_X = 0$;

3) a drift of not more than 70 mv over a period of 10 min when $U_X = 100$ v is multiplied by $U_y = 0$;

4) a drop in the amplitude response in both channels of not less than 5% for a frequency of up to 400 cps and for a commutation frequency of 10 kc.

The wiring diagram of the mock-up is not given here, since it was constructed only for checking the possibility of realizing the advantages of the considered structural scheme.

As another example, we shall consider the logarithmic time-pulse multiplier. The block diagram of the device for the case of single-quadrant multiplication is shown in Fig. 8a. Here, the transformation of the U_X, U_y, and U_Z voltages into relative durations of rectangular pulses at the output of triggers Tr1 and Tr2 is secured by comparing them with exponentially changing voltages.

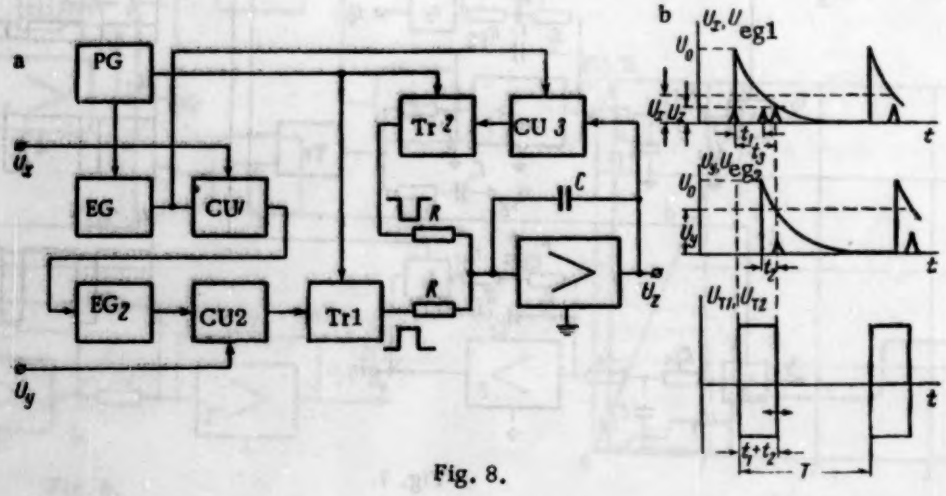

Fig. 8.

The pulse generator PG switches triggers Tr1 and Tr2 and actuates the exponential voltage generator EG1 whose output voltage $U_0 e^{-t/\tau}$ is compared with the U_x voltage by the comparison unit CU1. At the moment when these two voltages are equal, which occurs after the time $t_1 = -\tau \ln \frac{U_x}{U_0}$, a pulse which triggers EG2 appears at the CU1 output. A pulse at the CU2 output, which returns the Tr1 trigger into the initial position, appears after the time $t_2 = -\tau \ln \frac{U_y}{U_0}$.

The duration of the positive pulse at the Tr1 output is equal to the sum of the times $t_1 + t_2 = -\tau \ln \frac{U_x U_y}{U_0}$.

A pulse of negative polarity with an amplitude equal to the amplitude of the pulse supplied by trigger Tr1 is tapped off the output of trigger Tr2; therefore, the U_z voltage at the amplifier output is such that its duration is $t_3 = t_1 + t_2$.

Since $t_3 = -\tau \ln \frac{U_z}{U_0}$, $U_z = \frac{U_x U_y}{U_0}$.

If multiplication in four quadrants has to be secured, all circuit units have to be doubled and adapted for work with negative voltages.

The ease with which one can switch over to division operations and the considerable simplification in the case of the multiplication of several voltages constitute the advantages of this circuit.

With regard to accuracy, this circuit occupies a middle position between closed-loop and open-loop devices. With respect to open-loop circuits, the error of which usually exceeds 1%, the gain in accuracy is obtained by replacing the sawtooth voltage by an exponential voltage, which can be secured with very high accuracy.

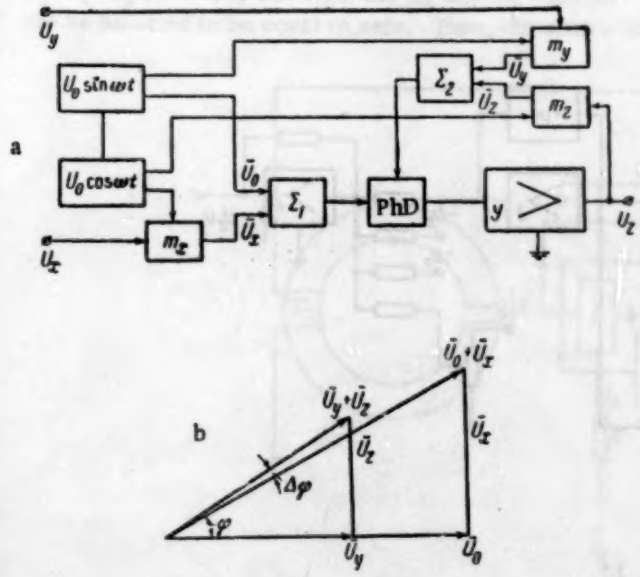

Fig. 9.

As in other time-pulse devices, the transmission band remains lower than the frequency of PG cyclic pulses by more than one order of magnitude.

An experimental check of the multiplier mock-up, which was constructed in accordance with the structural diagram and where standard elements used in computer units were utilized, yielded the following characteristics:

1) The accuracy was 0.5% with respect to a maximum output voltage of 100 v;

2) the frequency response remained horizontal for from zero to 20 cps for a commutation frequency of 1 kc.

As a rule, circuits based on different methods of signal modulation [14-22] are considerably more complicated than time-pulse circuits; however, due to the possibility of selecting a frequency of sinusoidal carrier oscillations which is considerably higher than the frequency of rectangular oscillations (from 100 to 1000 kc), these circuits have a broad transmission band (up to 1-10 kc). Attempts further to increase the carrier oscillation frequency lead to a sharp deterioration of accuracy, since the mutual influence of individual units becomes more pronounced. The design of, and comparison between, different variants of such circuits are given in [17] and [18].

Figure 9 shows a simplified variant of a multiplier circuit with amplitude modulation of signals; the circuit operating principle is based on phase relationships. Two high-frequency voltages with a phase shift of 90 deg are modulated by voltages U_x, U_y, and U_z by means of modulators m_x, m_y, and m_z.

The phase of the vector sum of voltages $\bar{U}_0 = U_0 \sin \omega t$ and $\bar{U}_x = m_x U_0 \cos \omega t$ is compared by the phase detector PhD with the phase of the vector sum $\bar{U}_y + \bar{U}_z = m_y U_0 \times \sin \omega t + m_z U_0 \cos \omega t$ (Fig. 9b). If the phases of these two sums do not coincide, an error voltage, which causes the output voltage to change until it assumes a magnitude proportional to the product of U_x and U_y, arises at the amplifier input.

With respect to accuracy and operating speed, such a circuit does not have any advantages over other devices with signal modulation, but it is considerably simpler and less expensive than the latter, and it secures a direct multiplication of factors with alternating signs. The fact that no stringent requirements are imposed on the amplifier transmission band, since the amplifier amplifies the already detected signal, also constitutes an advantage of this circuit.

The deficiencies of this circuit are the necessity for an accurate adjustment of circuits in the m_x, m_y, and m_z modulators and the requirement for a high carrier frequency stability.

An experimental mock-up of the multiplier constructed according to the diagram in Fig. 2 secured an accuracy of 0.5% for a transmission band of up to 5 kc. The carrier frequency was 465 kc.

By using a quartz oscillator, the device accuracy can be additionally improved.

3. Medium-Accuracy Multipliers with a Medium Transmission Band

This group comprises indirect-action multipliers, where the multiplication operation is replaced by summation and functional conversion operations [23-50], and multipliers based on the Hall effect in semiconductors [52 and 55].

The possibility of improving the accuracy of indirect-action circuits is limited by difficulties involved in constructing accurate nonlinear converters. Up to now, the best results (0.5-1%) were obtained with circuits based on the principle of sectionally linear approximation. The transmission band of indirect-action devices is limited by the parasitic parameters of functional converter elements. By using special corrective circuits, it can be brought up to a few tens and, in individual cases, even to a few hundreds of kilocycles [27, 37, and 38].

In circuits where the Hall effect in semiconductors is used, an accuracy of 0.3-1% can be secured for a transmission band from 1 to 10 kc [52-55].

Multiplier circuits with quadratic functional converters are most widely used at the present time, which is explained by their relative simplicity and the possibility of application for solving a relatively large number of problems.

The following circuit types are used for squaring: diode circuits [25, 28, 30, 31, 35, 36, 37, and 39], nonlinear semiconductor resistors of the thyrite or willemite type [32, 34, 46, 47, 48, 50, and 51], circuits with sawtooth voltage detection [23, 24, 33, and 42], electron-beam functional converters, etc. The quadratic sections of the volt-ampere characteristics of semiconductor or vacuum diodes, the quadratic dependence of the anode current on the grid voltage in three-electrode tubes [25, 29, 43, and 44], etc. can also be used.

Different variants of multiplier circuits based on quadrators, as well as surveys of these circuits with indications of past and possible future improvements, have been sufficiently treated in literature (see, for instance, [1]), and, therefore, we shall not consider them here.

In logarithmic multipliers [15, 63, and 65], the product is obtained as a result of finding the antilogarithm of the sum of logarithms of the input quantities. Such devices are usually constructed according to the diagram shown in Fig. 10. The determination of antilogarithms is here secured by connecting the logarithmic functional converter +ln to the circuit parallel to the decision amplifier. Voltages U_a and U_b are added to the U_x and U_y factors in order to secure the multiplication of quantities with alternating signs, since the logarithms are determined only for positive argument values. In this, the U_3 voltage at the output of amplifier 3 is set in such a manner that

$$-\ln(U_a + U_x) - \ln(U_b + U_y) = \ln U_3. \qquad (14)$$

i.e.,

$$U_3 = (U_a + U_x)(U_b + U_y).$$

For $U_a > |U_{x\max}|$ and $U_b > |U_{y\max}|$, all logarithms will be determined; however, in order to obtain the final result, the U_xU_b, U_yU_a, and U_aU_b components must be subtracted at the circuit output.

The character of error variations in the circuit is of theoretical interest. If we assume that all logarithmic converters have errors whose absolute values are $\Delta_{\ln}(U_x)$, $\Delta_{\ln}(U_y)$, and $\Delta_{\ln}(U_3)$, and the other operations are performed without errors, Eq. (14) should be rewritten in the following form:

$$-\ln(U_a + U_x)(U_b + U_y) =$$

$$= \ln U_3 + \ln\exp[\Delta_{\ln}(U_x) + \Delta_{\ln}(U_y) + \Delta_{\ln}(U_3)].$$

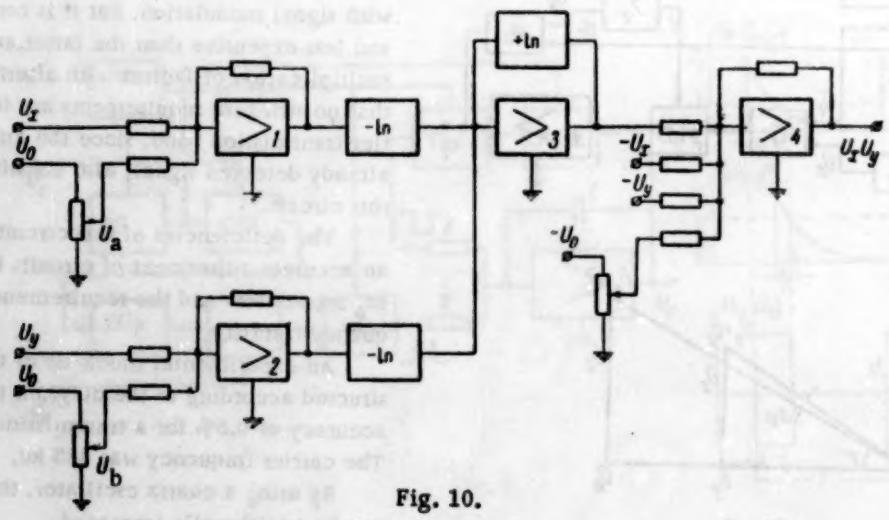

Fig. 10.

Hence,

$$U_3 =$$

$$=(U_a + U_x)(U_b + U_y)\exp[\Delta_{\ln}(U_x) + \Delta_{\ln}(U_y) + \Delta_{\ln}(U_3)].$$

The $\Delta_{\ln}(U_X)$, $\Delta_{\ln}(U_Y)$, and $\Delta_{\ln}(U_3)$ errors are small; therefore,

$$U_3 \approx (U_a + U_x)(U_b + U_y)$$
$$[1 + \Delta_{\ln}(U_x) + \Delta_{\ln}(U_y) + \Delta_{\ln}(U_3)]. \quad (15)$$

After subtracting the U_aU_b, U_aU_y, and U_bU_X components, we obtain

$$\delta(U_z) =$$

$$=\frac{U_{zi} - U_{za}}{U_{z\max}} = \frac{U_xU_y}{U_{z\max}}[\Delta_{\ln}(U_x) + \Delta_{\ln}(U_y) + \Delta_{\ln}(U_3)]. \quad (16)$$

Here, U_{zi} is the ideal product value, and U_{za} is the actual product value.

If we assume that the errors of functional converters are constant and equal and that they are independent of the argument values, the relative product error will be

$$\delta U_z = \frac{U_xU_y}{U_{z\max}}3\Delta_{\ln} + \frac{(U_aU_b + U_xU_b + U_yU_a)}{U_{z\max}}3\Delta_{\ln}. \quad (17)$$

Thus, the error depends linearly on the magnitude of the product itself and on each of the factors, and it contains a constant component. Physically, this is explained by the change in the transfer constant of amplifier 3, which is a consequence of connecting the amplifier to the functional converter feedback circuit.

In the case of single-quadrant multiplication, when U_X and U_Y have only one sign, the U_a and U_b voltages can be assumed to be equal to zero. Then, the error will decrease with a decrease in the product value, and its maximum value will not exceed $3\Delta_{\ln}$. Actually, for small argument values, this error will be larger, since the slope of the characteristics of logarithmic converters is in this case larger, and their error sharply increases.

The considered properties of logarithmic multipliers can be used when it is necessary to maintain a higher accuracy in a certain given range of argument changes.

From among the useful properties of logarithmic devices, one should mention also the possibility of direct multiplication of several factors, division, squaring, evolution, etc. However, their widespread use is hampered by difficulties in producing simple and sufficiently accurate logarithmic functional converters.

The following property of semiconductors is used in circuits based on the Hall effect: if a semiconductor plate is placed in a magnetic field and a current is transmitted through it, an emf will arise in the plate, the direction of which will be perpendicular to the current and the magnetic flux, i.e., $E = k_1BI$.

A number of multiplier circuits based on this principle are already in existence [52 and 53]; however, best results are obtained by using closed-loop circuits, such as, for instance, the circuit shown in Fig. 11. Here, two equal elements, I and II, are placed in a magnetic flux. A steady current I_0 is transmitted through the first element. The Hall emf in the first element is compared with the voltage U_X by means of a differential amplifier, whose output voltage causes the induction in the magnetic circuit gap to change in such a manner that $k_2E_1 = k_2k_1BI_0 = U_X$, where k_1 is the Hall constant, and k_2 is the proportionality factor. Hence, $B = \frac{U_X}{k_1k_2I_0}$.

If the $\frac{R_2}{R_1} = \frac{1}{k_2}$, the U_z voltage is equal to $\frac{U_XU_Y}{U_0}$. The circuit structure is the same as for other circuits with a controllable transfer constant; however, the controlled element is the variable emf.

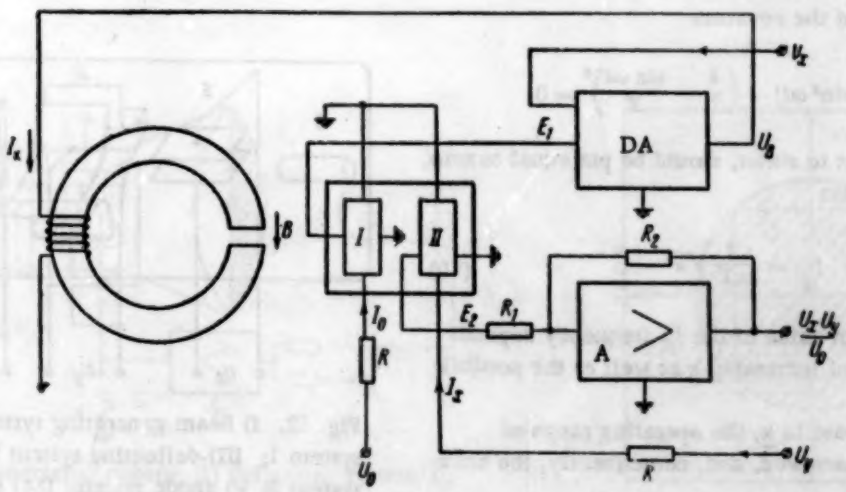

Fig. 11.

The circuit itself is purely electronic, but without the preliminary conversion of input voltages. This makes it possible to improve its dynamic properties in comparison with circuits where input voltage modulation is used; however, up to now, it was possible to secure transmission bands of only up to 10 kc. The reason for the limited possibility of broadening the transmission band in the U_X channel is the presence of the time constant $T = \frac{L}{r}$ (L is the coil inductance, and r is the coil resistance plus the differential amplifier output resistance) in the differential amplifier feedback circuit.

If the differential amplifier gain is sufficiently large, its output voltage will be related to the U_X voltage by the forcing element equation

$$U_B(p) = k_3(1 + pT)\,U_x(p). \qquad (18)$$

The proportionality factor k_3 depends on the Hall constant k_1, the current I_0, the magnetic system characteristics, the differential amplifier gain with respect to the E_1 signal, etc. The enumerated factors make it possible to vary k_3 in a sufficiently wide range; therefore, we shall take its value to be equal to 1 in order that $U_B = U_X$ under steady-state conditions. Then, if U_X changes, the voltage U_B will additionally increase in proportion to the rate of change in U_X.

If the differential amplifier linearity is limited by the value of $U_{B\,max}$, the maximum rate $\left(\frac{dU_X}{dt}\right)_{max}$ can be determined by

$$pU_x(p)_{max} = \frac{U_{B\,max}}{T} - \frac{U_x(p)}{T}. \qquad (19)$$

If we assume that, in the transient process, $U_{B\,max}$ can exceed k times the maximum value of U_B under steady-state conditions $U_{B\,op} = U_{X\,max}$ ($U_{B\,max} = kU_{B\,op}$), then, for determining the limiting value of the frequency $f_{li} = \frac{\omega_{li}}{2\pi}$ of the sinusoidal signal $U_X = U_{X\,max}\sin\omega t$, the discriminant of the equation

$$\omega^2(1 - \sin^2\omega t) - \left(\frac{k}{T} - \frac{\sin\omega t}{T}\right)^2 = 0,$$

solved with respect to $\sin\omega t$, should be put equal to zero. After this, we obtain

$$f_{li} = \frac{1}{2\pi T}\sqrt{k^2 - 1}. \qquad (20)$$

The maximum value of the f_{li} frequency depends on the possibility of increasing k as well as the possibility of reducing T.

With an increase in k, the operating range of changes in U_B is narrowed, and, consequently, the accuracy deteriorates.

The possibility of reducing the time constant T is limited for reasons of energy, since, if the rate of change $\frac{dB}{dt}$ increases, also the power taken from the differential amplifier increases.

Work proportional to the square of induction $A = aB^2$ is used up in creating the magnetic flux. Hence, the instantaneous power is

$$\frac{dA}{dt} = 2aB\frac{dB}{dt} = U_B I_k. \qquad (21)$$

For given values of induction B_{op} and $U_{B\,max}$,

$$\left(\frac{dB}{dt}\right)_{max} = \frac{U_{B\,max}\,I_{k\,max}}{2aB_{op}}. \qquad (22)$$

Consequently, the possibility of increasing the circuit operating speed also by increasing $I_{k\,max}$ or, which is the same, by decreasing T, is limited by the maximum amplifier power. For these reasons, multipliers based on the Hall effect have been grouped together with devices with a medium transmission band.

The accuracy of such devices is limited by instability and a considerable dependence of semiconductor properties on temperature.

At the present time Ge, Si, InSb, and InAs are used as Hall elements. Germanium and silicon elements have the largest Hall constant, and indium antimonide and indium arsenide make it possible to obtain a more powerful output. In comparison with other elements, the properties of InAs change slightly with temperature.

4. Approximate Broad-Band Multipliers

Such devices are provided with electron-beam tubes of a special design [56–61 and 66] or parametric linear circuits, where a current proportional to one factor is transmitted through a resistor which is controlled by the other factor [15].

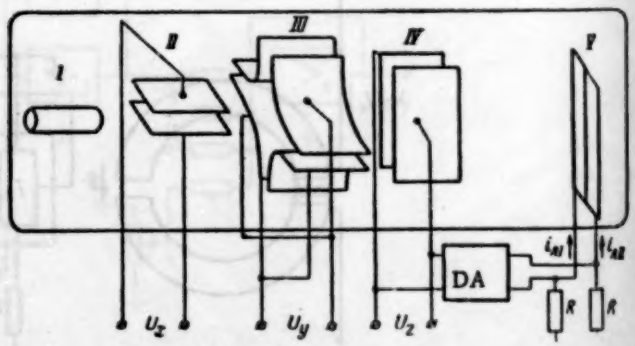

Fig. 12. I) Beam generating system; II) deflecting system 1; III) deflecting system 2; IV) deflecting system 3; V) anode system; DA) differential amplifier.

In circuits of the second type, usually the intrinsic characteristics of electron tubes are used, and, therefore, their accuracy is very low (5–10%).

A high accuracy (up to 0.5–1%) can be secured in circuits with electron-beam tubes. Here, it is extremely difficult to reduce the error, since it depends on the precision in manufacturing and assembling the tube electrodes.

As an example, Fig. 12c shows the circuit of a multiplier whose design is based on an electron-beam tube with a hyperbolic deflecting field [58]. In contrast to the uniform electrostatic field, the action of a hyperbolic field on the electronic beam is proportional, not only to the field strength, but also to the beam displacement with respect to the tube axis.

In the circuit in question, the electron beam is first deflected in the horizontal direction proportionally to the U_x voltage by means of an ordinary deflecting system, after which it enters the hyperbolic field, which is created by the factor U_y. The resulting beam deflection in the horizontal direction is proportional to the U_xU_y product, while the direction of beam deflection corresponds to the sign rule in multiplication. The hyperbolic field is created by four electrodes, whose sections with a vertical plane yields equal hyperbolic branches.

In order to obtain results in voltage form, a third deflecting system and an anode system are provided in the tube. When the beam is deflected with respect to the cut in the middle of the anode system, the equality of currents tapped off each of its halves is disturbed, and a voltage U_z, which returns the beam into its initial position, arises at the differential amplifier output. As a result, we obtain the following relation: $U_z = kU_xU_y$. According to the authors' data, the accuracy of such a device is 0.5%. The transmission band is 200 kc.

In another circuit, which is shown in Fig. 13 [56], the following well-known principle is used: an electron moving rectilinearly at the speed **V** in a magnetic field with the strength **H** is acted upon by a force equal to $\overline{\mathbf{H}} \times \overline{\mathbf{V}}$. Voltage U_x is applied to plates 1. The voltage U_y is converted into current I_k, which passes through the coil and creates the magnetic field. The greater the deflection of the beam by plates 1, the stronger the action of the magnetic field. The resulting action on the beam is proportional to the product of U_x and **H**. One-half of the screen in the tube is darkened, and, therefore, different signals are received by the photocell, in dependence on the beam position. As in the preceding case, there is a control circuit, due to which the Lorentz field, which acts on the beam electrons, is compensated by the amplifier A output voltage, which is equal to $U_z = kU_xU_y$. The error of such devices is equal to approximately 2%.

In the multiplier proposed in [60], an electron-beam tube with an ordinary electrostatic deflecting system is used. A plate, cut into four, as shown in Fig. 14, is mounted in the forward part of the tube. A current proportional to the surface area of the corresponding beam portion is tapped off each of the four plates. The currents are then summed according to the signs indicated in the figure. If the current density of the entire beam is uniform, and the factor voltages U_x and U_y are supplied to the deflecting plates, the total current will be proportional to their product, and the rule of signs will be observed. The fact that the beam cross section is not square has no importance, since the sum of segments complementing a square to form a circle is always equal to zero. The nonuniformity of the beam current density affects the device accuracy, which is low; it is equal to 3%. According to the authors' data, the transmission band is equal to 200 kc.

There is still another electron-beam tube variant [59], whose operating principle is illustrated in Fig. 15, which is intended for use in circuits with quadrators. The tube has a pair of deflecting plates, which direct a rectangular beam to a profiled parabolic screen. The beam current tapped off such a screen is proportional to the square of the voltage supplied to the plates. The beam operates with voltages of either sign, and, therefore, there is no necessity for separating the moduli in

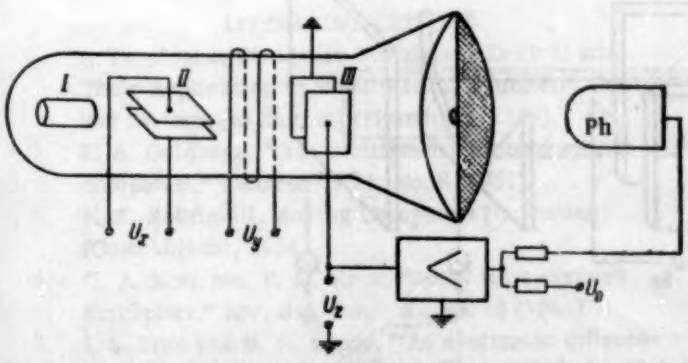

Fig. 13. I) Beam generating system; II) deflecting system 1; III) deflecting system 2; Ph) photomultiplier.

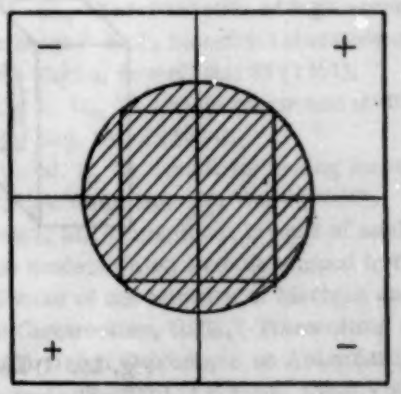

Fig. 14.

Comparative Table of Multiplier Technical Characteristics

Operating principle of the device	Static accuracy, %	Transmission band, cps
Very accurate, narrow-band with respect to one input, broad-band with respect to the other input		
Circuits with potentiometers which are controlled by a follow-up system	0.1	0.5
Circuits where the transfer constant changes stepwise	0.1	0.2
The same circuit with the application of the time-pulse interpolation method	0.1	1.2
The same circuit with place-by-place filling of the counter	0.1	1.3
The same circuit with automatic changing of the number of counter places	0.1	10
Accurate narrow-band multipliers		
Time-pulse multipliers [6]	0.4	12
Circuits with stabilized electron keys [7]	0.1	200
Logarithmic time-pulse devices	0.5	50
Time-pulse devices with combined connection of pulse dividers	0.2	400
Multipliers with amplitude modulation of input voltages [16]	0.1	10000
Multipliers based on phase relationships	1	5000
Devices of medium accuracy with a medium transmission-band		
Multipliers based on diode quadrators	0.5	10000
Multipliers based on thyrites	1	3000
Multipliers based on the Hall effect	0.5	1000
Approximate broad-band devices		
Multipliers based on Ohm's law	10	$2 \cdot 10^5$
Devices with electron-beam tubes	0.5	10^6
Combined devices with parallel channels		
Circuits with amplitude-separation of channels	0.02	100
Circuits with frequency-separation of channels	0.02	10000 and over

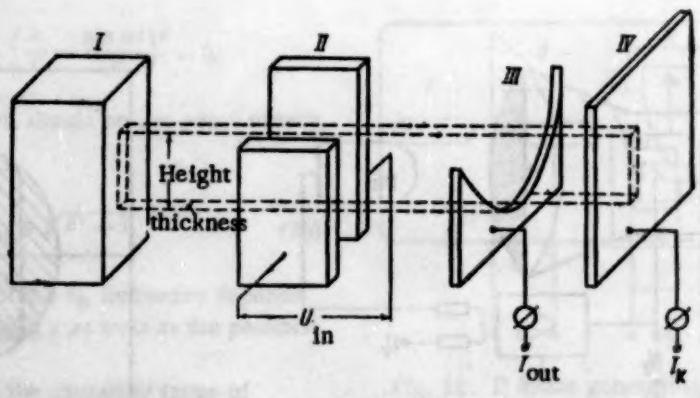

Fig. 15. I) Electron gun; II) deflecting plates; III) profiled screen; IV) collector.

using such a tube. According to the authors' data, the accuracy in squaring is 1%, and the transmission band attains several megacycles per second.

CONCLUSION

1. The above classification and survey of multipliers indicates that the use of any single principle in the design limits the maximum capabilities of these devices, either with respect to accuracy or with respect to operating speed (see Table of Technical Characteristics).

2. The considered well-known methods of increasing the operating speed of circuits where the transfer constant changes stepwise make it possible to broaden their transmission band only to a slight degree (from 0.2 to 1.3 cps). The method of automatically changing the number of binary counter places, which has been proposed here, makes it possible to improve the dynamic properties of a digital follow-up system up to 10 cps for a constant value of the product of accuracy and the transmission band.

3. In analyzing the possibilities of improving the accuracy and the operating speed of narrow-band multipliers, several new circuits have been proposed:

a) a circuit with combined connection of time-pulse dividers, which, for an accuracy of 0.2%, secures the broadening of the transmission band of time-pulse circuits to 400 cps;

b) a logarithmic time-pulse circuit, which secures an easy changeover to division operations and the possibility of direct multiplication of several factors;

c) a multiplier with signal amplitude modulation, which is based on phase relationships and which is characterized by the simplicity of its circuit and the possibility of direct four-quadrant multiplication.

On the basis of the obtained results, we can reach the conclusion that the design of a broad-band and, at the same time, accurate multiplier should not be based on any single principle, but on a combination of different circuits into a system which would make it possible to use the good dynamic properties of one principle and the high accuracy of another.

Combined multipliers will be considered in the next article [Avtomatika i Telemekhanika 21, 12 (1960)].

LITERATURE CITED

1. B. Ya. Kogan, Electronic Simulating Devices and Their Application in Investigating Automatic Control Systems [in Russian] (Fizmatgiz, 1959).
2. E. A. Goldberg, "Step multiplier in guided missile computers," Electronics 24, No. 8 (1951).
3. N. E. Kobrinskii, Analog Computers [in Russian] (Gostekhizdat, 1954).
4. G. A. Korn and T. M. Korn, "Relay time division multiplier," Rev. Sci. Instr. 25, No. 10 (1954).
5. I. S. Bruk and N. N. Lepov, "An electronic differential analyzer," Avtomat. i Telemekh. 17, No. 3 (1956)."
6. A. A. Fel'dbaum, Electrical Systems for Automatic Control [in Russian] (Oborongiz, 1957).
7. C. D. Morill and R. V. Baum, "Stabilized time division multiplier," Electronics 25, No. 12 (1952).
8. L. A. Finzi and R. A. Mathias, "An application of magnetic amplifier circuits to perform multiplication and other analytical operations," Trans. AIEE, 72 (Part I) (1953).
9. L. J. Graig, "The magnetic amplifier as analog computer component," Proc. IRE 41, No. 10 (1953).
10. R. L. van Allen, "Four-quadrant multiplication with transistors and magnetic core," Trans. AIEE, part I--Communication and Electronics No. 21 (1955).
11. D. N. Schaefer, "A static magnetic transistor analog divider," Trans. AIEE, part I-Electronics and Communication, No. 21 (1955).
12. E. A. Goldberg, "A high-accuracy time division multiplier," RCA Rev. 13, No. 3 (1952).
13. E. Flater and K. Fränz, "Multiplicador electronica par inpulsos modulados en duracion y amplitude," Revista Telegrafica Electronica 41 (Buenos Aires, 1952).
14. M. Mehron and W. Otto, "Instantaneous electronic analog computer design," Proc. NEC No. 2 (1954).
15. Generation of Electric Oscillations of a Special Form [Russian translation], ed. by L. Yu. Blumberg and T. R. Brakhtman (Izd. Sovet-skoe Radio (1951), Vols. 1 and 2, No. 4.
16. Lukashevich, L. A., "A multiplier circuit based on the principle of double amplitude modulation," Byull. Pol'skoi Akademii Nauk, Sect. IV 3, 3 (1955).
17. Erglis, K. É., An Electronic Circuit Multiplier of Instantaneous Values of Two Alternating-Sign Voltages, Candidate's Thesis [in Russian] (MEI, 1950).
18. McCool W. A., "An AM-FM electronic analog multiplier," Proc. IRE 41, No. 10 (1953).
19. McCann G. D., Wilts C. H., and Locanthi B. N., "Electronic technique applied to analog methods of computation," Proc. IRE 37, No. 8 (1949).
20. "Computer multiplier," Proc. IRE, No. 10 (1957).
21. Locathi B. H. "A high-speed multiplier for analog computers," Electric. Eng. 69, No. 8 (1950).
22. Price R. T. M., "AM multiplier of high accuracy and wide range," MIT, Research Laboratory of Electronics, Techn. Report, No. 21 (1951).
23. Norsworthy K. H., "A simple electronic multiplier," Electronic Eng. No. 2 (1954).
24. Somerville M. J., "A circuit for analog formation of xy/Z," Electronic Eng. 28, No. 9 (1956).
25. Vittenberg I. M., "Functional layouts of nonlinear electrical models which were developed in the Design Bureau of the Ministry of Machine and Instrument Construction, USSR," Transactions of the Second All-Union Conference on Automatic Control Theory [in Russian] (AN SSSR, 1955) Vol. 3.

26. Goff K. W. "An analog electronic correlator for acoustic measurement," J. Acoust. Soc. Am. 27, No. 2 (1955).
27. Mills R. L., "An accurate inexpensive electronic multiplier with wide dynamic range (Program of the Forty-Fifth Meeting of the Acoustical Society of America, May, 1953)," Acoust. Soc. of Am. No. 4 (1953).
28. Fitsner L. N., "A device for the multiplication of two quantities," Byull. Izobre. No. 2 (1955).
29. Holmes I. N. and Dukes M. A. "A speech-waveform correlator with magnetic tape delay and electronic multiplication," Proc. IRE, part III, No. 72 (July, 1954).
30. Pankolla H. "Ubersicht uber elektronische Multiplikationsverfahren," Messen Steuern Regeln, No. 6 (1960).
31. Trapeznikov V. A., Kogan B. Ya., Gurov V. V., and Maslov A. A., Description of the EMU-5 Electronic Mock-up [in Russian] (Inst. Telsh.- Ekonom. Inform. AN SSSR, 1956).
32. Gurov V. V., Evseev V. M., Kogan B. Ya., Maslov A. A., and Tranin F. E., Description of the EMU-8 Electronic Mock-up [in Russian] (Fil. Uses. Inst. Nauch. i Telsh. Inform. AN SSSR, 1957).
33. Maslov A. A. and Purlov Yu. G., "A universal functional converter based on the quadratic approximation principle," Avtomat. i Telemekh. 21, No. 2 (1960).
34. Kogan B. Ya., Maslov A. A., and Polonnikov D. E., "The EMU-8A electronic simulating apparatus," Vestnik Akad. Nauk SSSR, No. 7 (1958).
35. Maslov A. A., "Special diode functional converters based on semiconductor elements," Collection: Automation and Remote Control [in Russian] (Izd. AN SSSR, 1958).
36. Fitsner L. N., "A device for the multiplication of two quantities," Author's Certificate No. 100505 (November 25, 1952).
37. Coates H. M., "Simple square-law circuit with high frequency response," Electronic Eng. part I 29, No. 347 (1957).
38. Soltes A. S., "A wide-band square law computing amplifier," Trans. IRE, part VI 3, No. 2 (1954).
39. Fisher M. E., "The optimum design of quarter-squares, multipliers with segmented characteristics," J. Sci. Instr. 34, No. 8 (1957).
40. Keister G. L., "Square-wave analog multiplier," Transistor Circuits and Application (New York, McGraw Hill Book Co., 1957).
41. Sydnor R. L., O'Meara T. R., and Strathman J., "Analog multipliers and squarers using a multigrid modulator," Trans. IRE, EC-5, (June, 1956).
42. Pfeiffer Paul E. "A four-quadrant multiplier using triangular waves, diodes, resistors, and operational amplifiers," Trans. IRE EC-8, No. 2 (June, 1959).
43. Elias Peter, Multiplier Circuit, USA Pat, Class 235-61, No. 2741428, (April 10, 1956).
44. Stepanenko I. P., "Special uses of electronic tubes in automation and instrument construction," Collection: Progress in Electrovacuum Technology [in Russian] (Moscow - Leningrad, 1956).
45. Fisher M. E. "A wide-band analof multiplier using crystal diodes and its application to the study of a nonlinear differential equation," Electronic Eng. 29, No. 358 (1957).
46. Maslov A. A., "A multiplier - divider based on thyrites," Avtomat. i Telemekh. 18, No. 4(1957)."
47. Fitsner L. N., "A multiplier unit based on thyrites," Priborostroenie No. 4 (1956).
48. Kovach L. D., and Comley W., "An analog multiplier using thyrite," Trans. IRE EC-3, No. 2 (1954).
49. Balasanov G. N., Theoretical and Experimental Investigation of Static Power Converters with Semiconductor Resistors, Candidate's Thesis [in Russian] (IAT AN SSSR, 1954).
50. Benin V. L., "A wattmeter based on carborundum resistors," Avtomat. i Telemekh. 16, No. 2(1955).
51. Rozenblat M. A. and Sedykh O. A., "Electrical properties and application of carborundum resistors," Avtomat. i Telemekh. 12, No. 4 (1951).
52. Chasmar R. P. "An electrical multiplier utilizing the Hall Effect in indium arsenide," Electronic Eng. 30, No. 369 (1958).
53. Lofgren Lars, "Analog multiplier based on the Hall effect," Actes. Journees Internat. Calcul Analog, Brusels, 1955 (Brussels, 1956), III-151. Discuss 115.
54. Lofgren Lars, "Analog multiplier based on the Hall effect," J. of Appl. Phys. 29, No. 2 (1958).
55. Hilsum C., "Multiplication by semiconductors," Electronic Eng. (November, 1958).
56. Deeley E. M. and Mackey D. M., "Multiplication and division by electronic-analof methods," Nature, 163, No. 4147 (1949).
57. Miller I. A., Solter A. S., and Scott R. E., "Wide-band analof function multiplier," Electronics 28, 2, 11 (1955).
58. Schmidt W., "Die Hyperbeldrore, eine Electronestrahlrohre zum multiplizeeren in Analogie-Rechen gerafen," A. omgew. Phys., No. 2, (1956).
59. Soltes A. S., "Wide-band square-law circuit element," Trans. IRE ED-2, No. 2 (April, 1955).
60. Angela E. I., "An electron - beam tube for analog multiplier," Rev. Sci. Instr. 25, No. 3 (March,1954).
61. Cundlach F. W., "A new electron-beam multiplier with an electrostatic hyperbolic field," Journees Internat. Calcul. Analog (Brussels, 1955). Actes 1956.
62. Gurov V. V., Kogan B. Ya., Talantsev A. D., and Trapeznikov V. A., "The new electronic simula-

tion apparatus of the Institute of Automation and Remote Control, Academy of Sciences, USSR," Avtomat. i Telemekh. 17, No. 1 (1956).*

63. Davis B. E. and Swift I. H., "An analog computer technique using magnetic amplifiers," Trans. AIEE, part I – Communication and Electronics, No. 16 (Jan., 1955).
64. Breitbart (ed.) Parts and Units for Radar Stations [in Russian] (Sovetskow Radio, 1953) Part 3.
65. Burgin B. Sh., "Electrical multiplication and division and their application for measurement and control purposes," Élektrichestvo No. 9 (1958).
66. Choundhury A. K. and Nag B. R., "Analog multiplier and function generator with cathode-ray tube," Indian J. Phys. 33, (1958).

*See English translation.

LETTER TO THE EDITOR

J. Matyáš

Translated from Avtomatika i Telemekhanika, Vol. 21, No. 10,
pp. 1433-1434, October, 1960

In its issue No. 1 of 1960, the journal Avtomatika i Telemekhanika published the article, "On methods for the simulation of rational-fraction transfer functions without differentiating elements" by B. Ya. Kogan [1]. Before the appearance of this article, no such surveys and comparisons of different methods for the solution of this problem were available in literature. Since certain methods for the simulation of transfer functions have special advantages in various practical applications, the article by B. Ya. Kogan must be recognized as being of interest to persons engaged in solving practical problems by means of simulating devices.

At the same time, the journal Slaboproudý Obzor No. 1, 1960, published my article, "Methods for programming differential equations with constant coefficients by means of simulating devices" [2]. The above article treated also some other methods for the reproduction of programming block diagrams by means of simulating devices, which were different from those proposed in [1]. I would like to give here a brief presentation of these methods, thereby supplementing B. Ya. Kogan's article.

First, a few remarks concerning article [1].

1. The circuit in Fig. 1 [1] represents a circuit for dividing the input voltages by the coefficient a_3. Consequently, this circuit is stable for all $a_3>0$ (and not only for $a_3>1$, as was stated in [1]). For $0<a_3<1$, the resistor with the admittance a_3-1 is negative, but it can be connected to another feedback resistor. Thus, a resistor with admittance a_0 will be obtained in the feedback. For very small values of the a_3 coefficient, we shall obtain a circuit with a large amplification factor, which will be stable for all $a_3>0$. (The above circuit is unstable only for $a_3\leq 0$.) For $a_3<0$, the initial equation is multiplied by -1; for $a_3=0$, we shall obviously obtain an equation of a lower order. The case where $a_3=1$ is most often encountered in practice (generally, $a_n=1$).

2. In the method of decomposing the initial differential equation into a system of first-order equations [1], the new coefficients α_1 (see Fig. 6a and the systems of equations (15), (16), and (16a) [1]) represent the initial conditions for the pulse transfer function $w(t) = L^{-1}\{W(s)\}$ of the system under consideration, which is given by

$$\alpha_{n-k} = w^{(k-1)}(0).$$

This statement has been proved in [2].

Composition of Block Diagrams for the Programming of Rational-Fraction Functions by Means of Simulating Devices without Auxiliary Computations

Programming diagrams which contain all coefficients of the initial differential equation in nontransformed form have great advantages. In the above-mentioned article by B. Ya. Kogan, only the direct integration method and the method of combining the derivatives for $b_n=0$ have this property. The diagrams obtained as a result of using these methods are inverse (adjoint) with respect to each other.

For $m<n$, other diagrams which have this property can be obtained by various methods. All such diagrams can be completely described by means of feedbacks and couplings "which supply a forward signal." Any such diagram can be composed in a purely formal manner without any auxiliary calculations by using the following rules and conditions:

Rule 1. Any coefficient a_k on the left-hand side of the initial differential equation corresponds in the diagram to a feedback loop through $n-k$ integrators with the open-loop feedback gain $-a_k$.

Rule 2. Any coefficient b_k on the right-hand side of the initial differential equation corresponds in the programming diagram to a loop supplying a forward signal through k integrators (passing from the system input to the system output through $n-k$ integrators) with the gain b_k.

Condition 1. All loops supplying a forward signal must either go out from the system input (see Fig. 2 [1]) or converge to the system output (see Fig. 7 [1]).

Condition 2. Each integrator or summator in the diagram between the beginning of any feedback loop and the system output has only one input (no feedback loop or a loop supplying the forward signal must terminate in it).

Every programming block diagram set up according to rules 1 and 2, and satisfying conditions 1 and 2, represents a diagram which contains all coefficients of the initial differential equation in nontransformed form, and, conversely, any system which contains all the coefficients in nontransformed form can be composed in a purely formal manner according to the above rules and conditions.

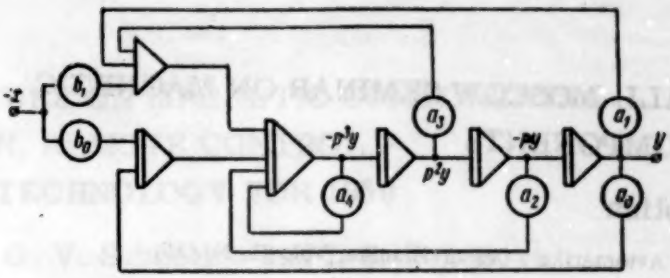

As an example, the figure shows a programming block diagram for the case where n = 5 and m = 1. (The gains of all integrators and summators are assumed to be equal to −1.)

Programming diagrams which contain all coefficients of the initial differential equation in nontransformed form have the following important advantages:

a) The programming block diagram can be obtained without any auxiliary calculations in a purely formal manner according to the above-formulated rules 1 and 2 and conditions 1 and 2.

b) The change in any coefficient of the initial equation can be effected independently of other coefficients by means of a suitable potentiometer.

c) Among these programming block diagrams, there are such diagrams which provide derivatives of the output quantity at the outputs of some of its integrators up to the n-m-1 order (see figure).

It follows from the above that programming block diagrams which contain all coefficients of the initial differential equation in nontransformed form often have important advantages over other diagrams in solving practical problems. They are described in detail in [2].

LITERATURE CITED

1. B. Ya. Kogan, "On methods for the simulation of rational-fraction transfer functions without differentiating elements," Avtomat. i Telemekh. 21, No. 1 (1960).*
2. J. Matyáš, "Programování lineárních diferenciálních rovnic s konstantními koeficienty na dif. analysátorech," Slaboproudý obzor, No. 1 (1960).

* See English translation.

WORK OF THE ALL-MOSCOW SEMINAR ON MAGNETIC AUTOMATION COMPONENTS

G. V. Subbotina

Translated from Avtomatika i Telemekhanika, Vol. 21, No. 10, p. 1435, October, 1960

During the first half of 1960, the All-Moscow Seminar on Magnetic Automation Components continued its work. The Seminar is being held at the Institute of Automation and Remote Control, Academy of Sciences, USSR, under the guidance of Dr. Tech. Sci. Prof. M. A. Rozenblat.

At the Seminar session which was held on February 24th, M. A. Rozenblat and G. V. Subbotina submitted a report entitled " Stability of multistage magnetic amplifiers." The report dealt with a method for determining the transfer function of a multistage summing magnetic amplifier and an investigation of stability criteria of magnetic amplifiers with internal feedback (self-magnetization) by using frequency criteria and considering the lag in load circuits. The authors showed that the obtained stability criterion makes it possible to synthesize a stable two-stage magnetic amplifier with an assigned error for a certain given gain.

In their report "Reversive dc magnetic amplifiers of greater efficiency," which was submitted on March 23rd, M. A. Boyarchenkov and M. A. Rozenblat presented the general principles for the design of highly efficient reversive amplifiers for work with dc loads. A number of new transformerless reversive amplifier circuits have been proposed.

On April 13th, N. P. Vasil'eva and I. S. Gashkovets submitted a report entitled "Stability of long circuits with logic elements," which dealt with the requirements for the "input — output" characteristics of logic elements for securing stable operation of annular or long circuits composed of identical logical repeaters or identical inverters, as well as circuits satisfying these requirements.

On April 27th, R. A. Lipman and A. I. Moskalev reported on the results of investigations of magnetic amplifiers with self-magnetization and a dc output with a circuit for voltage doubling by means of capacitors. This circuit secures a twice greater amplification with respect to voltage in comparison with the ordinarily used two-core circuits of this type. The circuit sensitivity to the feed voltage shape, which must be sinusoidal, constitutes a deficiency of this circuit.

In his report, "Magnetic transistor pulse amplifiers with dc feed," which was submitted on May 11th, L. N. Kiselev analyzed a circuit with both magnetic amplifiers and transistors, operating under switching conditions, where the magnetic amplifier plays the role of the duty regulator. Since the magnetic amplifier represents the input stage, the transistor invertors for feeding and controlling the magnetic amplifier must secure only a power sufficient for feeding the low-power magnetic amplifier and for controlling the output stage triodes. The characteristics of a 2-kw amplifier with an output stage based on four P-207 transistors connected in parallel were given.

On May 25th, M. A. Ol'shvang reported on the development of magnetic semiconductor amplifiers with ac outputs. A magnetic amplifier is used for the first stage, and a push-pull amplifier with transistors which operate under switching conditions is used as the second stage. The semiconductor stage gain is considerably increased by providing positive feedback with respect to the load current by means of a feedback transformer. Such amplifier circuits for the control of two- and three-phase asynchronous motors, as well as a reversive circuit with a half-wave dc output, were described.

The last session of the Seminar in the first half of this year was held on June 8th. At this session, Yu. A. Avakhom submitted the report, "Control of cores with a rectangular hysteresis loop." The author proposed a new method of controlling cores for magnetic amplifiers with internal feedback with respect to the quasi-load characteristic which is close to the actual characteristic of magnetic amplifier control. The simulation of operating conditions for small and large control circuit resistances was secured by means of two different measuring circuits.

The participants at the Seminar noted that the subjects of the reports are important and of interest from the theoretical point of view, as well as for practical application. The reports were recommended for publication.

LIST OF LITERATURE ON MAGNETIC COMPONENTS FOR AUTOMATION, REMOTE CONTROL, AND COMPUTER TECHNOLOGY FOR 1959

Compiled by G. V. Subbotina and I. S. Trefilova

Translated from Avtomatika i Telemekhanika, Vol. 21, No. 10, pp. 1436-1450, October, 1960

GENERAL PROBLEMS
(Terminology, bibliography, standardization problems, etc.)

Measurement of magnetic parameters. Domestic and foreign book and periodical literature for 1955-1958; 13 titles (No. 1767). Composite Bibliographic Index of Technical Papers, 1958 (Gos. Publich. Nauchno-Tekh. SO AN SSR, Moscow, 1959) p. 171.

A. D. Nesterenko, On the Terminology in the Field of Magnetic Measurements. Problems in Magnetic Measurements (Izd. AN UkrSSR, Kiev, 1959) p. 5.

I. I. Pekker, "All-Union seminar on contactless magnetic components for automation, remote control, and computer technology, Moscow, October, 1959", Izvest. Vyssh Ucheb. Zaved., Élektromekhanika, 11, 137 (1959).

G. V. Subbotina, "Work of the All-Moscow seminar on magnetic automation components in ", Avtomat.i Telemekh. 20, 12, 1698 (1959).*

G. V. Subbotina, "List of literature on magnetic amplifiers and contactless magnetic components for 1956 (supplement)", Avtomat. i Telemekh. 20, 3, 376 (1959).*

G. V. Subbotina and I. S. Trefilova, "Magnetic components for automation, remote control, and computer technology". Annotated literature index for 1957 (Sovetskoe Radio Izd., 1959) p. 71.

G. V. Subbotina and I. S. Trefilova, "List of literature on magnetic components for automation, remote control, and computer technology for 1958 (list of domestic papers)" Avtomat. i Telemekh. 20, 9, 1902 (1959).*

Yu. P. Filimonov and M. I. Kaplan, "Literature on contactless magnetic components with a rectangular hysteresis loop", Radioélektr. Promy., 15, 55 (1959).

FERROMAGNETIC MATERIALS AND CORES

a) Magnetic Materials

V. G. Borisenko, "On suitable methods of determining the magnetic properties of cold-rolled transformer steel", Zavodskaya Lab. 25, 12, 1422 (1959)* Fig. 2, Table 3; Bibl. 4.

V. G. Vasil'ev and V. A. Zverev, "Electronic simulation of hysteresis characteristics of ferromagnetic materials", Izvest. Vyssh. Ucheb. Zaved., Élektromekhanika, 9, 3 (1959)* Bibl. 3.

V. I. Prozhzhina and N. V. Erofeeva, "On the structure of the family of symmetric hysteresis loops in ferromagnetic materials", Izvest. Akad. Nauk SSSR, Sev. Fiz. 23, 3, 304 (1959)* Fig. 2, Bibl. 5.

R. K. Kalinin', "Ratio of magnetic losses in ferrite cores with an open-loop magnetic circuit," Tr. Inst. Fiz. AN LatvSSR, 11, 73 (1959) Bibl. 8.

L. V. Kirenskii, et al., "On technical magnetization of ferromagnetic materials," Doklady Akad. Nauk SSSR 128, 2, 288 (1959) Bibl. 10.

I. Kraus, "On the problem of securing a rectangular hysteresis loop in manganese ferrites," Czechoslovak Physics Journal 9, 3, 408 (1959).

N. I. Lapkin and V. S. Mes'kin, "On the effect of high-temperature annealing on the magnetic properties of magnetically soft alloys," Izvest. Akad. Nauk SSR, Ser. Fiz. 23, 3, 280 (1959) Fig. 6, Bibl. 5.

G. Matveev and V. Khomich, "Ferrites: new magnetic materials," Radio, 8, 52 (1959).

"On the determination of the properties of electrical steel" [Résumé of the discussion in the journal Zavodskaya Laboratoriya 25, 4 (1959)] Zavodskaya Lab. 25, 12, 1415 (1959)* Bibl. 9.

A. I. Pirogov, "Effect of temperature on the magnetic reversal process in ferrite cores," Inzh. Fiz. Zhur. (Minsk, 1959).

K. A. Piskarev, "An oxide magnetic material," Author's Certificate, Class 21g, 303, No. 123259. Byull. Izobre., 20 (1959).

I. M. Puzei, "Temperature-stabilization of the magnetic properties of Permalloy," Doklady Akad. Nauk SSSR 120, 4, 768 (1958).

L. I. Rabkin, "A magnetic core", Author's Certificate, Class 21d^2, 48, 117963. Byull. Izobret. , No. 3 (1959).

L. I. Rabkin, "Certain problems in magnetic dielectrics physics," Izvest. Akad. Nauk SSSR, Ser. Fiz., 22, 10, 1276 (1958) Bibl. 6.

L. I. Rabkin and Z. I. Novikova, "Electrical properties of magnetic dielectrics and ferrites," Izvest. Akad. Nauk SSR, Ser. Fiz. 23, 3, 388 (1959) Fig. 15, Bibl. 2.

N. S. Siunov and V. M. Pavlinin, "Simultaneous magnetization of steel by currents of different frequency (50 and 200 cps), "Izvest. Vyssh. Ucheb. Zaved., Elektromekhanika, 3, 7 (1959) Fig. 12, Bibl. 4.

L. V. Sobolev, "Voltampere characteristics and the temperature dependence of the conductivity of nickel–zinc ferrites, " Vest. Mosk. Ser. Unt., Matem., Mekhan., Astron., Fiz., Khim 1, 117 (1959) Bibl. 4.

R. V. Telesnin, T. V. Dmitrieva, and S. A. Matevosyan, "On the temperature dependence of the magnetic ductility of iron and some iron–nickel alloys," Nauchnye Doklady Vysshei Shkoy Fiz. i Matem. 5, 205 (1958) Fig. 6, Bibl. 7.

"Standard ferrite cores, " Radio, 8, 55 (1959).

Ya. S. Shvartsbart, "Magnetically soft materials produced by the Elektrostal' Plant," Collection: Magnetic Amplifiers (Mat. Nauch.–Tekh. Goveshchariya, Khar'kov, 1958 Moscow, 1959) pp. 72-77, Table 4.

b) Magnetization Processes and the Dynamic Characteristics of Ferromagnetic Materials (Losses, Eddy Currents, Viscosity, etc.)

V. V. Bardizh and V. V. Kobelev, "Calculation of magnetic reversal curves for ferrite cores," Izvest. ITM and VT AN SSSR (1959) p. 26, Fig. 15; Bibl. 3.

V. F. Belyavskii and K. M. Polivanov, "On the dynamic characteristics of ferromagnetic cores," Nauch. Doklady Vyssh. Shkol., Élektromekhanika i Avtomatika 2, 14 (1959), Fig. 12, Bibl. 12.

V. F. Belyavskii and K. M. Polivanov, "Cores made of anisotropic ferromagnetic strips," Izvest. Vyssh. Ucheb. Zaved., Élektrotekhnika, 10, 3 (1959) Bibl. 1.

V. Gaiko and I. Daniel–Sabo, "Effect of variable magnetic fields on the residual state of magnetically soft material," Czechoslovak.Physics Journal 9, 1, 37 (1959) Bibl. 5.

E. I. Gurvich and E. I. Kondorskii, "Effect of microscopic inhomogeneities on the dynamic characteristics of magnetically soft alloys in weak fields," Izvest. Akad. Nauk SSSR, Ser. Fiz. 23, 3, 324 (1959) Fig. 3, Bibl. 12.

V. L. Dyatlov, "Consideration of eddy currents and viscosity in the magnetic reversal of strip cores in large fields," Nauch. Doklady Vyssh. Shkol., Élektromekhanika i Avtomatika, 2, 3 (1959) Fig. 7, Bibl. 10.

V. G. Elkin and A. I. Pirogov, "Dynamic characteristics of ferrites and their application in designing circuits with ferrite cores, " Tr. VIRTU, Minsk, No. 15 (1959).

E. I. Klepfer and G. M. Tikhomirov, "Problems in the theory of ferrite cells," Izvest. Vyssh. Ucheb. Zaved., Élektromekhanika, No. 12 (1959).

A. I. Pirogov, "Dynamics of pulse magnetic reversal in ferrites with a rectangular hysteresis loop," Collection: Tr. VTs AN SSSR (1959).

A. I. Pirogov, Pulse Magnetic Reversal in Ferrites with a Rectangular Hysteresis Loop, Candidate's Thesis (Mosk. Énerg. Inst., Moscow, 1959).

M. A. Rozenblat, "Effect of eddy currents on the characteristics of magnetic amplifiers with feedback in the case of low-resistance control circuits," Avtomat. i Telemekh. 20, 12, 1659 (1959)* Fig. 8, Bibl. 4.

N. A. Smol'kov and V. F. Belov, "Certain properties of ferrites under pulse conditions," Izvest. Akad. Nauk SSSR, Ser. Fiz. 23, 3, 357 (1959) Fig. 5, Bibl. 15.

R. V. Telesnin and E. F. Kuritsyn, "On the magnetic reversal rate in ferrites," Izvest. Akad. Nauk SSSR, Ser. Fiz. 23, 3, 352 (1959) Fig. 6, Bibl. 9.

R. V. Telesnin and A. G. Shishkov, "Effect of magnetic viscosity on the frequency characteristics of ferrites," Izvest. Akad. Nauk SSSR Ser. Fiz. 23, 3, 343 (1959) Fig. 8, Bibl. 8.

Yu. M. Shamaev, V. L. Dyatlov, and A. I. Pirogov, "Dynamic characteristics of ferrites," Nauch. Doklady Vyssh. Shkol., Élektromekhanika No. 1 (1959).

c) Core Design and Production Technology

I. S. Babayants and A. I. Ivanov, " A device for automatically maintaining a constant rotation speed of the bobbin in toroidal winding of cores." Author's Certificate, Class 21g, 1_{01}, No. 123627. Byull. Izobret., 21 (1959).

A. M. Bamdas, V. A. Somov, and A. O. Shmidt, "Certain design variants of single-phase and three-phase transformers which are controlled by shunt magnetization," Tr. Gor'kovskogo Politekhnicheskogo 15, 4, 27 (1959) Fig. 15, Bibl. 7.

N. I. Vorob'ev, "The use of enamel as insulation material between sheets in magnetic cores made of electrical strip steel," Izvest. Vysshikh Ucheb. Zaved., Élektromekhanika, 1, 125 (1959) Fig. 6, Bibl. 2.

I. K. Levochkin, "The present state of development of a new line of magnetic amplifiers with magnetic circuits made of II-shaped plates," Collection: Magnetic Amplifiers (Scientificotechnical Conference Transactions, Khar'kov, 1958; Moscow, 1959) p. 40, Fig. 5.

A. V. Netushil, "Effect of insulation thickness on the magnetic properties of foliated cores," Tr. MÉI, 30, 142 (1958).

L. I. Rabkin, "A magnetic core," Author's Certificate, Class 21g, 31_{03}, No. 120621. Byull. Izobre. 12 (1959).

B. G. Sokolov, "A line of 30- to 3000-w magnetic amplifiers with magnetic circuits consisting of three-leg plates," Collection: Magnetic Amplifiers (Scientificotechnical Conference Transactions, Khar'kov, 1958; Moscow, 1959) pp. 78-85, Fig. 4.

V. M. Kharlamov, "A method for the rejection of unsuitable magnetic materials," Author's Certificate, Class 21e, 37_{10}, No. 118902 (594056 of March 7, 1958). Byull. Izobret., 7 (1959).

T. K. Tsogoev, "An adapter to the winding device for fastening the wire end at the lead-out of components (in particular, chokes)," Author's Certificate, Class 21g, 1_{01}, No. 123626. Byull. Izobret., 21 (1959).

3. General Problems in the Theory of Nonlinear Magnetic Circuits (Calculation of Circuits with Steel Components, Ferroresonance, etc.)

L. A. Bessonov, "On the theory of oscillations in one of the ferroresonance circuits," Izvest. Vysshikh Ucheb. Zaved., Élektromekhanika, 2, 43 (1959) Fig. 12, Bibl. 2.

B. K. Bul', "Investigation of the field in the vicinity of the air gap and the calculation of permeance," Vest. Élektropromy. 9, 66 (1959).

E. F. Galteev and V. G. Morozov, "Compound ferroresonance voltage stabilizer for ac generators with permanent magnets," Nauchnye Doklady Vysshei Shkoly, Élektromekhanika i Avtomatika, 2, 151 (1959) Fig. 8, Bibl. 3.

V. P. Glukhov, "Design of a circuit consisting of a resistor and a choke with steel," Vestn. Élektropromy., 10, 42 (1959).

B. Z. Zil'berman, "Condition for the maximum accuracy of ferroresonance voltage stabilizers," Radiotekhnika 14, 4, 75 (1959).

V. D. Krochakevich, Transient Processes in Three-Phase Circuits with Rectifier Bridges. Candidate's Thesis (Lenin Komsomol Riga Aircraft-Engineering Military Academy, 1959).

M. S. Libkind and G. I. Kugushev, "Graphs for determining the harmonic composition of magnetizing currents in superimposing a steady field on a variable field," Élektrichestvo, 7, 55 (1959) Fig. 5, Bibl. 1.

E. M. Pevzner, "On the investigation of transient processes by means of dc currents in electric circuits with steel components," Izvest. Vysshikh Ucheb. Zaved., Priborostroenie, 1, 63 (1959) Fig. 1, Bibl. 1.

S. P. Pivovarov, "Design of ferroresonance voltage stabilizers," Vest. Élektroprom., 6, 60 (1959) Fig. 3, Bibl. 5.

B. A. Piontkovskii, "A ferroresonance voltage stabilizer," Author's Certificate, Class $21a^4$, 35_{14}, No. 121485. Byull. Izobret., 15 (1959).

G. M. Tikhomirov, "Representation of the hysteresis loop equation in the form of an integral with a variable upper limit," Izvest. Vysshikh Ucheb. Zaved., Élektromekhanika, 6, 3 (1959).

4. Magnetic Amplifiers, Theory, Circuits, and Design

a) Books, Monographs, and Dissertations

M. A. Boyarchenkov and M. A. Rozenblat, Fast Reversive Electric Drives with Magnetic Amplifiers (Society for the Dissemination of Political and Scientific Knowledge of the RSFSR. Dzerzhinskii Moscow NTP Institute, Moscow, 1959) p. 42.

N. P. Vasil'eva, O. A. Sedykh, and M. A. Boyarchenkov, Magnetic Amplifier Design (GÉI, Moscow–Leningrad, 1959) p. 336, Fig. 155, Bibl. 44.

N. P. Vasil'eva, Design of Magnetic Power Amplifiers. Lecture delivered as a part of the course "Electromagnetic Components and Devices" (VZÉI, Moscow, 1959) p. 46.

V. A. Geiger, Magnetic Amplifier Circuits [Russian translation from English] (GÉI, Moscow–Leningrad, 1959) Transl. by D. A. Lipman and I. I. Ratgauz, ed. by I. Ya. Lekhtman, p. 400, Fig. 154, Bibl. 548.

Li Fêng, Thermal Calculations and Investigation of the Heating of Magnetic Amplifiers with Three-Leg Cores. Candidate's Thesis (MÉI, Moscow, 1959).

A. L. Pisarev, Investigation of Steady-State Operating Conditions of Six-Choke Magnetic Amplifier Circuits with a Three-Phase Load. Candidate's Thesis (Moscow, 1959).

L. V. Safris, "A method for designing magnetic amplifiers with respect to linearized characteristics" (Central Institute for Technicoeconomic Information, Advanced Scientificotechnical and Industrial Experience, Thesis 27, No. É-59-54/24 (Moscow, 1959) p. 27

O. A. Sedykh, Problems in Selecting the Optimum Design Parameters of Magnetic Amplifiers. Candidate's Thesis (IAT AN SSSR, Moscow, 1959).

b) Single-Ended Magnetic Amplifiers

G. A. Antonov, "A differential magnetic amplifier," Author's Certificate, Class $21a^2$ 18_{08} No. 120538 (590715/24 of January 27, 1959) Byull. Izobre., 12 (1959).

V. P. Vasil'ev and N. N. Aleksandrov, "Operation of magnetic amplifiers which are controlled by means of semiconductor triodes," Sborn. Tr. Slushatelei Leningrad. Voenno-Vozdushnoi Inzh. Akad. im. A. F. Mozhaisk. 27, 138 (1959), Fig. 12, Bibl. 4.

V. S. Vysochanskii, "A single-ended magnetic amplifier with an ac output," Author's Certificate, Class $21a^2$, 18_{08}, $21e^1$, 30_{20}, No. 116921 (January 19, 1959).

N. A. Givartovskaya, "Design of a choke-coupled magnetic amplifier." Second lecture of the course "Electromagnetic components and devices" (Ugletekhizdat, Moscow, 1959) p. 20.

V. P. Glukhov, "The design of magnetic amplifiers with respect to the universal characteristics determined by physical simulation," Collection: Magnetic Amplifiers (Scientificotechnical Conference Transactions, Khar'kov, 1958, Moscow, 1959) pp. 120-130, Fig. 9.

V. P. Glukhov, "Design of a magnetic amplifier with respect to the universal characteristics obtained by

physical simulation," Izvest. AN LatvSSR, 2, 51-60 (1959), Fig. 5, Bibl. 4.

V. P. Glukhov, General Theoretical Characteristics of Choke-Coupled Magnetic Amplifiers. Electrical Equipment Systems for Vehicles (Izd. AN LatvSSR, 1959) Vol. 2; Tr. Instituta Énergetiki i Élektrotekhniki AN LatvSSR, 7, 63-81 (1959).

V. P. Glukhov and É. A. Yakubaitis, "Simulation of choke-coupled magnetic amplifiers," Avtomat. i Telemekh. 20, 7, 955 (1959)*Fig. 4, Bibl. 5.

A. I. Guzenko, "Design of single-ended magnetic power amplifiers." Collection: Automatic Regulation and Control Systems (Mashgiz, Moscow, 1959) No. 97, pp. 85-96, Fig. 4, Bibl. 2.

E. D. Demidenko, "An engineering method of calculating saturation power chokes," Vest. Élektroprom., 2, 63 (1959) Fig. 5, Bibl. 3.

A. G. Zdrok, "On the design of magnetic amplifiers with active-inductive rectified loads," Élektrichestvo, 5, 25-31 (1959) Fig. 8, Bibl. 5.

N. A. Kaluzhnikov, "On the design of ac circuits of choke-coupled magnetic amplifiers with internal feedback," Avtomat. i Telemekh. 20, 5, 606 (1959)*Fig. 11, Table 1, Bibl. 8.

B. E. Kubyshin, "Problems in the linear theory of magnetic amplifiers," Sbornik Trudov Instituta Élektrotekhniki AN UkrSSR, 16, 113 (1959) Bibl. 7.

B. E. Kubyshin, "A method for calculating magnetic amplifiers on the basis of the linear theory," Sborn. Trud. Inst. Élektrotekhniki AN UkrSSR, 16, 174 (1959).

G. I. Kudryavtseva, "Certain problems in the theory and practice of fast magnetic amplifiers for follow-up systems," Transactions of the Third All-Union Conference on Automation of Industrial Processes in Machine Construction and Automated Electric Drives (Moscow, 1959).

V. S. Lerner, "Transfer functions of a magnetic amplifier for active loads," Avtomatika, AN UkrSSR, 1, 58 (1959) Fig. 4, Bibl. 11.

R. A. Lipman and I. B. Negnevitskii, "Design of single-ended magnetic amplifiers with internal feedback," Transactions of the Third All-Union Conference on Automation of Industrial Processes in Machine Construction and Automated Electric Drives (Moscow, 1959).

L. N. Lupaev and N. N. Aleksandrov, "Control of magnetic amplifiers by varying the control voltage phase," Sborn. Trud. Slushatelei Leningrad. Voenno-Vozdushnoi Inzh. Akad. im. A. F. Mozhaiskogo, 27, 158 (1959) Fig. 7b, Bibl. 3.

E. L. L'vov, "Application of the similarity theory in designing magnetic amplifiers," Nauchnye Doklady Vysshei Shkoly, Élektromekhanika i Avtomatika, 3, 119-134 (1958) Bibl. 3.

A. G. Pinchuk, "A transformer magnetic amplifier," Author's Certificate, Class $21a^2$, 18_{08}, No. 97021. Byull. Izobre., 2 (1959).

O. B. Rosenbauli, "A method for designing optimum choke-coupled magnetic amplifiers," Nauchnye Doklady Vysshei Shkoly, Élektromekhanika i Avtomatika 2, 174 (1959).

O. B. Rosenbauli and R. N. Rodin, "Design of current transformers with magnetization," Élektrichestvo, 4, 63 (1959) Fig. 12.

L. L. Samurina, "Operation of a half-wave magnetic amplifier with an active-inductive load," Izvest. Vysshikh Ucheb. Zaved., Élektromekhanika, 2, 81 (1958) Fig. 6, Table 3, Bibl. 3.

Hu Chia-yao and V. A. Shubenko, "Transient processes in magnetic amplifiers with an inductive load which is connected through a rectifier bridge," Izvest. Vysshikh Ucheb. Zaved., Élektromekhanika, 4, 84 (1959) Bibl. 94.

N. M. Yakovlev, "On the design of differential magnetic amplifiers with an ac output," Izvest. Vysshikh Ucheb. Zaved., Priborostroenie, 1, 55(1959) Bibl. 6.

N. M. Yakovlev, "Determination of the transfer function of magnetic amplifiers," Izvest. Vysshikh Ucheb. Zaved., Priborostroenie, 2, 13-21(1958) Fig. 3, Bibl. 2.

É. A. Yakubaitis and V. P. Glukhov, "Physical simulation of circuits with choke-coupled magnetic amplifiers," Izvest. AN LatvSSR, 4, 129 (1958) Fig. 2, Bibl. 5.

c) Push-Pull Magnetic Amplifiers

O. A. Kossov, "A push-pull magnetic amplifier with a dc output," Author's Certificate, Class $21a^2$, 18_{08}, No. 117345. Byull. Izobret., 2 (1959).

O. A. Kossov, "A magnetic crystal amplifier," Avotma. i Telemek. 20, 7, 988 (1959) Fig. 5, Bibl. 3.

V. E. Pankin, "A push-pull bridge magnetic amplifier," Author's Certificate, Class $21a^2$, 18_{08}, No. 122495, March 31, 1958. Byull. Izobre. ,18 (1959).

M. A. Rozenblat, "A push-pull magnetic amplifier with a dc output," Author's Certificate, Class $21a^2$, 18_{08}, No. 122777, March 26, 1959. Byull. Izobre., 19 (1959).

M. A. Rozenblat and G. V. Subbotina, "Improvement of the efficiency of reversive dc magnetic amplifiers by means of transistors," Avtomat. i Telemekh. 20, 9, 1268 (1959)*Fig. 4, Bibl. 5.

O. B. Rosenbauli and R. N. Rodin, "A push-pull transformer magnetic amplifier," Author's Certificate, Class $21a^2$, 18_{08}, No. 118523 (580205 of July 9, 1957). Byull. Izobret., 6 (1959).

L. L. Samurina, "Analysis of fast push-pull magnetic amplifiers," Nauchnye Doklady Vysshei Shkoly, Élektromekhanika i Avtomatika, 3, 26 (1958) Fig. 8, Bibl. 3.

V. A. Faradzhev, "A fast reversive full-wave magnetic amplifier," Author's Certificate, Class $21a^2$, 18_{08}, No. 121817, March 8, 1958. Byull. Izobret., 16 (1959).

d) Multiphase Magnetic Amplifiers

V. V. Gorskii, "A three-phase magnetic amplifier," Author's Certificate, Class $21a^2$, 18_{08}, No. 97548. Byull. Izobret., 5 (1959).

V. A. Kulinich and A. M. Bamdas, "A device for balancing linear currents in three-phase circuits," Author's Certificate, Class $21a^2$, 43, No. 121951, January 14, 1959. Byull. Izobre., 16 (1959).

A. L. Pisarev, "Investigation of the operation of magnetic amplifiers with self-saturation for a three-phase load," Avtomat. i Telemekh. 20, 9, 1274 (1959)* Fig. 8, Bibl. 4.

A. L. Pisarev, "On the control characteristic of magnetic amplifiers operating with a three-phase load," Avtomat. i Telemekh. 20, 5, 622 (1959)*Fig. 10, Bibl. 1.

V. P. Shipillo, "A three-phase reversive magnetic amplifier," Author's Certificate, Class $21a^2$, 18_{08}, No. 121174, December 4, 1958. Byull. Izobre., 17 (1959).

e) Multistage Magnetic Amplifiers

S. I. Khmel'nik, "Functional current converter in the load of a two-stage magnetic amplifier circuit, Author's Certificate, Class $21a^2$, 18/08, No. 114548, August 21, 1958.

f) Decision Magnetic Amplifiers

V. P. Milovzorov, "Summing magnetic amplifiers," Tr. Ryazanskogo Radiotekh. Inst. 3, 95 (1958) Fig. 6, Bibl. 2.

G. I. Takhvanov, "Feedback in decision amplifiers," Tr. Ryazanskogo Radiotekh. Inst. 3, 124 (1958) Fig. 8, Bibl. 3.

MAGNETIC AMPLIFIERS, APPLICATION OF MAGNETIC AMPLIFIERS

a) General Application Problems

D. A. Alenchikov, "Development and utilization in industry of a line of magnetic amplifiers and saturation chokes," Collection: Magnetic Amplifiers (Scientificotechnical Conference Transactions, Khar'kov, 1958, Moscow, 1959) pp. 4-19, Fig. 8, Bibl. 19.

M. E. Aizenshtat, "A line of toroidal magnetic amplifiers and units with toroidal amplifiers," Collection: Magnetic Amplifiers (Scientificotechnical Conference Transactions, Khar'kov, 1958, Moscow, 1959) pp. 56-59.

B. K. Karpenko, "A nonlinear electronic amplifier for compensating the nonlinearity of rotary and magnetic amplifiers" (VINITI Branch, Moscow, 1959) p. 11; Referat. Zhur. Élektr., 4, 2947 (1960) Fig. 4.

Ya. M. Kleinman, "On the experience gained in using magnetic amplifiers in devices and equipment produced by the Yuvmetallurgavtomatika Plant," Collection: Magnetic Amplifiers (Scientificotechnical Conference Transactions, Khar'kov, 1958, Moscow, 1959) pp. 160-164, Fig. 4.

Magnetic Amplifiers. Collection of Articles Based on Scientificotechnical Conference Transactions (Ts-INTI of the Electrical Engineering Industry and Instrument Construction, Moscow, 1959) p. 178, Fig. 116, Bibl. 35.

M. A. Rozenblat, "Magnetic amplifiers for automatic control systems," Collection: Automatic Control and Computer Techniques (Moscow, 1959) Vol. 1, pp. 182-204, Fig. 23.

Ya. B. Rozman and V. A. Naidis, "Magnetic amplifiers as electrical components of machines and machine tools," Collection: Magnetic Amplifiers (Scientificotechnical Conference Transactions, Khar'kov, 1958, Moscow, 1959) pp. 20-27.

Ya. Yu. Solodukho, "Magnetic amplifiers in the automation of continuous-rolling mills," Collection: Magnetic Amplifiers (Scientificotechnical Conference Transactions, Khar'kov, 1958, Moscow, 1959) pp. 86-98, Fig. 12.

T. Kh. Stefanovich, "Magnetic amplifiers for automatic control systems and systems for regulating industrial electric drives," Transactions of the Third All-Union Conference on the Automation of Industrial Processes in Machine Construction and Automated Electric Drives (Moscow, 1959).

T. Kh. Stefanovich, "Magnetic amplifiers for automatic control systems and systems for regulating electric drives," Tr. Nauchno-Issle. Inst. Élektroprom., Élektroprivod i Sreds'tva Avtomatizatsii 5, 462-476 (1959) Fig. 5.

T. Kh. Stefanovich, "Development of TUM magnetic amplifiers and complete assemblies of devices based on TUM amplifiers for industrial equipment automation," Collection: Magnetic Amplifiers (Scientificotechnical Conference Transactions, Khar'kov, 1958, Moscow, 1959) pp. 46-55, Fig. 6.

F. A. Stupel', "Problems in designing fast electromagnetic mechanisms," Tr. Khar'kovskogo Politekhnicheskogo Instituta 27, 1, 25-33 (1959) Fig. 8, Bibl. 2.

M. V. Khapatetov and M. A. Borisov, "Low-power TUM magnetic amplifiers with toroidal cores"(VINITI Branch, Advanced Scientificotechnical and Industrial Experience, Thesis 27, No. É-59-52/23 Moscow, 1959) p. 14.

É. A. Yakubaitis, "A self-oscillation synchronous oscillator with variable frequency," Choke-Coupled Magnetic Amplifiers (AN LatvSSR Press, 1959) Chap. 5, pp. 187-231, Fig. 27.

b) Application for Control of Electrical Machines

D. A. Alenchikov, "A method of calculating the characteristic of dc electric drives with choke control, which is based on using the family of external characteristics of rectifier-choke converters," Tr. Nauchno-Issle. Inst. Élektroprom., Élektroprivod i Sreds'tva Avtomatizatsii 5, 57-68 (1959) Fig. 5, Bibl. 14.

D. A. Alenchikov, "A method of calculating the characteristics of dc electric drives with choke control, which is based on using the family of external characteristics of rectifier-choke converters," Transactions of the

Third All-Union Conference on Automation of Industrial Processes in Machine Construction and on Automatic Electric Drives (Moscow, 1959).

D. A. Alenchikov, "Calculation of the static characteristics of systems with choke control," Avotmat. i Telemekh. 20, 5, 595 (1959) Fig. 10, Bibl. 5.

D. A. Alenchikov, Control of dc Motors by Means of Saturation Chokes and Semiconductor Rectifiers (Ts-BTI NII Élektropromyshlennosti, Moscow, 1959) p. 120.

D. A. Alenchikov and V. S. Kulebakin, "A method of calculating the characteristics of dc motors with choke control," Avtomat. i Telemekh. 20, 7, 908(1959) Fig. 5, Bibl. 4.

M. I. Aronov, "A device for automatic excitation control in dc oscillators," Author's Certificate, Class 21d, 38_{20}, No. 118102. Byull. Izobre., 4 (1959).

G. M. Bider, "Application of magnetic amplifiers in automation circuits for metallurgical electric drives," Byull. Tsnilchermeta, 5 (361), 54 (1959) Fig. 3.

B. S. Bochkov, L. L. Gol'dina, and L. V. Rosman, "A device for automatic unloading of synchronous machines in the case of overloads," Author's Certificate, Class 21c, 68_{01}, No. 117597. Byull. Izobret., 2 (1959).

Ya. S. Brovman, "Magnetic amplifiers with half-wave fast action in the controllable electric drive for the main motion of heavy machine tools," Collection: Magnetic Amplifiers (Scientificotechnical Conference Transactions, Khar'kov, 1958, Moscow, 1959) pp. 131-137, Fig. 9, Bibl. 5.

A. L. Vil'nyanskii, "Magnetic amplifiers as dc generators or drivers" (VINITI Branch, Advanced Scientificotechnical and Industrial Experience, Thesis 27, No. É-59-7/2, Moscow, 1959) p. 16.

V. S. Volodin, E. D. Larin, M. A. Rozenblat, and G. V. Subbotina, "A fast push-pull magnetic semiconductor amplifier for power follow-up drives," Avtomat. i Telemekh. 20, 3, 323 (1959) Fig. 12, Bibl. 5.

K. P. Garionov, "A contactless self-regulating circuit for controlling heat-powered drives with electric transmission to the moving shafts," Sborn. Leningrad. Inst. Inzh. Zheleznodorozhnogo Trans., 159, 258 (1958) Fig. 7, Bibl. 3.

L. A. Gasparyan and O. B. Rosenbauli, "A device for synchronous generator phase compounding," Author's Certificate, Class $21d^2$, 6_{01}, No. 122202, December 2, 1959. Byull. Izobret., 17 (1959).

L. A. Gasparyan, O. B. Rosenbauli, A. N. Larionov, F. F. Galteev, and T. N. Verbitskaya, "A device for regulating the voltage of synchronous generators," Author's Certificate, Class $21d^2$, 6_{01}, No. 122803, March 23, 1959. Byull. Izobret., 19 (1959).

L. V. Dranitskii, "Application of drives with magnetic amplifiers in machine tools produced by the Moscow Plant for Jig Borers," Collection: Magnetic Amplifiers (Scientificotechnical Conference Transactions, Khar'kov, 1958, Moscow, 1959) pp. 36-39, Fig. 3.

A. G. Efanov, N. G. Kozlov, and Yu. R. Reingol'd, "Results of the industrial testing of the automated dc electric drive for ÉVG-6 excavators with magnetic excitation amplifiers," Tr. Nauchn.-Issle. Inst. Élektroprom., Electric Drives and Automation Equipment 5, 283 (1959) Fig. 5.

M. N. Zaritskii, "Regulation of the automatic control system for a synchronous electric drive with choke control," Nauchnye Doklady Vysshei Shkoly, Gornoe Delo, 4, 161 (1958).

Yu. D. Kapuntsov, "A device for the control of synchronous three-phase motors," Author's Certificate, Class 21c, 59_{30}, 121838, December 7, 1958. Byull. Izobre., 16 (1959).

I. P. Kopylov, "Motors-amplifiers combining a magnetic amplifier with an electric motor," Transactions of the Third All-Union Conference on Automation of Industrial Processes in Machine Construction and Automated Electric Drives (Moscow, 1959).

I. P. Kopylov, "Motor-amplifiers for dc and ac Current," Collection: Magnetic Amplifiers (Scientificotechnical Conference Transactions, Khar'kov, 1958, Moscow, 1959) pp. 165-173, Fig. 6, Bibl. 4.

I. P. Kopylov, L. M. Polyak, and V. I. Radin, "A differential rotary amplifier with magnetization," Nauchnye Doklady Vysshei Shkoly, Élektromekhanika i Avtomatika, 1, 136 (1958) Fig. 5, Bibl. 4.

I. P. Kopylov and V. I. Radin, "An ac motor-amplifier," Élektrichestvo, 11 (1959).

O. M. Kostyuk, "An automatic voltage regulator for synchronous motors," Author's Certificate, Class $21c^2$ 57_{34}, No. 123228. Byull. Izobret., 20 (1959).

O. M. Kostyuk, "Current transformers with magnetization by dc current and particularities in their design for circuits used in automatic control of synchronous generator excitation," Sbornik Trudov Instituta Élektrotekhniki AN UkrSSR Problems in the Stability and Automation of Power Systems, 16, 135 (1959) Fig. 9, Bibl. 6.

V. S. Kulebakin and D. A. Alenchikov, "Application of saturation chokes and magnetic amplifiers in automated electric drives," Collection: Magnetic Amplifiers (Scientificotechnical Conference Transactions, Khar'kov, 1958, Moscow, 1959) pp. 60-71, Fig. 6, Bibl. 6.

A. M. Lyubavin, "A controllable electric drive with magnetic amplifiers," Tr. Nauchn.-Issle. Inst. Élektroprom., Electric Drives and Automation Equipment 5, 46 (1959) Fig. 5.

A. M. Lyubavin, "A controllable electric drive with a magnetic amplifier," Transactions of the Third All-Union Conference on Automation of Industrial Processes in Machine Construction and Automated Electric Drives (Moscow, 1959).

Kh. M. Mamisurov, "The maximum allowable number of times an asynchronous short-circuited motor can be switched on in the case of choke control," Collec-

tion: Sudovaya Élektrotekhnika i Svyaz', 8, 19-24 (1959) Bibl. 4.

L. A. Milovidov, "Results of investigations of the static characteristics of a three-phase asynchronous electric drive system with choke control and feedback with respect to speed," Collection: Magnetic Amplifiers (Scientificotechnical Conference Transactions, Khar'kov, 1958, Moscow, 1959) pp. 138-151, Fig. 12, Bibl. 12.

L. A. Milovidov, Theoretical and Experimental Investigation of an Asynchronous Electric Drive System with Choke Control and Feedback with Respect to Speed, Candidate's Thesis (IAT AN SSSR, Moscow, 1958).

O. A. Nekrasov and A. Ya. Shikhin, "On the self-regulation of diesel locomotive generators by means of magnetic amplifiers," Élektrichestvo, 5, 31 (1959).

M. N. Osokhin, "Power characteristics of a crane asynchronous electric drive with saturation chokes," Élektrichestvo, 12, 47-50 (1959) Fig. 2, Bibl. 3.

D. P. Pampura and B. A. Kuznetsov, "Conversion of the mechanical characteristics of asynchronous electric motors for mining shaft elevators by means of saturation chokes in the stator circuit," Izvest. Vysshikh Ucheb. Zaved., Gornoe Delo, 5, 64 (1958).

A. Ya. Petrovskii, "A line of electric drive assemblies 0.1- to 4-kw magnetic amplifiers (PMU)," Collection: Magnetic Amplifiers (Scientificotechnical Conference Transactions, Khar'kov, 1958, Moscow, 1959) pp. 28-35, Fig. 8.

A. L. Pisarev, "Application of saturation chokes and magnetic amplifiers in automated electric drives for elevators in inclined mining shafts," Collection: Magnetic Amplifiers (Scientificotechnical Conference Transactions, Khar'kov, 1958, Moscow, 1959) pp. 99-106, Fig. 5.

M. M. Rasulov, "A system for regulating the excitation of synchronous generators with magnetic amplifiers," Tr. Énerge. Inst. im. I. G. Es'man, AN AzerSSR 14, 53-68 (1959) Fig. 14, Bibl. 6.

Yu. R. Reingol'd, "Investigation of the dynamic properties of a generator-motor system with rotary and magnetic amplifiers by the method of experimental frequency characteristics," Tr. Nauchno-Issle. Inst. Élektroprom., Electric Drives and Automation Equipment 5, 29 (1959) Fig. 7, Bibl. 11.

O. B. Rosenbauli and R. N. Rodin, "A graphoanalytical method for calculating the characteristics of the choke control of asynchronous motors with a heavy Shenfer rotor," Avtomat. i Telemekh. 20, 6, 793 (1959) Fig. 6, Bibl. 2.

O. B. Rosenbauli and R. N. Rodin, "Circuits for motor speed stabilization with three-winding transformers," Avtomat. i Telemekh. 20, 3, 318 (1959) Fig. 3, Bibl. 1.

O. B. Rosenbauli and R. N. Rodin, "A device for the speed stabilization of three-phase asynchronous motors," Author's Certificate, Class 21c, 59_{01}, No. 118538 (586290 of November 18, 1957). Byull. Izobre., 6 (1959).

N. P. Rybalko, "A speed regulator for mining shaft elevators," Author's Certificate, Class 21c, 59_{34}, No. 117272. Byull. Izobret., 2 (1959).

V. V. Sarv, Speed-Control of Asynchronous Motors with Phase Rotors by Using Saturation Chokes in the Case of Balanced and Unbalanced Feed, Candidate's Thesis (Leningrad Institute of Electrical Engineering, 1959).

V. V. Sarv, "Speed-control of asynchronous motors by means of saturation chokes," Information Bulletin (Council of National Economy, Power Supply Management "Éstonénergo" Énergosbyt), 6, 33-39 (1959) Fig. 5.

V. V. Semenov and É. F. Stepura, "An electrohydraulic speed regulator for hydraulic turbines," Author's Certificate, Class 21c, 64_{57}, No. 123231. Byull. Izobret., 20 (1959).

O. V. Slezhanovskii, "A system of contactless control for reversive dc electric drives," Tr. Nauchn.-Issle. Inst. Élektroprom., Electric Drives and Automation Equipment 5, 79-93 (1959) Fig. 6, Bibl. 2.

M. M. Sokolov and Yu. D. Kapuntsov, "A controllable asynchronous electric drive for crane mechanisms with saturation coils," Élektrichestvo, 11 (1959) Fig. 4, Table 1, Bibl. 1.

É. F. Stepura and V. V. Semenov, "A nonlinear magnetic device for restricting the armature current in electrical machines," Author's Certificate, Class 21c, 59_{29}, No. 121837, January 16, 1959. Byull. Izobret., 16 (1959).

M.S. Ter-Mkhitarov, "Possibilities of using magnetic amplifiers in the generator excitation circuit of generator-motor systems," Collection of Scientific Papers (Perm Mining Institute), 2, 159-165 (1958).

"A device (self-operator) for the automatic control of hydroelectric power station units," Author's Certificate, Class 21c, 64_{53}, No. 120570 (589971/24 of January 15, 1958).

N. V. Sharygin, "Application of magnetic power amplifiers in high-frequency voltage-stabilization circuits of rotary generators and in infrasonic-frequency power amplifier circuits," Collection: Magnetic Amplifiers (Scientificotechnical Conference Transactions, Khar'kov, 1958, Moscow, 1959) pp. 107-112, Fig. 3.

É. A. Yakubaitis, "Static self-excitation systems with magnetic amplifiers and germanium triodes for synchronous generators operating at variable frequency," Collection: Magnetic Amplifiers (Scientificotechnical Conference Transactions, Khar'kov, 1958, Moscow, 1959) pp. 113-119, Fig. 5.

É. A. Yakubaitis and A. Z. Libman, "Railway-car electric power stations with ac generators and semiconductor rectifiers," Vest. Vses. Nauchn.-Issle. Inst. Zheleznodorozhnogo Transp., 7, 55-57 (1958) Fig. 2, Bibl. 6.

c) Application in Current and Voltage Stabilizers

L. M. Al'tshul', "An electromagnetic voltage stabilizer," Author's Certificate, Class $21d^2$, 42_{01}, No. 118104. Byull. Izobret., 4(1959).

A. M. Bamdas, V. A. Somov, and S. V. Shapiro, "New powerful ac stator stabilizers," Vest. Elektroprom., 9, 8 (1959), Fig. 5, Bibl. 4.

D. I. Bogdanov, "On the theory of voltage stabilizers with series ferroresonance," Vest. Elektroprom., 3, 53 (1959) Fig. 4, Bibl. 1.

V. S. Volodin and M. A. Rozenbiat, "A stable dc voltage source with magnetic and semiconductor components," Izvest. Akad. Nauk SSSR, Otdel. Tekh. Nauk, Power Engineering and Automation, 4, 208 (1959) Fig. 4.

Yu. K. Zakharov and V. G. Nikulin, "A choke-coupled ac voltage stabilizer," Author's Certificate, Class $21d^2$, 42_{01}, No. 121182. Byull. Izobret.,14 (1959).

P. N. Loiter and E. V. Ershova, "A voltage stabilizer," Author's Certificate, Class $21d^2$, 42_{01}, No. 121850. Byull. Izobret., 16 (1959).

G. F. Neplokhov, "A device for rectified stabilization," Author's Certificate, Class $21d^2$, 42_{01}, No. 124981. Byull. Isobret., 24 (1959).

I. L. Pekker and V. V. Tsokanov, "A voltage stabilizer," Author's Certificate, Class 21c, 67_{10}, No. 124502. Byull. Izobre.,23 (1959).

S. G. Popov, "A voltage stabilizer," Author's Certificate, Class $21d^2$, 42_{01}, No. 120592. Byull. Izobret., 12 (1959).

Yu. N. Pryadilov, "Effect of load reactance on the accuracy of ac voltage stabilizers with saturation chokes," Tr. Mosk. Aviat. Tekh. Inst.,41, 47-53 (1959).

S. F. Pyatkin and P. G. Yantsev, "A contactless method for automatic stabilization of temperature in electric furnaces," Steklo i Keramika, 10, 35 (1958).

F. Sokolov, "The 28-SN-1.25 voltage stabilizer," Kinomekhanik, 6, 31 (1959).

V. P. Soskovets, "A direct-control voltage stabilizer," Vestnik Svyazi, 12, 10-11 (1959) Fig. 4.

A. S. Tofanyuk, Voltage Stabilizers (Voenizdat, Moscow, 1958) p. 83.

G. S. Finogin and A. A. Fedosin, "A current stabilizer," Author's Certificate, Class $21d^2$, 53_{02}, No. 121852, January 26, 1959. Byull. Izobret.,16 (1959).

S. V. Shapiro, "Starting stabilizers with a transformer controlled by shunt magnetization," Tr. Gor'kov. Politekh. Inst. 15, 4, 80 (1959).

d) Application in Measuring Devices

K. P. Garionov, "Multiplier circuits with magnetic amplifiers as data transmitters for voltage, power, and current in voltage self-regulation systems for diesel locomotive traction generators," Collection: Tr. Leningrad. Inst. Inzh. Zheleznodorozhnogo Transp., 159, 268 (1958) Fig. 6, Bibl. 8.

I. Ya. Kaverkin, "Two types of measuring magnetic amplifiers," Informat. Tekh. Sborn. TsBTI, 16 (145), 28 (1958) Fig. 8, Bibl. 1.

O. N. Mel'nikov, "On the application of push-pull magnetic amplifiers as components for measuring large dc current values in control systems," Elektrichestvo, 8, 36-40 (1959) Fig. 5, Bibl. 3.

A. M. Ryvkin, "A device for dc current measurements," Author's Certificate, Class 21e, 36_{01}, No. 120603 (599161/24 of May 9, 1958).

e) Other Applications

A. S. Baginskaya, "Differential protection of synchronous generators by means of current transformers with magnetization by secondary current " Izvest. Tomsk. Politekh. Inst. 94, 166 (1959), Fig. 6, Bibl. 2.

A. S. Baginskaya, "Current transformers with magnetization by secondary current for differential protection," Izvest. Tomsk. Politekh. Inst. 94, 161 (1959) Fig. 6, Bibl. 3.

I. V. Gavrilov, "Application of half-wave magnetic amplifiers in the grid control circuit of mercury rectifiers," Collection: Magnetic Amplifiers (Scientifico-technical Conference Transactions, Khar'kov, 1958, Moscow, 1959) pp. 152-159, Fig. 11.

L. S. Golubev, "A contactless device for automatic charging of storage batteries," Author's Certificate, Class 21b, 26_{02}, No. 124487. Byull. Izobret., 23 (1959).

O. I. Danilevich, "A method for starting mechanical rectifiers," Author's Certificate, Class 21g, 15_{02}, No. 121880, December 18, 1958. Byull. Izobret., 16 (1959).

Ya. A. Kantin, "A controllable transformer," Author's Certificate, Class $21d^2$, 53_{02}, No. 123602. Byull. Izobret., 21 (1959).

Yu. A. Rashkovskii, "Application of current transformers with magnetization in relay protection circuits," Tr. Khar'kov. Politekh. Inst. 27, 1, 43 (1959) Fig. 3, Bibl. 3.

MAGNETIC VOLTAGE AMPLIFIERS, MODULATORS, AND PROBES (MAGNETOMETERS)

R. Ya. Berkman and V. N. Mikhailovskii, "Measurement of variable weak magnetic low-frequency fields in geophysical prospecting," Izvest. Akad. Nauk SSSR, Ser. Geofiz.,6 (1959).

R. Ya. Berkman and V. N. Mikhailovskii, "A method for measuring variable weak low-frequency magnetic fields and its application in technology and applied physics," Avtomat. Kontrol' i Izmeritel'naya Tekh., 3 (1959).

I. G. Gol'dreer, "A converter for transforming dc signals into ac signals," Author's Certificate, Class $21d^2$, No. 124522. Byull. Izobret.,23 (1959).

K. P. Egorov and T'ung K'ai, "Magnetic modulators and the possibilities of their application in multichannel communication equipment, " Tr. Leningrad.

Élektrotekh. Inst. Svyazi, 3 (36) 51 (1958) Fig. 9, Table 3, Bibl. 5.

S. P. Kolosov, "Calculation of the static characteristics of push-pull magnetic voltage amplifiers (for automatic systems)," Nauchnye Doklady Vysshei Shkoly, Élektromekhanika i Avtomatika, 2, 43 (1959) Fig. 3, Bibl. 4.

S. A. Levitan and I. B. Negnevitskii, "A magnetic modulator," Author's Certificate, Class $21d^2$, 12_{64}, No. 124521. Byull. Izobret., 23 (1959).

V. N. Mikhailovskii, B. I. Blazhkevich, R. Ya. Berkman, R. E. Martynyuk-Lototskii, Yu. I. Spektor, and E. A. Andrievskii, "z-Magnetometers with magnetic-modulation data tramsitters of the second harmonic type," Avtomat. Kontrol' i Izmeritel'naya Tekh., 3 (1959).

R. I. Yanus, L. A. Fridman, and V. I. Drozhzhina, "On the theory of differential ferroprobes with longitudinal excitation," Tr. Inst. Fiz. Metall. AN SSSR, 21, 313-326 (1959).

DISCRETE-ACTION MAGNETIC COMPONENTS

a) Books, Monographs, and Dissertations

O. V. Bachin, Possibilities of Using Transfluxors in Memory and Programming Devices (ITM and VT AN SSSR Press, 1959) p. 37.

É. D. Demin and L. A. Chinenkov, Pulse Devices with Ferrites and Semiconductors in Radio Electronics (Novosibirsk, 1959) p. 168, Fig. 98.

V. M. Doklart and G. Ya. Novik, Application of Transistor and Magnetic Components in Digital Computers (Izd. Sovetskoe Radio, 1959), p. 232.

É. I. Zarubina, "Electromagnetic lag lines with ferrite cores" (VINITI Branch, Advanced Scientifico-technical and Industrial Experience, Thesis 42, No. P-59-112/9 Moscow, 1959) p. 12.

Ya. G. Koblents, Design of Circuits and Units for Contactless ATS Magnetic Control (Svyaz'izdat, Moscow, 1959) p. 65, Fig. 30, Bibl. 12.

Ya. G. Koblents, Magnetic Commutation Fundamentals (Svyaz'izdat, Moscow, 1959) p. 58, Fig. 24, Bibl. 11.

Yu. A. Makhmudov, Exploration of the Possibility of Designing a Universal Digital Computer with Magnetic (Ferrite) Components. Candidate's Thesis (Electrical Simulation Laboratory, Academy of Sciences, USSR, 1959).

V. D. Panasenko, "Components for automatic and remote control devices," Tr. Aviats. Inzh. Akademii im. Dzerzhinskogo, Moscow, 39, 272 (1959) Table 187, Bibl. 54.

I. V. Prangishvili, Development and Investigation of Units and Assemblies of Contactless Remote Control Systems with Magnetic and Semiconductor Components. Candidate's Thesis (IAT AN SSSR, 1959).

Application of Transistor and Magnetic Components in Digital Computers. Collection of articles [Russian translation] ed. V. K. Lyubchenko and S. M. Nikulin (Sovetskoe Radio, Moscow, 1959) p. 232.

b) Application of, and Surveys Pertaining to, Discrete Components in Control Systems and Computers

Ya. A. Bedrov, "An indicator of the static state of circuits with two stable equilibrium states," Author's Certificate USSR, Class $21a^1$, 26, No. 111719, June 25, 1958.

N. P. Vasil'eva and N. L. Prokhorov, "Magnetic logical components for automatic control circuits," Avtomat. i Telemekh. 20, 12, 1647 (1959) Fig. 23, Bibl. 6.

K. Guiskii, "A linear commutator with ferrites and semiconductor triodes and a single-cycle input," Sborn. Nauchn.-Issle. Rabot Studentov Élektromekh. Fakul'teta, Leningrad Politekh. Inst., 4, 80 (1959) Fig. 5.

É. A. Demin and L. A. Chinenkov, "Semiconductor current pulse generators for the switching of commutation circuits with ferrites with a rectangular hysteresis loop," Nauchnye Doklady Vysshei Shkoy, Inzh. Radio i Elektronika, 4, 218 (1958) Fig. 12, Bibl. 3.

A. D. Drozdov, V. P. Sabadashev, and Yu. A. Vegera, "A phase-selecting device with alternating pulse current for remote control," Izvest. Vysshikh Ucheb. Zaved., Élektromekhanika, 2, 90-93 (1959) Fig. 3, Bibl. 3.

Z. S. Zorina and E. A. Shkabara, Computers Based on Ferrite Cores with Crystal Triode Control. Problems in Computer Mathematics and Technology (AN UkrSSR Press, Kiev, 1958) pp. 84-93, Fig. 9, Bibl. 5.

Yu. N. Ivenskii, Ya. A. Slepyan, and I. M. Kaplan, "Contactless end switches," Byull. Tekh.-Ékonom. Inform. Council of National Economy of the BelorusSR, 4-5, 76 (1958).

M. I. Kaplan, "A distributor based on magnetic components," Author's Certificate, Class $21a^1$, 36, No. 123201. Byull. Izobret., 20 (1959).

Ya. G. Koblents, "Design and analysis of single-cycle magnetic logical and trigger commutation circuits," Élektrosvyaz' 3, 3, 73-81 (1959) Bibl. 8.

Ya. G. Koblents and E. I. Glaz, "Opposing ATS complex of industrial equipment based on contactless magnetic components," Élektrosvyaz' 3, 11, 58 (1959) Fig. 3, Bibl. 5.

Yu. A. Makhmudov, "A compact universal digital computer based on magnetic (ferrite) LÉM-1 components," Radiotekhnika 14, 3, 47 (1959), Fig. 1, Table 1, Bibl. 3.

K. G. Mityushkin, "The BMT-S-58 cableless remote signal device," Élektricheskie Stantsii, 8, 86 (1959) Fig. 1.

V. N. Mikhailovskii, V. N. Okhotskaya, and K. D. Nadtochii, "Contactless remote control components"

(TsITÉI Advanced Scientificotechnical and Industrial Experience, 1959), Thesis 42, No. P-59-109/8.

E. A. Nemtseva and V. P. Sabadashev, "Development of devices for the storage and circulating transmission of remote control signals with magnetic components," Collection: Nauchn. Rabot. Student. Énerget. Élektromekh. i Mekh. Fakul'tetov Novocherkasskogo Politekh. Inst.,2, 33 (1959) Fig. 7.

K. I. Petukhov, "A magnetic storage device for mining control centralization," Sbor. Leningrad. Inst. Inzh. Zheleznodorozhnogo Transp.,161, 298 (1958) Fig. 8.

I. V. Prangishvili, "Analysis of the operation of magnetic pulse components in contactless remote control devices," Avtomat. i Telemekh. 20, 4, 473 (1959) Fig. 8, Bibl. 6.

A. K. Romanov, "Operation of magnetic single-cycle shift recorders with simultaneous magnetization reversal in additional cores," Élektrosvyaz', 10, 43 (1959), Bibl . 7.

V. P. Sabadashev and Yu. A. Vegera, "A contactless fast phase device for remote control using ac pulses," Izvest. Vysshikh Ucheb. Zaved., Élektromekhanika,2, 94 (1959) Fig. 6, Bibl. 1.

V. E. Khazatskii and V. A. Leonov, "A cyclic-action contactless commutator," Author's Certificate, Class 21c, 47_{50}, No. 121165. Byull. Izobre.,14 (1959).

c) Components Consisting of Magnetic Amplifiers with Feedback

Ya. G. Koblents, D. A. Yakovenko, and N. P. Margacheva, "A magnetic time relay," Author's Certificate, Class 21, 4/05, 21c, 68/60, No. 115510, November 29, 1958.

E. P. Krasovskii, V V. Lauér, and A. G. Shapovalenko, "An ac time relay with a magnetic amplifier," Izvest. Vysshikh Ucheb. Zaved., Énergetika, 1, 59-64 (1958) Fig. 4, Bibl. 2.

I. S. Mikadze and V. G. Kikalishvili, "A time relay with a magnetic amplifier," Tr. Tbilisskogo Nauchn. Issle. Inst. Priborostroeniya i Sredstv Avtomat. 1, 79 (Tbilisi, 1957) Fig. 6, Bibl. 2.

I. V. Prangishvili, "A contactless relay," Author's Certificate, Class 21c, 45_{01}, No. 117663. Byull. Izobret., 2 (1959).

I. I. Ratgauz, "A contactless time relay," Author's Certificate, Class 21c, 44, No. 75562. Byull. Izobret., 2 (1959).

Yu. I. Sumarokov, L. V. Shul'gin, and N. D. Sokolova, "A magnetic trigger," Author's Certificate, Class 21g, 4_{05}, No. 117666. Byull. Izobret.,2 (1959).

V. E. Khazatskii, "A magnetic trigger amplifier," Author's Certificate, Class $21a^1$, 36, No. 119892. Byull. Izobret.,10 (1959).

N. V. Khrushcheva and L. N. Bykov, "A contactless time relay," Author's Certificate, Class 21g, 4_{05}, No. 117587. Byull. Izobret.,2 (1959).

N. I. Chicherin and Yu. M. Kozlov, "A contactless three-position relay," Author's Certificate, Class $21a^1$ 27, No. 123208. Byull. Izobret.,20 (1959).

B. K. Shchukin, "A contactless relay," Author's Certificate, Class 21g, 4_{05}, No. 94434. Byull. Izobret. , 2 (1959).

d) Components with Hysteresis

V. G. Glotov and L. A. Pronin, "On the shape of the hysteresis loop of ferrite cores for memories," Vestn. Élektroprom.,7, 64 (1959) Fig. 4, Bibl. 4.

V. G. Glotov and L. A. Pronin, "Ferrites with a rectangular hysteresis loop for memories," Tr. Nauchn. Issle. Inst. Élektroprom. 4, 53-58 (1959) Fig. 5, Bibl. 5.

Yu. N. Glukhov, V. I. Zolotarevskii, M. A. Kartsev, V. P. Konstantinov, and R. P. Shidlovskii, A Ferrite Memory for 4096 Numbers. Digital Techniques and Computers (Izd. AN SSSR, 1959) pp. 5-27, Fig. 18.

L. V. Ivanov and E. N. Filinov, Control Devices for the Preparation and Adjustment of Ferrite Memories. Digital Techniques and Computers (Izd. AN SSSR, 1959) pp. 28-41, Fig. 9, Bibl. 2.

A. I. Korolev, "A contactless number code data transmitter with magnetic storage devices," Sborn. Leningrad. Inst. Inzh. Zheleznodorozhnogo Trans.,161, 292 (1958) Fig. 3.

V. R. Kulikov, "On the selection of parameters of magnetic automation components with hysteresis," Tr. Khar'kov. Politekh. Inst. 27, 1, 35 (1959) Fig. 3, Bibl. 4.

E. I. Mamonov, "A method for determining the switching time of magnetic components," Author's Certificate, Class 21e, 12, No. 124049. Byull. Izobret., 22 (1959).

A. K. Romanov, "Stability of magnetic push-pull shift recorders," Nauchnye Doklady Vysshei Shkoly, Radiotekh. i Élektron., 2, 303 (1959) Bibl. 5.

N. Ya. Matyukhin and O. V. Rosnitskii, "On the operation of ferrite cores in matrix memories," Collection: Computer Techniques (Izd. AN SSSR Moscow, 1959) pp. 119-130, Fig. 11, Bibl. 5.

L. A. Chinenkov and É. D. Demin, "A closed-loop shift recorder with magnetic components with a rectangular hysteresis loop," Author's Certificate, Class $21a^1$, 36, No. 119893. Byull. Izobret. 10 (1959).

e) Magnetic Transistor Components

É. I. Galynker, A Decimal Counter with Ferrite–Transistor Triggers. Digital Techniques and Computers (Izd. AN SSSR, 1959), pp. 183-185, Fig. 4.

M. G. Reinberg and V. A. Tret'yukhin, Ferrite–Transistor Triggers with a Single Transistor. Digital Techniques and Computers(Izd. AN SSSR, 1959) pp. 179-182, Fig. 4, Bibl. 1.

Yu. I. Serenkov and I. S. Vorontsova, "Experimental investigations of the simultaneous operation of ferrite-transistor logical cells in computer mock-ups," Nauchn.

Tekh. Informat. Byull. Leningrad. Politekh. Inst. im. M. I. Kalinina, 1, 66 (1959) Bibl. 6.

f) Ferroresonance Components

I. L. Tanatarova and V. P. Sabadashev, "Development and investigation of fast remote control devices with ferroresonance components," Collection: Nauchn. Raboty Studentov Énerget. Élektromekh. i Mekhan. Takul'tetov Novocherkasskogo Politekh. Inst., 3, 21 (1959) Fig. 9, Bibl. 2.

MAGNETIC OSCILLATORS AND FREQUENCY CONVERTERS

A. M. Bamdas and V. I. Zagryadskii, "A contactless induction frequency converter," Izvest. Vysshikh Ucheb. Zaved., Élektromekhanika, 2, 105 (1959) Fig. 3, Bibl. 14.

A. M. Bamdas and V. A. Kulinich, "Automatic balancing of a three-phase circuit feeding an active single-phase load of variable magnitude," Izvest. Vysshikh Ucheb. Zaved., Énergetika, 9, 53 (1959) Bibl. 14.

A. M. Bamdas and V. A. Kulinich, "Static converters with magnetic amplifiers for transforming single-phase currents into three-phase currents," Tr. Gor'kov. Politekh. Inst. im. Zhdanova 15, 4, 37 (1959) Fig. 6, Bibl. 13.

A. M. Bamdas and V. A. Kulinich, "A static device for transforming a single-phase system into a three-phase system," Author's Certificate, Class $21d^2$, 52, No. 120594. Byull. Izobret., 12 (1959).

K. I. Vil'pert, "A converter with semiconductor triodes for transforming dc current into ac current," Author's Certificate, Class $21d^2$, 12_{03}, No. 124520. Byull. Izobret. 23 (1959).

V. I. Zhitomirskii and E. N. Men'chukov, "A frequency divider circuit," Author's Certificate, Class $21a^4$, 48_{15}, No. 119208. Byull. Izobret., 8 (1959).

A. I. Zaitsev and Ya. V. Petrov, "A resonance three-phase frequency trebler," Izvest. Tomskogo Politekh. Inst. 97, 12 (1959), Fig. 10, Bibl. 4.

V. A. Kulinich, "Static transformation of single-phase currents into three-phase currents with balance stabilization," Izvest. Vysshikh Ucheb. Zaved., Élektromekhanika, 7, 66 (1959) Fig. 9, Bibl. 17.

Ya. V. Petrov and A. I. Zaitsev, "On the circuits of three-phase ferromagnetic frequency treblers," Izvest. Tomskogo Politekh. Inst. 97, 22 (1959) Fig. 6, Bibl. 5.

A. G. Pinchuk, "A device for frequency multiplication," Author's Certificate, Class $21d^2$, 51, No. 94694. Byull. Izobret., 1 (1959).

S. V. Pokrovskii, On the Method of Designing Static Frequency Doublers. Candidate's Thesis (MÉI, Moscow, 1959).

A. M. Pshenichnikov, "Analysis of the operation of Roer multivibrators in industrial remote measurement devices," Avtomat. i Telemekh. 20, 9, 1250-1261 (1959) Fig. 12, Bibl. 6.

V. A. Rayushkin, "Analytical determination of idling and short-circuit regimes of frequency doublers by taking into account the higher harmonics," Tr. Khar'kov. Politekh. Inst. 27, 1, 5 (1959) Fig. 9, Bibl. 11.

L. L. Rozhanskii, "A static frequency doubler with magnetization by direct current," Tr. Khar'kov. Politekh. Inst. 27, 1, 19 (1959) Fig. 3, Bibl. 4.

A. G. Rubinshtein, D. F. Tartakovskii, and I. I. Vinshtein, "A magnetic oscillator," Author's Certificate, Class $21a^4$, 13, No. 122782, February 7, 1959. Byull. Izobret., 19 (1959).

A. B. Flerov and V. P. Sabadashev, "Investigation of extrinsic characteristics of magnetic frequency treblers," Collection: Nauchnye Raboty Studentov Énerget. Élektromekh. i Mekhani. Fakul'tetov Novocherkasskogo Politekh. Inst., 3, 41-50 (1959), Fig. 9, Bibl. 4.

L. A. Chinenkov and É. A. Demin, "Frequency dividers with ferrites and semiconductor triodes," Élektrosvyaz' 6, 6, 11 (1959) Bibl. 8.

V. I. Shchitnikov, "A method for dividing the pulse repetition frequency," Author's Certificate, Class $21a^1$, 36, No. 124003, Byull. Izobret., 22 (1959).

MAGNETIC MEASUREMENTS AND METHODS FOR TESTING MAGNETIC COMPONENTS

Yu. A. Avakh, "A new method for controlling magnetic amplifiers," Nauchnye Doklady Vysshei Shkoly, Mashinostroenie i Priborostroenie, 2, 175-182 (1959).

Yu. A. Avakh, "A device for testing magnetic amplifiers which are controlled by direct current," Author's Certificate, Class 21e, 36_{10}, No. 121874, December 18, 1958. Byull. Izobret., 16 (1959).

O. N. Al'tgauzen and N. A. Semenova, "On the method of measuring the magnetic properties of electrical steel in weak and medium fields," Zavodskaya Lab. 25, 4, 426-428 (1959) Fig. 3, Bibl. 4.

"Methods and equipment for inspecting ferrite toroidal cores with respect to their magnetic properties," 1953-1957, 14 titles (01 No. 1301), Novo. Zarubezhnoi Radioélekt. VNT MO SSSR, 7, 32 (April, 1959)

R. Kh. Bal'yan, V. I. Laletin, and I. V. Trofimov, "A method for demagnetizing the cores of pulse transformers," Radiotekhnika 14, 8, 40 (1959) Fig. 2, Bibl. 2.

R. Kh. Bal'yan, V. I. Laletin, and I. V. Trofimov, "A device for demagnetizing the cores of pulse transformers," Author's Certificate, Class $21d^2$, 12_{02}, No. 121501. Byull. Izobret., 15 (1959).

A. A. Bondar', "A method for dividing losses in magnetic cores," Author's Certificate, Class 21e, 12, No. 123249. Byull. Izobret., 20 (1959).

G. Kh. Vyal'yamyaé, "A device for determining the magnetic properties of ferromagnetic materials," Author's Certificate, Class 21e, 12, No. 123607. Byull. Izobret., 21 (1959).

L. N. Gertsiger, "The IMI-2 magnetic induction meter," Priborostroenie, 5, 27 (1959).

K. K. Gomoyunov, "A method for determining the magnetic properties of ferromagnetic cores," Author's Certificate, Class 21e, 12, No. 119249. Byull. Izobret., 8 (1959).

G. L. Gornshtein and M.M. Leshchines, "The problem of measuring magnetic induction in electrical steel in a magnetic field of 10 at/cm," Zavodskaya Lab. 25, 12, 1427 (1959) Fig. 1, Table 2, Bibl. 2.

V. V. Druzhinin, "On the shape of specimens for determining the magnetic characteristics of electrical steel," Zavodskaya Lab. 25, 4, 429 (1959) Fig. 2, Table 5.

V. V. Druzhinin, Yu. E. Zubov, A. A. Kozhurov, and R. I. Yanus, "A device for magnetic and electrical investigation of whole electrical steel sheets," Author's Certificate, No. 118903, March 7, 1959.

V. V. Druzhinin and I. P. Kudryavtsev, "On the quantitative determination of texture in cold-rolled transformer steel," Zavodskaya Lab. 25, 12, 1425 (1959) Fig. 3, Bibl. 4.

E. L. Kantor, "Inspection of the basic ferromagnetic characteristics of toroidal cores in mass production," Priborostroenie, 11, 21 (1959).

V. P. Karpenko, Possibilities of Using T-Circuits for Magnetic Measurements, Magnetic Measurement Problems(Izd. AN UkrSSR, Kiev, 1959) pp. 105-119, Fig. 11, Bibl. 4.

V. P. Karpenko, A Calorimetric Method of Measuring Losses in Ferromagnetic Materials. Magnetic Measurement Problems (Izd. AN UkrSSR, Kiev, 1959) pp. 96-104, Fig. 2, Bibl. 5.

I. I. Kifer, "Magnetic measurement methods and equipment," Zavodskaya Lab. 25, 4, 423-425 (1959).

I. I. Kifer and V. U. Marguleva, "On the oscillographic method of testing magnetically soft materials," Zavodsk. Lab. 25, 4, 434(1959) Fig. 3, Table 4, Bibl. 3.

B. E. Kubyshin, Determination of the Permeability of Substances in Variable Fields. Magnetic Measurement Problems (Izd. AN UkrSSR, Kiev, 1959) pp. 6-19 Fig. 5, Bibl. 3.

E. D. Mamontov, "A method for measuring the permeability of closed-loop cores in variable magnetic fields," Author's Certificate, Class 21e, 37_{10}, No. 122548, January 17, 1959. Byull. Izobret., 18 (1959).

V. M. Mezhenin, "A new device for testing magnetic amplifiers" (VINITI Branch, Moscow, 1959) p. 11, Ref. Zh. Elektrotekh., 4, 2947 (1960).

V. I. Molotkov, "A method for determining the hysteresis loop of ferromagnetic materials," Author's Certificate, Class 21e, 37_{10}, No. 123620. Byull. Izobret., 21 (1959).

A. D. Nesterenko, The Use of Balancing Circuits for Testing Magnetically Soft Materials in Steady Magnetic Fields. Magnetic Measurement Problems. (AN Izd. Ukr. SSR, Kiev, 1959) pp. 53-61, Fig. 8, Bibl. 5.

V. F. Petrochenko, "Separation of losses in steel by the method of two different frequencies in the case of constant losses due to eddy currents," Magnetic Measurement Problems (Izd. AN UkrSSR Kiev, 1959) pp. 45-52, Table 2, Bibl. 6.

L. I. Rabkin, E. V. Ébanoidze, Z. A. Isaeva, and N. P. Goryachev, "A method of testing ferrites," Author's Certificate, Class 21e, 37_{10}, No. 119935. Byull. Izobret., 10 (1959).

I. M. Rozhanovskii, "Magnetic characteristics of electrical steels in variable magnetic fields," Magnetic Measurement Problems (Izd. AN UkrSSR, Kiev, 1959) pp. 20-32, Fig. 14, Table 4.

I. M. Rozhanovskii, "Recommended methods for separating losses in electrical steels," Magnetic Measurement Problems (Izd. AN UkrSSR, Kiev, 1959) pp. 33-44, Fig. 4, Table 2, Bibl. 8.

A. A. Roitman, "On magnetic tests of cold-rolled textured electrical steel," Zavodskaya Lab. 25, 4, 433 (1959).

N. M. Rudnyi, A. Z. Veksler, and I. F. Kobyakov, "A stabilized sinusoidal current source for checking electrical measuring instruments," Collection of Reports on Scientific Investigations Performed in the Institutes of Measures and Measuring Instruments of the Council of Ministers of the Standartgiz, Moscow–Leningrad, 3, 77 (1959), Report No. 288.

N. A. Semenova and O. N. Al'tgauzen, "On the method of determining magnetic properties in the Epstein apparatus," Zavodskaya Lab. 25, 12, 1418 (1959) Fig. 3, Bibl. 5.

O. P. Sidorov, "A device for measuring hysteresis losses in ferromagnetic materials," Author's Certificate, Class 21e, 37_{10}, No. 119262. Byull. Izobret., 8 (1959).

E. K. Ul'yanova, "A device for determining the pulse characteristics of ferrite cores," Tr. Nauchn. Issle. Inst. Élektropro. 4, 59 (1959) Fig. 3.

E. N. Chechurina, "Peculiarities in testing ferromagnetic materials in the case of simultaneous magnetization in steady and variable fields," Tr. VNIIM: Investigations in the Field of Electrical Measurements, Standartgiz, Moscow–Leningrad, 38 (98), 126-135 (1959) Fig. 7, Table 4, Bibl. 7.

N. G. Chernysheva, "On methods of determining the properties of electrical steel," Zavodskaya Lab. 25, 4, 437 (1959).

E. T. Chernyshev, E. N. Chechurina, N. G. Chernysheva, and I. A. Oralova, "Development of methods and equipment for testing normal magnetic material specimens at frequencies over 1000 cps in the 10,000-gauss induction range," Collection of Reports on Scientific Investigations performed in the Institutes of the Committee for the Council of Ministers of the Standards, Measures, and Measuring Instruments USSR (Standartgiz, Moscow–Leningrad, 1959), No. 3, p. 77, Report No. 289.

Yu. M. Shamaev, F. G. Lisitsyn, and A. I. Pirogov, "Measurement method and the results obtained in measuring the static and dynamic characteristics of ferrites with a rectangular hysteresis loop," Nauchnye Doklady Vysshei Shkoly, Élektromekhanika i Avtomatika, 3, 3 (1958), Fig. 16, Bibl. 7.

R. I. Yanus, Certain Problems in the Theory and Techniques of Magnetic Measurements. Author's Abst. of Ph. D. Dissertation (UF AN SSSR, Sverdlovsk, 1959).

R. I. Yanus, "On nondestructive methods for testing electrical sheet steel," Zavodskaya Lab. 25, 12, 1421-1422 (1959)* Bibl. 9.

R. I. Yanus and Yu. A. Vdovin, "A method for determining the magnetic properties of electrical steel," Author's Certificate, Class 21e, 37_{10}, No. 124547. Byull. Izobret., 23 (1959).

R. I. Yanus, V. V. Kubarev, Yu. A. Vdovin, and I. P. Kolpakov, "An automatic device for sorting electrical steel sheets," Zavodskaya Lab. 25, 4, 480 (1959)*

R. I. Yanus and T. M. Senkevich, "A simple electromagnetic device for thickness measurement," Tr. Inst. Fiz. Metallov AN SSSR, 21, 131 (1959).

Automation and Remote Control